A UNITED STATES DEPARTMENT OF COMMERCE PUBLICATION

Engineering and Instrumentation

SECTION C

JOURNAL OF RESEARCH

NATIONAL BUREAU OF STANDARDS

Volume 73C

Numbers 3 and 4

July–Dec. 1969

J. Res. Nat. Bur. Stand. (U. S.), C
CODEN: JNBCA
73C (3 & 4) 47–118 (1969)

Journal of Research

of the

National Bureau of Standards

C. Engineering and Instrumentation

July–Dec. • 1969

VOLUME • 73C

NUMBERS • 3 and 4

Editor: Martin Greenspan

Associate Editors: G. F. Montgomery, R. V. Smith, A. F. Schmidt

Publication dates:
Feb. 15, May 15, Aug. 15, Nov. 15, 1969

JOURNAL OF RESEARCH

The National Bureau of Standards Journal of Research reports research and development in the fields of activity shown at right. Also included from time to time are survey articles on topics closely related to the Bureau's scientific and technical program.

The Journal is published in three separate sections as follows:

A. Physics and Chemistry

Contains papers of interest primarily to scientists working in these fields. Issued six times a year. Annual subscription: domestic, $9.50; foreign, $11.75. Single copy, varies.

B. Mathematical Sciences

Presents studies and compilations designed mainly for the mathematician and the theoretical physicist. Issued quarterly. Annual subscription: domestic, $5.00; foreign, $6.25. Single copy, $1.25.

C. Engineering and Instrumentation

Reports research and development results of interest chiefly to the engineer and the applied scientist. Issued quarterly. Annual subscription: domestic, $5.00; foreign, $6.25. Single copy, $1.25.

The National Bureau of Standards[1] was established by an act of Congress March 3, 1901. Today, in addition to serving as the Nation's central measurement laboratory, the Bureau is a principal focal point in the Federal Government for assuring maximum application of the physical and engineering sciences to the advancement of technology in industry and commerce. To this end the Bureau conducts research and provides central national services in four broad program areas. These are: (1) basic measurements and standards, (2) materials measurements and standards, (3) technological measurements and standards, and (4) transfer of technology.

The Bureau comprises the Institute for Basic Standards, the Institute for Materials Research, the Institute for Applied Technology, the Center for Radiation Research, the Center for Computer Sciences and Technology, and the Office for Information Programs.

THE INSTITUTE FOR BASIC STANDARDS provides the central basis within the United States of a complete and consistent system of physical measurement; coordinates that system with measurement systems of other nations; and furnishes essential services leading to accurate and uniform physical measurements throughout the Nation's scientific community, industry, and commerce. The Institute consists of an Office of Measurement Services and the following technical divisions:

Applied Mathematics—Electricity—Metrology—Mechanics—Heat—Atomic and Molecular Physics—Radio Physics[2]—Radio Engineering[2]—Time and Frequency[2]—Astrophysics[2]—Cryogenics.[2]

THE INSTITUTE FOR MATERIALS RESEARCH conducts materials research leading to improved methods of measurement standards, and data on the properties of well-characterized materials needed by industry, commerce, educational institutions, and Government; develops, produces, and distributes standard reference materials; relates the physical and chemical properties of materials to their behavior and their interaction with their environments; and provides advisory and research services to other Government agencies. The Institute consists of an Office of Standard Reference Materials and the following divisions:

Analytical Chemistry—Polymers—Metallurgy—Inorganic Materials—Physical Chemistry.

THE INSTITUTE FOR APPLIED TECHNOLOGY provides technical services to promote the use of available technology and to facilitate technological innovation in industry and Government; cooperates with public and private organizations in the development of technological standards, and test methodologies; and provides advisory and research services for Federal state, and local government agencies. The Institute consists of the following technical divisions and offices:

Engineering Standards—Weights and Measures—Invention and Innovation—Vehicle Systems Research—Product Evaluation—Building Research—Instrument Shops—Measurement Engineering—Electronic Technology—Technical Analysis.

THE CENTER FOR RADIATION RESEARCH engages in research, measurement, and application of radiation to the solution of Bureau mission problems and the problems of other agencies and institutions. The Center consists of the following divisions:

Reactor Radiation—Linac Radiation—Nuclear Radiation—Applied Radiation.

THE CENTER FOR COMPUTER SCIENCES AND TECHNOLOGY conducts research and provides technical services designed to aid Government agencies in the selection, acquisition, and effective use of automatic data processing equipment; and serves as the principal focus for the development of Federal standards for automatic data processing equipment, techniques, and computer languages. The Center consists of the following offices and divisions:

Information Processing Standards—Computer Information—Computer Services—Systems Development—Information Processing Technology.

THE OFFICE FOR INFORMATION PROGRAMS promotes optimum dissemination and accessibility of scientific information generated within NBS and other agencies of the Federal Government; promotes the development of the National Standard Reference Data System and a system of information analysis centers dealing with the broader aspects of the National Measurement System, and provides appropriate services to ensure that the NBS staff has optimum accessibility to the scientific information of the world. The Office consists of the following organizational units:

Office of Standard Reference Data—Clearinghouse for Federal Scientific and Technical Information[3]—Office of Technical Information and Publications—Library—Office of Public Information—Office of International Relations.

[1] Headquarters and Laboratories at Gaithersburg, Maryland, unless otherwise noted; mailing address Washington, D.C. 20234.
[2] Located at Boulder, Colorado 80302.
[3] Located at 5285 Port Royal, Springfield, Virginia 22151.

U.S. DEPARTMENT OF COMMERCE
Maurice H. Stans, Secretary
NATIONAL BUREAU OF STANDARDS
Lewis M. Branscomb, Director

Order all publications from the Superintendent of Documents
U.S. Government Printing Office, Washington, D.C. 20402.

Use of funds for printing this publication approved by the Director of the Bureau of the Budget (June 22, 1966).

JOURNAL OF RESEARCH of the National Bureau of Standards—C. Engineering and Instrumentation
Vol. 73C, Nos. 3 & 4, July–December 1969

Design Features of a Precision AC-DC Converter

Louis A. Marzetta

Institute for Applied Technology, National Bureau of Standards, Washington, D.C. 20234

and

Donald R. Flach

Institute for Basic Standards, National Bureau of Standards, Washington, D.C. 20234

(August 5, 1969)

With the availability today of high performance operational amplifiers and related components, it is possible to construct an instrument for ac-dc transfer work that meets the requirements of a standards laboratory. Transformation of measured average a-c values into d-c voltage is possible with a predictable accuracy of 20 parts per million up to 1 kHz. Precision of operation is assured from dc to 100 kHz.

Key words: AC; DC; operational; precision; rectifier; transfer.

1. Introduction

Reference to precise a-c measurement has always implied an rms evaluation. This has been so because the majority of physical results in experiments and other usage are related to transformation of electrical energy, to heat or mechanical work, and electrical laboratories have found the best accuracy in square-law responding instruments. With the availability today of highly stable, nearly pure sine-wave power sources and precision linear operational devices, the situation has changed. For some ac-dc transfer work such as amplitude monitoring [1],[1] the average a-c responding systems to be described can have a superiority of precision over rms converters. In addition, the wide usage of average responding instruments such as digital voltmeters with a-c options and sampling devices has increased the need for a basic average transfer standard. This paper will delve into design factors that demonstrate the ability of transforming the average value into d-c voltage with a high order of accuracy.

2. Operational Rectifier Stage

The choice of systems and circuits for average a-c measurement is more limited than for rms. An average responding circuit is involved with some form of rectification—that is, it has to average either the positive or the negative values of the voltage wave, or both without regard to sign. It is the defects in the rectifying elements that affect precision and accuracy. The object of the operational rectifier circuit, figure 1, is to place the rectifying components in the feedback loop at the output of the amplifier wherein the full loop gain amplification can be used to greatly reduce the diode weaknesses. The device is a unity gain circuit (if equal value resistors are used at the input and feedback connections) whereby half-sine waves are generated at each output.

Because of the unwieldy nature of transfer expressions in circuits with diodes, a linear amplifier type analysis in the frequency domain will be pursued first, by neglecting the diode imperfections.

2.1. Finite Gain Error

Using superposition theory and writing a current balance at the input summing junction, we find that the transfer function of a unity-gain inverting operational amplifier with perfect ratio resistors is

$$V_{out}/V_{in} = -\frac{1}{1+(2/A_f)} \qquad (1)$$

where A_f is the open-loop voltage amplification of an

[1] Figures in brackets indicate the literature references at the end of this paper.

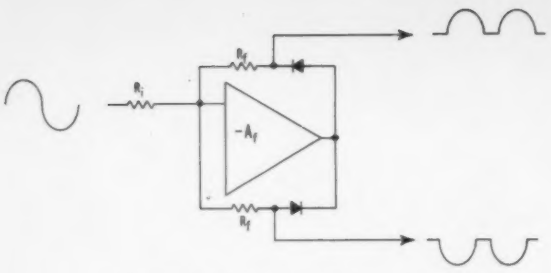

FIGURE 1. *Basic operational rectifier.*

operational amplifier with ideal characteristics but finite amplification.

To avoid commonly observed errors in the usual exact-gain formula due to neglect of the phasor nature of the open-loop voltage amplification, A_f, the general formula can be expressed in a more usable form as follows

$$V_{out}/V_{in} = -(Z_f/Z_i) \cdot \frac{1}{1+(1/A_f)(\cos\theta - j\sin\theta)[1+(Z_f/Z_i)]} \quad (2)$$

where θ is the open loop phase angle of the amplifier, and A_f is now the magnitude of the open loop amplification. Starting with zero degrees at direct current, θ usually increases with a minus sign (lag) as the frequency increases. Z_f and Z_i are feedback and input impedances, respectively. In most literature a reader tends to interpret the closed-loop gain expression as an output that falls off with frequency because of the drop in open loop amplification. Careful tests corroborate expression (2) and show that this is not necessarily so. The output can actually rise with frequency for a constant input in spite of a dropping A_f in the region where θ has shifted beyond 90 degrees lag, the reason being that the phase lag has created a real component of positive feedback.

The transfer error in ppm (parts per million) for an inverting unity gain situation is the difference between unity and the magnitude of V_{out}/V_{in}. Except for angles near 90°, the error can be closely approximated as $\pm(2/A_f)\cdot(\cos\theta)\cdot 10^6$; the minus sign for phase lag less than 90° and plus sign for phase lag greater than 90°, where $(A_f \gg 1)$. Exactly at 90° the error reduces to $2/A_f^2$, and reaches zero error slightly beyond 90°. However, effectiveness of quadrature error reduction does drop off rapidly for phase deviations from the 90° region.

Since phase characteristics are rarely given in operational amplifier literature, the transfer error calculation of the operational rectifier will be hampered. Using the worst case basis of $(2/A_f)\cdot 10^6$ for the error, for an amplifier with zero phase shift, it could be expected that an operational amplifier would exhibit a gain transfer error of 100 ppm at the frequency where the open loop amplification is 20 000 and that the error would double each octave increase of frequency. However, it was found from actual test data that the error function did not behave in this manner but that the output remains quite constant for a wide frequency range, in some cases rising at the higher frequencies due to the previously described phase properties. Hence it can be assumed that the $(2/A_f)\cdot 10^6$ error factor is quite conservative.

2.2. Finite Diode Conduction Level Error

Another source of error arises from the finite conduction level of the diodes. Time is lost at the amplifier in order for its output to reach the diode conduction voltage, which means that there is a "lost area" at the beginning of the half sine wave output. The overall error in average value with a first order approximation can be expressed as the ratio of the lost small area to the half-wave area. It is desirable to analyze the factors that may influence this particular error.

For the period of a half-sine wave with V_m peak volts, the average value is $(2/\pi)V_m$. Hence the area under the function is $(2/\pi)(V_m)(\pi)$ or $2V_m$ volt-radians. The lost area in question can be found by formal integration as

$$\text{Lost Area} = V_m \int_0^{\phi_c} \sin\phi d\phi \quad (4)$$

where ϕ_c is the angle measured from the zero crossing point to the diode conduction point. For small angles, $\cos\phi = 1-(\phi^2/2)$ and the lost area from expression (4) is

$$\text{Lost Area} = V_m|-\cos\phi|_0^{\phi_c} = V_m(\phi_c^2/2) \text{ volt-radians.} \quad (5)$$

At angle ϕ_c the diode conduction voltage, V_c, at the amplifier output is

$$V_c = A_f V_s \quad (6)$$

where V_s is the potential at the operational amplifier's summing input junction and A_f is the open-loop voltage amplification. Also for small radian angles

$$V_s = \phi_c V_m. \quad (7)$$

Substituting (7) into (6), the angle at conduction point becomes

$$\phi_c = V_c/V_m A_f. \quad (8)$$

Using expressions (5) and (8)

$$\text{Lost Area} = V_c^2/2V_m A_f^2. \quad (9)$$

Taking the ratio of the lost area (9) to the half-wave area $(2V_m)$, the overall error is

$$\text{error, } \epsilon = V_c^2/4V_m^2 A_f^2. \quad (10)$$

Because of the squared value for A_f in the expression,

the error due to the finite diode conduction level is considerably less than the closed-loop gain error noted in expression (2).

2.3. Slew Rate Error

A second source of possible error from the diode conduction level is found in the consideration of the operational amplifier–rectifier in the time domain. Included in the data on operational amplifiers is the "slew rate"–a measure of the device's transient response. Slewing rate, S, or maximum output voltage change with respect to time is expressed as

$$S = (dV_0/dt)_{max} = V_p(\omega_h/10^6) \text{ volts per microsecond} \quad (11)$$

where V_p is the peak output voltage and ω_h is the maximum frequency in radians per second for full output of the device. Using the stated slew rate, the time lost in reaching diode conduction can be found and used to compute the lost area. The elapsed time (t_c) from zero crossing to conduction, V_c is

$$t_c = V_c/S \text{ seconds.} \quad (12)$$

The angle, ϕ_c, of expression (4) can be expressed as

$$\phi_c = (t_c/t_0)\ (2\pi) \text{ radians} \quad (13)$$

where t_0 is the time for one period of the operating frequency, f_0. Substituting (12) in (13)

$$\phi_c = V_c 2\pi f_0/S \text{ radians.} \quad (14)$$

Using the lost area expression (5) and expression (14) for ϕ_c

$$\text{Lost area due to } S = V_m[V_c 2\pi f_0/S]^2/2. \quad (15)$$

As in expression (10) the overall error, ϵ, comes from the ratio of lost area to half-wave area.

$$\text{error, } \epsilon = V_c^2(2\pi f_0)^2/S^2. \quad (16)$$

Comparing expressions (16) and (10)–for example: if $f_0 = 16$ kHz, V_c is about 0.6 V, an amplifier with $A_f = 10^4$ and a slew rate of 10 V per microsecond, the error from expression (10) with an input signal of $V_m = 7$ V becomes approximately two parts in 10^{11}. Using expression (16) the error is about ten parts in 10^6.

In this example the slew rate factor contributed a greater error than the A_f gain factor. However, the slew rate figure alone is not a reliable measure of an amplifier's ability to be used as a precision operational rectifier. It is possible for a device to have both a relatively low A_f and a high slew rate since the two are independent design features of the amplifier. Such a rectifier would suffer a possible error from expression (10). Fortunately all amplifiers investigated that have the desired open-loop amplification also have sufficient slew rate. One additional note is that amplifier output overshoot at the beginning and end of the half-sine wave has not been a troublesome factor.

Thus far the discussion of the operational rectifier has been concerned with its a-c requirements; however the precision of its average value output also demands a strict dc stability. Not very long ago it was possible to achieve low drift results only with chopper-stabilized devices. High a-c performance operational amplifiers are now available in differential, nonchopper design wherein the drift error contribution with a 5 V input signal can be kept below 20 ppm for hours. Bias current variations at the input are low enough so as to be negligible in producing d-c output variations with feedback resistors encountered (1 kΩ to 100 kΩ).

2.4. Feed-Forward Operational Amplifiers

In the course of experimenting with a number of available operational amplifiers a certain group of them were found to exhibit a marked anomalous behavior. These particular amplifiers showed a monotonically decreasing response with frequency that was much sharper than was predictable with the conservative error factor bases. An inquiry into design of these amplifiers revealed them as "feed-forward" type devices. Briefly this means the input signal assumes different paths through the overall amplifier chain depending upon the input frequency, in the manner of a chopper stabilized amplifier. They can sometimes be spotted in the literature as wide-band devices with a high capacitance at the inverting input, as much as 0.02 μF. While feed-forward type operational amplifiers can be used as operational rectifiers, FET differential amplifiers characterized by their low input capacitance at both inputs (5 pF or less) are generally preferred.

3. Operational Filter Stage

The operational stage following the rectifier is the filter. (Fig. 2) Basically it is an accurate unity gain stage with a large enough time constant to filter out the half-sine-wave ripple to a level tolerable to the d-c detector. It also provides nearly ideal impedance buffering between the rectifier output and the d-c detector. The filter operational amplifier a-c response performance is unimportant, but like the operational rectifier, the need for low d-c voltage drift must be met. To preserve the unity gain accuracy and to present a low output impedance, the open loop d-c voltage amplification should be at least 200 000–a figure that is easily found in today's devices.

The feedback filter capacitor should have enough capacitance to achieve the desired time constant in conjunction with the feedback resistor (10 kΩ to 50 kΩ) to meet the detector requirements. Capacitor leakage resistance is important; the value should be at least 10^5 times the feedback resistor value. Polycarbonate dielectric capacitors are available in a 40 μF value, meeting the low leakage requirements.

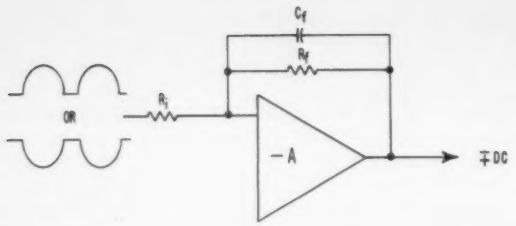

FIGURE 2. *Basic operational filter.*

4. Choice of Precision Resistors for the Rectifier and Filter Stages

The principal factor in the gain-setting accuracy of an operational stage is the ratio accuracy of the circuit resistors external to the component amplifier. Wire-wound resistors of various forms are available with both individual and ratio accuracies of 5 ppm. Extensive tests have demonstrated their ability to perform well in operational circuits. With little complexity it is possible to detect by d-c null techniques a difference of less than 5 ppm in a pair of high quality wire wound resistors by interchanging their respective positions at the input and feedback of an operational amplifier. The problem with some wire wound resistors is that they can exhibit a noticeable dc-ac error for frequencies above 5 kHz, amounting to several hundred ppm at 50 kHz. While it is possible to partially compensate for the error by using networks tailored to the resistor characteristics, it is the purpose of this article to describe systems of high precision that are void of compensation schemes. Fortunately there are available metal film resistors with desirable properties for the immediate application. These possess a virtually zero dc-ac difference over the range of interest (dc to 100 kHz). They are readily available with better than 100 ppm ratio accuracy with a relative temperature coefficient of a few ppm per degree. For wide band work in the area of 100 ppm accuracy, the metal film resistors are highly recommended; for high-accuracy, low-frequency applications of say 20 ppm, wire wound resistors may be more suitable.

5. Selection of Diodes at Operational Rectifier

The role of reverse leakage current and junction capacitance of a chosen diode must be considered in relation to the feedback resistor. It is possible to use a single silicon diode in each feedback path of the rectifier circuit since they are available with leakage currents less than 10^{-9} A. The usual operational forward diode current is 10^{-3} A, hence the error is 1 ppm for the stated leakage current. A more conservative approach is to use a pair of diodes in series, with a resistive shunt path between them for the leakage current; an arrangement conceived by Richman [1]. The series feature also reduces the resultant capacitance at full reverse bias; typically 1 pF.

The junction capacitance at the diode can introduce an error by adding a component of reverse current to the diode's forward signal current. However the net effect can be small because of the quadrature phase relationship of the currents. The error expression can be derived from the circuit impedances in the current branches. For small values of capacitance or high ratio of capacitive reactance to series feedback resistance, the error becomes $= 1/2(R_f/X_c)^2 \cdot 10^6$ ppm. For example at an operating frequency of 16 kHz and a feedback resistance of 10^4 Ω, a 1 pF diode capacitance would introduce an error of about 1/2 ppm.

With two silicon diodes in series the output must reach about 1.2 V before conduction takes place. This quadruples the small error in average value because of the "lost area" as explained previously. The latest development of "hot carrier" diodes can be used to good advantage. These high-speed diodes have the low-leakage feature of silicon diodes and a low forward conduction voltage similar to germanium less than 0.39 V.

Reverse recovery or effective minority carrier lifetime in a diode is a measure of its ability to turn off in going from forward to reverse conduction. In the operational rectifier this factor affects the termination of the half sine wave function, resulting in an error in average value. The analysis of the error is nearly the same as for the case of limited amplifier slew rate discussed previously with the error showing up as a lost area. Fortunately the diodes described in this section have recovery times in the vicinity of 10^{-9} s. Using the same procedure as with the example of the slew rate discussion, the error contributed at 16 kHz with the stated recovery time is found from expression (6). The error is equal to $\theta^2/4$ or $(10^5 \cdot 10^{-9})^2/4 = 10^{-8}/4$ which is negligible.

6. Stabilization of Operational Rectifier

To prevent high frequency oscillation a small capacitor is generally needed across the feedback resistor of an operational device. The resultant time constant places an upper corner frequency, F_h, having a direct bearing on the gain accuracy at some lower operating frequency, F_0. For large separation of the two frequencies, the asymptotic slope error is nearly $(F_0/F_h)^2 \cdot 10^6$, in ppm where $F_h = 1/2\pi R_f C_f$. The analysis is correct for a linear system; however in the rectifier configuration the capacitor is across both the feedback resistor and diode string resulting in a marked reduction of corner frequency, F_h which is difficult to calculate. Experience has shown that a series pair of 5 pF capacitors has been effective in stabilizing all amplifiers tested. However, this value of stabilizing capacitance can degrade the gain accuracy by 50 ppm at 20 kHz with a 5 kΩ feedback resistance.

7. Unity-Gain Input Isolation Amplifier Stage

The combination of the operational rectifier stage and filter stage is sufficient to meet the needs of most

average ac-dc transfer requirements. This system has an input impedance equal to the input resistor of the operational rectifier stage, typically 5 kΩ. In some cases this may be annoying because of the loading affect on a-c sources and a-c attenuators. For these reasons the effectiveness of an operational unity-gain impedance transforming circuit was investigated for use in applications where 100 ppm accuracy is sufficient.

The basic circuit is shown in figure 3. It is recognized as a noninverting amplifier with unity gain for the indicated input-output connection. Note that no precision resistors are involved in its operation and that it is able to take advantage of the high input impedance available with FET type differential devices—around 10^{11} Ω shunted by 3.5 pF of capacitance. In order for the stage to have the desired gain accuracy from d-c through the highest operating frequency, the selected operational differential amplifier must have both a wide-band high open loop amplification and a wide-band high common-mode rejection ratio, CMRR. The latter factor is a measure of the amplifier's ability to precisely respond only to the instantaneous amplitude difference value between the two input terminals; hence it desirably produces no output when both inputs are at the same potential and polarity. Analytically the CMRR of a differential amplifier is the ratio of a voltage V_m to the difference of the potentials at the two inputs required for a null output; expressed as

$$\text{CMRR} = V_n/[(V_n \pm e_+) - (V_n \pm e_-)]. \qquad (17)$$

Each of the terms in the denominator of (17) is an equivalent potential at each input consisting of a magnitude V_n and an apparent error potential, $\pm e$. For example if V_n is 1 V and the difference of the two equivalent input potentials is 0.001 V, the CMRR is 1000 : 1. Its polarity is a function of the polarity of the symmetry inperfections, e_+ and e_-. Writing circuit voltage loops, the transfer function of the stage is expressed as

$$V_{out}/V_{in} = \frac{1 \pm 1/\text{CMRR}}{1 + (\cos\theta - j \sin\theta)/A_f} \qquad (18)$$

The effect of wide band CMRR and A_f with phase lag that is greater than 90°, can be seen in figure 4 for three situations: (A) high CMRR and low A_f; (B) high A_f and low CMRR; (C) both CMRR and A_f are high. The figure is a plot from laboratory data on actual devices and corroborates and predicted behavior from expression (18) though the slope of curve (B) could have been lower for a minus polarity effect of the CMRR. The three devices shown in figure 4 are high-performance units, and the use of the terms "low A_f" or "low CMRR are in a relative sense, keeping in mind that the total ordinate value is less than 0.1 percent error.

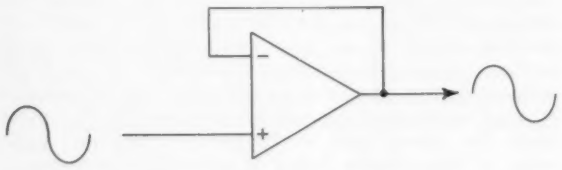

FIGURE 3. *Unity-gain isolation amplifier.*

The stage also has a desirable low output impedance—a dynamic impedance equal to the amplifier intrinsic output impedance divided by the value of A_f. A typical amplifier is capable of delivering ± 10 V output at 10^6 Hz, with a load current of 10 mA. In summary, the operational stage described is a rather elegant impedance transformer with an impedance ratio of at least 10^6: 1 operating from dc through 100 kHz with a gain accuracy of 200 ppm to at least 20 kHz.

8. Test Results

A large number of tests were performed involving a variety of operational amplifiers for use as precision rectifier, filter, and unity-gain impedance coupling stages. The tests could be grouped in three broad areas of interest: accuracy at a reference frequency, precision (stability and repeatability) and frequency response (ac-dc deviation).

8.1. Tests for Accuracy

The first group of tests were concerned with the accuracy of transformation of ac to dc by an operational rectifier; i.e., the relation between the average value of the output (half-wave) and the rms value of the input, with a voltage wave of very low distortion, so that $V_{ave} = V_{rms} \cdot \sqrt{2}/\pi$. The operational amplifiers available for these tests were of the chopper-stabilized type having very high open-loop amplification at frequencies below 5 kHz. Their d-c drift was less than 5 μv for periods of several hours. Oil-filled, wire-wound resistors matched to a few ppm in unity-ratio value were employed, with resistance values from 1 to 25 kΩ. The major components of the measuring system for these tests, shown in figure 5, included a low-distortion, highly stable a-c power source, (total harmonic distortion below 0.01%) a seven-dial calibrated, precision d-c power supply, a standards laboratory differential thermal voltage comparator (called a DTVC), [4] sensitive d-c null meter, and the average ac-dc converter under test. The magnitude of each harmonic of the source (up through the 9th) was measured. Its effect on the form factor of the voltage wave was calculated to be less than 10 ppm, assuming the worst possible phase angle with respect to the fundamental.

The standard was the rms responding DTVC unit, having the function of monitoring the sine-wave signal to be measured and matching it by null method to the d-c supply of the equivalent rms value. In turn the d-c supply was scaled down by a factor of $\sqrt{2}/\pi$, by the attenuator, and nulled against the d-c output of the average converter. The d-c difference is the error of

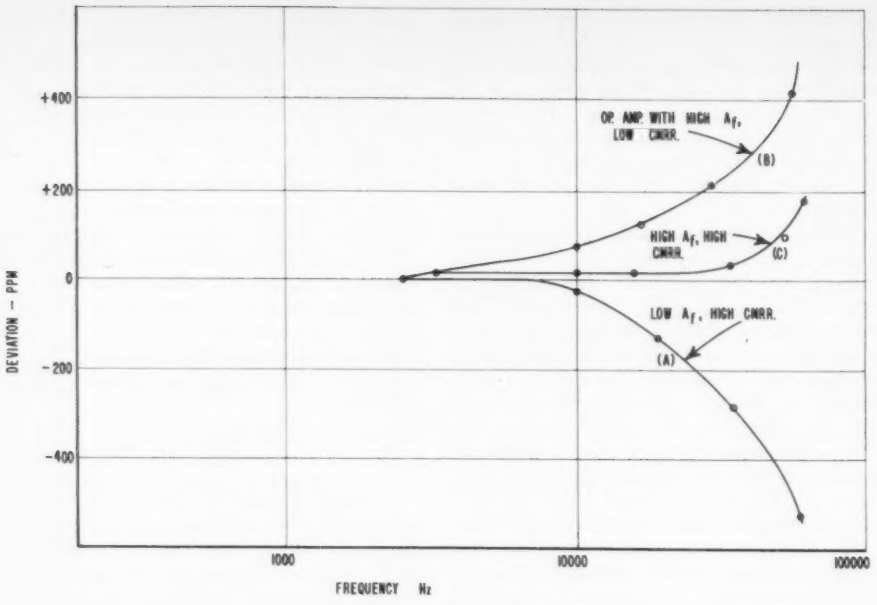

FIGURE 4. *Frequency response of figure 3.*

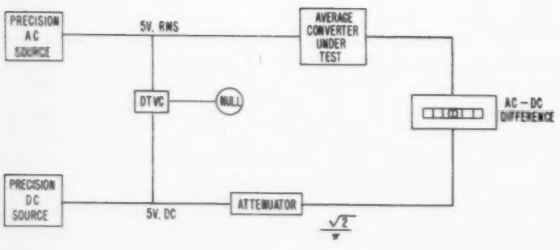

FIGURE 5. *Testing system.*

the device under test. Since the entire system has d-c response, scale factor inaccuracies at any position in the system could be checked by substituting the same d-c supply potential for the a-c signal (the average unit has identical input-output polarity correspondence). By using the same d-c supply as both signal and reference, its amplitude could be varied at will, allowing a check on dynamic range and on d-c offset. A 5 V rms a-c level was used in all the tests in order to avoid approaching the usual ± 10 V operational amplifier output limit. Operating voltages below 5 V are not recommended because most of the error factors discussed would be increased.

The results of these tests in figure 6 show that the operational rectification and filtering combination could yield a d-c voltage whose amplitude can be related to the rms value of a-c input with an accuracy of better than 20 ppm for frequencies out to 1000 Hz. At higher frequencies the accuracy was degraded because this was a feed forward type of amplifier. Short term perturbations of output were in the vicinity of 1 ppm, and possibly less.

These tests have demonstrated high accuracy performance at low and mid range audio frequencies. The next emphasis was on the design factors needed to extend the operating frequency range to 100 000 Hz and to include a high input impedance stage ahead of the rectifier.

8.2 Tests for Frequency Response

This group of tests involved the latest differential FET operational amplifiers having wide-band, high-value open-loop amplification figures. In addition, for reasons previously stated in the section on precision resistors, metal film resistance components were used in these tests. Since the question of measurement accuracy had been settled in the previously described group of tests, the test circuit arrangement was modified to demonstrate operational precision. Rather than employing the primary standard DTVC unit, a much simpler version of differential thermal comparator was used to monitor the output of the a-c signal power source for the purpose of maintaining constant amplitude. A peak ac-dc voltage comparator, though sensitive to waveform distortion, could be used in place of an rms comparator since an ac source of low distortion is specified. An in-depth analysis of the effects of ac distortion on the rectified average value can be found in reference [3]. For these tests the stress was on frequency response, exact value of magnitudes being of secondary importance. The recorded values were the measured differences

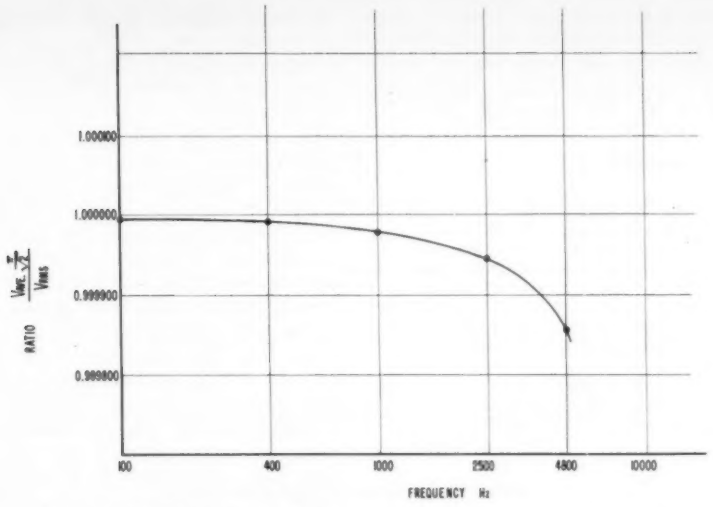

FIGURE 6. *Transfer accuracy of ac-dc converter (Chopper-stabilized amplifier).*

between the average d-c output and the fixed d-c reference power supply, expressed in ppm and plotted versus frequency. Normalizing the error values at some low frequency starting point is a means of removing the error offset due to any imprecision of resistor ratio and d-c offset at the amplifier stages.

The crosses in figure 7 show the test values obtained with an operational rectifier-filter combination which had metal film resistors.[2] Considering the number of instruments involved in the tests and their individual contribution to the end precision, the assignment of $\pm$ 150 ppm for the wide-band ac-dc error of the average measuring instrument is conservative. At the same time of the tests shown in figure 7, a unity-gain input isolation amplifier stage was added ahead of the operational rectifier state. In figure 7, the circles show the results of three runs; again all the values taken are plotted. Comparison of the circles and crosses shows that very little was changed in the response characteristic with the addition of the isolating amplifier. The benefit realized is substantial; the impedance presented to the a-c source increased from 5 kΩ to 10 MΩ. All frequency test points were within 200 ppm of the normalized value.

9. Some Wiring Suggestions

Circuit wiring, especially in the operational rectifier circuit should be short for minimum lead inductance and arranged in a manner for minimum shunt capacitance. One of the most critical points in the connection from the selected polarity output of the rectifier to the input resistor of the filter stage. Distortion of the half-sine wave resulting from shunt capacitance at this point could affect the accuracy of the average value.

[2] Four tests were made at each frequency, but were not separately plotted when the results differed by only small amounts.

It is strongly suggested the electronic circuit be d-c isolated from chassis ground. Removing the input and output common terminal from ground helps in eliminating the noisy effects of circulating d-c ground currents. Both a-c and d-c isolation can be had by a guarded circuit which offers low electrical capacity from the common terminals to chassis. This form of isolation requires a box-within-a-box type construction plus a special power supply. Such regulated supplies with a multi-shielded transformer are available with 10 000 megohm d-c insulation and 0.1 pF line-power input to d-c output isolation.

10. Initial D-C Offset Voltage Adjustments

After a sufficient warm-up period (usually 1 hr) the voltage offset of the filter stage is trimmed for zero output voltage with its input connection from the input resistor momentarily tied to common. The operational rectifier stage offset can be likewise adjusted by shorting to common the input side of the input resistor and trimming for zero output voltage. For this stage the diodes must be temporarily short-circuited. Effectiveness of input-output transfer of the instrument can be observed by applying some d-c value from 1 to 10 V to the input and comparing it to the instrument output by means of a null meter; the diode rectifier polarity output must be correctly selected. The d-c input-output agreement should be within the ratio accuracy of the resistors at the rectifier and filter stages.

11. Suggested Circuit

Figure 8 is a schematic diagram of a line-up of operational stages for use as an average ac-dc converting instrument. The circuit is capable of serving either the need for accuracy or for operational precision.

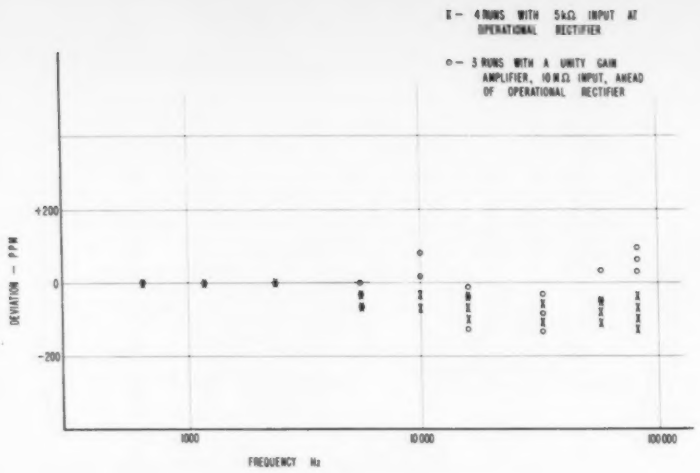

FIGURE 7. *Frequency response of converter.*

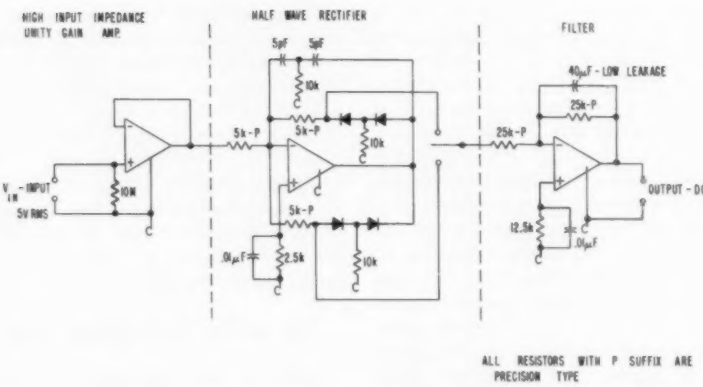

FIGURE 8. *Schematic diagram.*

If accuracy of 20 ppm is desired for ac-dc transfer, wherein the measured values can be related on an rms basis, the following points are pertinent. The high input impedance operational first stage must be deleted and the input signal applied to the second stage—the operational rectifier. The reason for this precaution is that the available amplifiers for use as a noninverting stage have marginal open loop gain and CMRR figures for accuracy work below 100 ppm. As for the rectifier stage, the selected operational amplifier must have a very high open loop gain and a low d-c drift. An open loop gain of 200 000 at 1 kHz is needed if the contributed error is to be less than 10 ppm. The voltage drift should be in the area of 1 μV/°C and 10^{-10} A/°C for the current drift. While differential FET type operational amplifiers come close to meeting these specifications, the accuracy results reported in this writing have been obtained with chopper stabilized devices. Because of their possible feed-forward design the 20 ppm operating accuracy is limited to frequencies below 1 kHz and the gain setting resistors at the rectifier stage are restricted to values of 1 kΩ or less. The latter components should have a ratio accuracy error of less than 5 ppm, available in oil filled, wire wound resistors. A signal level of 5 V rms at the a-c source is suggested. The a-c signal power source should have a total harmonic distortion of less than 50 ppm and freedom from a d-c component, if the rms value is desired. The operational amplifier at the filter stage need only have the stated d-c precision of the rectifier stage.

The three stages shown in figure 8 can offer an operating precision and flatness of amplitude response with frequency of better than 200 ppm over the range from d-c to 100 KHz, as described previously under the section heading of Test Results. FET-type differ-

ential operational amplifiers can be found to meet the requirements of each stage. If the sole interest is operational precision in the form of stability and repeatability, the principal concern in selecting the operational amplifiers is the d-c drift characteristics. However, the open loop voltage gain has to be considered in order to maintain the desired transfer gain ratio. With a voltage drift value below 10 μV/°C and a current drift under 10^{-10}A/°C the operating precision can be held to better than 100 ppm. For situations requiring accuracy of measurement or if flatness of amplitude response with frequency is important, the wide-band open loop voltage gain deserves additional attention. In the case of the noninverting first stage the CMRR figure is also important. If the input stage is to have a unity gain accuracy of 100 ppm at 5 kHz, both the open loop gain and the CMRR at that frequency should be at least 20 000 for the selected operational amplifier. For the rectifier stage the same values of 20 000 is needed at 5 kHz for 100 ppm accuracy but the CMRR can be neglected. The filter stage as usual need only have the stated d-c operating characteristics. Again, in the case of rms measurements of accuracy the a-c signal source must have appropriate purity—no more than 200 ppm total harmonic distortion for 100 ppm transfer accuracy.

12. References

[1] Richman, P., Operational Rectifier, U.S. Patent No. 3311835, March 28, 1967, assigned to Weston Instruments, Inc.

[2] Marzetta, L. A., A Peak AC–DC Voltage Comparator for Use in a Standards Laboratory, NBS Technical Note No. 280, issued January 17, 1966.

[3] Richman, P., Modern AC Voltage Calibration for Audio and Sub-Audio Frequencies, presented at 19th Annual ISA Conference, October 12–15, 1964, New York, Preprint No. 21, 4–2–64.

[4] Hermach, F. L., Griffin, J. E., and Williams, E. S., A System for Accurate Direct & Alternating Voltage Measurements, IEEE Trans. on Instrumentation & Measurement IM14 p215–224, 1965.

(Paper 73C3&4–288)

JOURNAL OF RESEARCH of the National Bureau of Standards—C. Engineering and Instrumentation
Vol. 73C, Nos. 3 & 4, July–December 1969

An Improved High-Precision Calibration Procedure For Reference Standard Hydrometers

Horace A. Bowman and William H. Gallagher

Institute for Basic Standards, National Bureau of Standards, Washington, D.C. 20234

(June 24, 1969)

This paper describes a method of calibrating hydrometers which, although no more accurate that the technique used heretofore at the National Bureau of Standards, reduces calibration time from several days to a few hours. The procedure is based upon easily measured hydrometer weight, stem scale geometry, and flotation level measurements at only one liquid density. The reliability of this single level is improved by observing the hydrometer flotation under various weight loads. The calibration experiment is oriented toward automatic data reduction so the finished calibration report is of much wider applicability than the simple correction table derived from the older experiment.

Key words: Calibration; density; hydrometer; hydrometer calibration; reference hydrometer; specific gravity; standard hydrometer.

1. Objectives and Results

There are two classes of hydrometers, which although identical in construction, differ significantly in their method of calibration and the use to which they are put. *Working hydrometers* are used extensively in science and industry for moderate precision measurements of liquid densities. *Reference standard hydrometers* are used exclusively for the calibration of working hydrometers using comparison techniques described in the appendix. These reference standard hydrometers are calibrated by comparing their observed flotation levels to bath densities independently determined by hydrostatically weighing solid object density standards.

The comparison experiment used in the past at NBS for calibration of reference standard hydrometers was fundamentally sound under specified conditions, but it was time-consuming and its range of applicability was restricted. Hydrometers were tested in the liquid in which they were to be used, and several baths of this liquid were prepared covering the density range shown on the hydrometer stem scale. It was difficult to obtain more than five such comparisons in a day, although the requirements of some calibrations were such that fifteen or more comparisons had to be performed. Additionally, if the hydrometer was to be used in a liquid of different surface tension, a different calibration was required.

We have devised a calibration procedure in which only one comparison bath is required which can be completed in less than three hours, and the data are of such form that corrections can be deduced for any (or all) points on the stem scale. Even though the hydrometer is to be used in fluids of radically different surface tension or temperature, additional calibration effort is not required.

This new procedure is based upon knowledge of the hydrometer weight and stem scale geometry (both easily measured to adequate accuracy) and knowledge of the level at which the hydrometer floats in *one bath* of known properties. Hydrometer flotation levels are observed to one-tenth scale division. In estimating tenths of divisions, most observers are biased for or against certain numbers, and when reading the same level repeatedly, they will usually continue to make the same estimate. As a result, multiple observations on the same level are little better than a single observation. To minimize such reading errors, only one observation is made on the freely floating hydrometer. Thereafter it is loaded by small weights, causing it to sink to lower levels, each of which is recorded. From knowledge of the weights and stem scale geometry it is possible to calculate independent values of the unloaded flotation level. Averaging the single observed value with the various calculated values provides a more reliable figure for the true flotation level of the unloaded hydrometer in the bath. This bath may be set up to have ideal properties such as transparency, surface tension, or any other characteristic considered important by the experimenter. The requirement is that it float the hydrometer near the lower end of its scale.

Based upon long standing custom the densities of different classes of fluids are measured on different scales of density; for example, oils are usually measured in "degrees API," alcohol in "percent of proof

spirit," and acids in "specific gravity." This has forced NBS to maintain an inventory of currently calibrated reference standard hydrometers whose scales are graduated in different systems but covering the *same density range*. Our new calibration procedure is oriented for automatic data reduction. This yields a byproduct. With appropriate computer instructions, we are able to obtain a table of scale corrections to convert readings into many other density scales without additional laboratory work, so a single calibration experiment of the type described can take the place of several of the older experiments.

The National Physical Laboratory [1] [1] calibrates its reference hydrometers by partially suspending them from a balance while floating in a xylene bath at some previously selected scale graduation. The bath density is measured by a special finely divided hydrometer. By varying the suspension length and the xylene level so that each cardinal point is examined, comparison between gravitational and buoyant forces provides the required correction.

2. The Calibration Experiment

There are four steps in the laboratory work demanded by the new procedure. As pointed out above, about three hours is required for completion.

1. The hydrometer is weighed on a laboratory balance to determine its apparent weight in air, $\bar{W}_H$, defined and discussed in section 4.

2. The hydrometer stem scale of N cardinal points is laid alongside a centimeter scale (actually a linear comparator, see fig. 1) and a table of values of L_1, L_2, L_3, . . . L_N is prepared indicating the distance of each cardinal point from some arbitrary zero reference. At the same time the distance to the upper tip of the hydrometer, L_T, is recorded.

3. An indicator micrometer, see figure 1, is used to measure the stem diameter at each cardinal point. Two measurements, 90° apart, are averaged and a table of values D_1, D_2, D_3 . . . D_N is prepared showing these average stem diameters.

4. The hydrometer is floated in a bath of density ρ, which is measured by hydrostatically weighing a solid-object density standard as discussed in section 4. The hydrometer flotation level is noted. After this, four (or more) hat-shaped objects of weights in air $\bar{W}_A$, $\bar{W}_B$, $\bar{W}_C$, and $\bar{W}_D$ are placed on the upper tip of the hydrometer, causing it to sink deeper into the bath. The flotation level with each hat in place is noted.

3. Data Recording and Reduction

Raw data are recorded on forms designed so that a typist can most conveniently transcribe them on a punched tape acceptable to the NBS ADP system and receive the finished calibration report from the printout. This requires about six minutes.

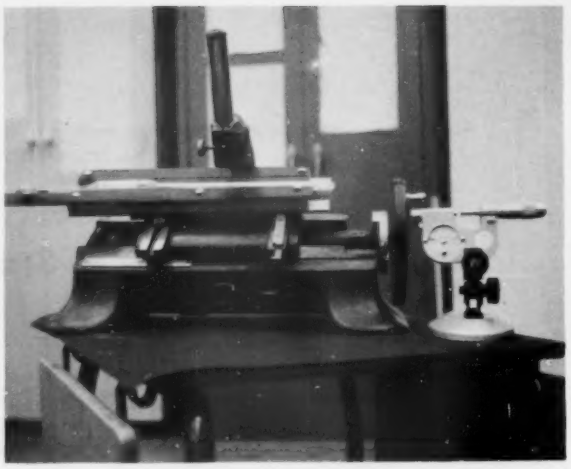

FIGURE 1. *The two devices used to measure hydrometer stem geometry.*

The linear comparator on the left is used to convert the stem scale graduations from density indications to linear distances. Stem diameters are measured by the indicator micrometer shown on the right.

The computer program is based upon the following arguments:

1. The five equilibrium flotation levels observed during the flotation tests (sec. 2.4) are observed on the hydrometer stem scale in terms of the scale units. These levels must be expressed in ordinary length units, centimeters. This is accomplished by interpolation in the table of centimeter equivalents prepared in section 2.2, after which we have L_0, L_A, L_B, L_C, and L_D representing the level in centimeters at which hydrometer flotation occurs with no hat, with hat A, with hat B, with hat C, etc. If the bath temperature is different from the room temperature during geometric measurements, then the geometric measurements are corrected to the bath temperature by suitable application of the thermal coefficient of expansion of the hydrometer.

2. By similar interpolation we obtain from the table of stem diameters (sec. 2.3) the stem diameter at each flotation level. Values of D_0, D_A, D_B, D_C, and D_D are the stem diameters at each of the five flotation levels—no hat, with hat A, with hat B, with hat C, etc.

3. We now calculate the average stem diameter between the "no hat" flotation level and each of the "with hat" levels. Values of $\bar{D}_A$, $\bar{D}_B$, $\bar{D}_C$, $\bar{D}_D$ are the average stem diameter between L_0 and L_A, between L_0 and L_B between L_0 and L_C, and between L_0 and L_D.

4. From knowledge of the surface tension of the test bath, γ, and the various stem diameters involved, we calculate the weight in air of the meniscus, m, which would form at each flotation level and cardinal point, thus

$$m = \frac{\pi D \gamma}{980}$$

[1] Figures in brackets indicate the literature references on page

where D is the stem diameter at the level of interest.[2] Meniscus weights at the various flotation levels are named m_0, m_A, m_B, m_C, and m_D depending upon the hat in use. At the cardinal points, they are labeled $m_1, m_2, m_3 \ldots m_N$.

5. The standard deviation of a single observation on the flotation level of a hydrometer may be as large as 1/4 mm when observing conditions are non-ideal. Step 2.4 in the experimental procedure yields only one value of the flotation level, L_0, of the hydrometer (by itself with no hat load) in the test bath. The objections to repeated observations of the same stem scale graduation to improve assurance were discussed above. We calculate an additional value of this flotation level from each of the "with hat" flotation level observations. These additional values are independent of the original observed value, and they are largely, but not entirely, independent of one another.

The flotation level under no load is taken under the following conditions of equilibrium, see figure 2:

$$M + m_0 - \rho V_0 - \rho_A (V - V_0) = 0 \qquad (1)$$

where M and V are the mass and volume of the hydrometer, ρ_A the air density, and V_0 is the immersed volume. The comparable equation of equilibrium for flotation when the hydrometer is loaded by hat "A" (with the hydrometer floating at stem level L_A) is given by

$$M + \bar{W}_A + m_A - \rho V_0 - \rho V_A - \rho_A (V - V_0 - V_A) = 0 \quad (2)$$

where V_A is the stem volume between L_0 and L_A. Subtracting eq (2) from (1) we get a value for V_A

$$V_A = \frac{\bar{W}_A + m_A - m_0}{\rho - \rho_A}. \qquad (3)$$

Based upon stem geometry we can write a different equation for V_A

$$V_A = \frac{\pi \bar{D}_A^2}{4} (L_0 - L_A) \qquad (4)$$

where $\bar{D}_A$ is the average stem diameter between L_0 and L_A. Equating (3) and (4) yields a new value of L_0, thus

$$L_0 = L_A - \frac{4(\bar{W}_A + m_A - m_0)}{\pi \bar{D}_A^2 (\rho - \rho_A)}. \qquad (5)$$

Using this procedure, we calculate a value of L_0 for each "with hat" observation and take the average to give the reference level, L; thus

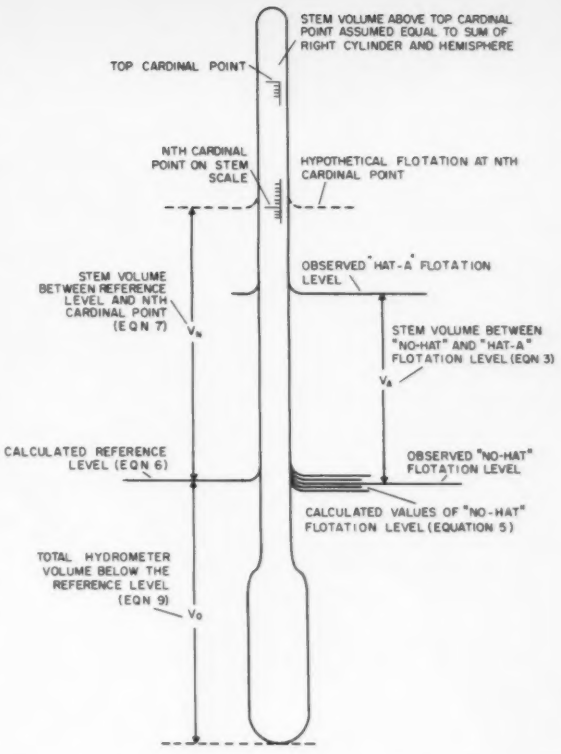
STEM VOLUME ABOVE TOP CARDINAL POINT ASSUMED EQUAL TO SUM OF RIGHT CYLINDER AND HEMISPHERE
TOP CARDINAL POINT
NTH CARDINAL POINT ON STEM SCALE
HYPOTHETICAL FLOTATION AT NTH CARDINAL POINT
OBSERVED "HAT-A" FLOTATION LEVEL
STEM VOLUME BETWEEN REFERENCE LEVEL AND NTH CARDINAL POINT (EQN 7)
V_N
STEM VOLUME BETWEEN "NO-HAT" AND "HAT-A" FLOTATION LEVEL (EQN 3)
V_A
CALCULATED REFERENCE LEVEL (EQN 6)
OBSERVED "NO-HAT" FLOTATION LEVEL
CALCULATED VALUES OF "NO-HAT" FLOTATION LEVEL (EQUATION 5)
TOTAL HYDROMETER VOLUME BELOW THE REFERENCE LEVEL (EQN 9)
V_0

FIGURE 2. *Various stem scale levels and volumes used in the data-reduction argument.*

$$L = \frac{L_0(\text{obs}) + L_0(\text{hat } A) + L_0(\text{hat } B) + L_0(\text{hat } C) + L_0(\text{hat } D)}{5}. \qquad (6)$$

The variability in these values of L_0 is mostly random and is associated with imperfect flotation and geometric observations.

6. We next calculate a table of stem volumes between the reference level, L, and each cardinal point on the stem scale. Values of V_1, V_2, $V_3 \ldots V_N$ are obtained from

$$V_N = \frac{\pi \bar{D}_N^2}{4} (L - L_N) \qquad (7)$$

where $\bar{D}_N$ is the average stem diameter between L and L_N.

7. Based upon our knowledge that the hydrometer floats at the reference level, L, under "no hat" conditions when test bath temperature, density and surface tension are t, ρ, and γ respectively, we can calculate a table of bath densities $\rho_1, \rho_2, \rho_3, \rho_4 \ldots \rho_N$ which will float the hydrometer at each of the N cardinal points under conditions of t and γ.

[2] If γ is a pure force, then m as defined here would be mass, not weight in air. However, air buoyancy is ignored in most surface tension measurements, so γ is usually an apparent force. If γ is a pure force, the meniscus weight in air is

$$\frac{\pi D \gamma}{980} \left[1 - \frac{\rho_A}{\rho}\right]$$

where ρ_A is air density and ρ the fluid density. For the average hydrometer, the difference between meniscus weight and mass is about 1 ppm of the hydrometer weight—insignificant in this experiment.

Equilibrium conditions for flotation at the reference level, L, are given by

$$m_0+(M-\rho_A V)-\rho V_0+\rho_A V_0=0 \qquad (8)$$

where V_0 is the hydrometer volume below L. As explained in section 4, the apparent weight in air of the hydrometer, $\bar{W}_H$, is given by $M-\rho_A V$. Making this substitution and solving for V_0 we get

$$V_0=\frac{\bar{W}_H+m_0}{\rho-\rho_A}. \qquad (9)$$

By similar reasoning we can write the equilibrium equation for flotation at L_N (the level of the Nth cardinal point)

$$M+m_N-\rho_N(V_0+V_N)-\rho_A(V-V_0-V_N)=0 \quad (10A)$$

$$\bar{W}_H+m_N-\rho_N(V_0+V_N)+\rho_A(V_0+V_N)=0. \quad (10B)$$

The immersed volume, V_i, is the sum of V_0 and V_N. Looking to eqs (7) and (9) for numerical values of V_0 and V_N, we get

$$V_i=V_0+V_N=\frac{\bar{W}_H+m_0}{\rho-\rho_A}+\frac{\pi\bar{D}_N^2}{4}(L-L_N). \qquad (11)$$

All terms in (14) represent vertical forces on the hydrometer, positive down. Inasmuch as we want the hydrometer to float at the *same* level (namely the Nth cardinal point) under both initial and final conditions, the sum of terms involving Δ (after expansion of (14)) must be held to zero.

Expanding (14) and subtracting (13) leaves

$$\Delta m_N-\rho_N\Delta V_i-\Delta\rho_N V_i-\Delta\rho_N\Delta V_i-\rho_A\Delta V_e=0 \qquad (15)$$

and

$$\Delta\rho_N=-\frac{\rho_N\Delta V_i+\rho_A\Delta V_e-\Delta m_N}{V_i+\Delta V_i}. \qquad (16)$$

Inasmuch as volumes are functions of temperature, and meniscus weight is a function of surface tension

$$\begin{aligned}\Delta V_i&=\alpha(T-t)V_i=\alpha(T-t)(V_0+V_N)\\ \Delta V_e&=\alpha(T-t)V_e=\alpha(T-t)(V-V_0-V_N)\\ \Delta m_N&=\frac{\pi D_N}{980}(\Gamma-\gamma)\end{aligned} \qquad (17)$$

where α is the volumetric coefficient of expansion of the hydrometer. Substituting values of the Δ terms in (17) back into (16) we get

$$\Delta\rho_N=-\frac{\alpha(T-t)[\rho_N(V_0+V_N)+\rho_A(V-V_0-V_N)]-\frac{\pi D_N}{980}(\Gamma-\gamma)}{(V_0+V_N)[1+\alpha(T-t)]}. \qquad (18)$$

With a numerical value of V_i from (11) we solve (10B) for ρ_N

$$\rho_N=\frac{\bar{W}_H+m_N+\rho_A V_i}{V_i}. \qquad (12)$$

8. Values of $\rho_1, \rho_2, \rho_3, \ldots \rho_N$ calculated in eq (12) are valid only when the flotation liquid is identical to the test bath in that it has the same temperature, t, and the same surface tension, γ. We must, therefore, construct a table of densities which will float the hydrometer at each of the N cardinal points under the general conditions of temperature, T, and surface tension, Γ.

Equation (10A) shows equilibrium conditions at the Nth cardinal point under t and γ. The exposed volume of the hydrometer, V_e, is given by

$$V_e=V-V_0-V_N.$$

Then from (10A)

$$M+m_N-\rho_N V_i-\rho_A V_e=0. \qquad (13)$$

Since altering t and γ of the bath will cause changes in m_N, ρ_N, V_i, and V_e, eq (13) becomes

$$M+(m_N+\Delta m_N)-(\rho_N+\Delta\rho_N)(V_i+\Delta V_i)-\rho_A(V_e+\Delta V_e)=0. \qquad (14)$$

From (10A) the bracketed term of the numerator of (18) is seen to be equal to $(M+m_N)$, so that

$$\Delta\rho_N=-\frac{\alpha(T-t)(M+m_N)-\frac{\pi D_N}{980}(\Gamma-\gamma)}{V_i[1+\alpha(T-t)]}. \qquad (19)$$

After selecting values for T and Γ, all terms on the right side of (19) are known,[3] and

$$R_N=\rho_N+\Delta\rho_N \qquad (20)$$

where R_N is the liquid density which will float the hydrometer at its Nth cardinal point when the liquid temperature is T and its surface tension is Γ.

If geometric measurements associated with this test are made in centimeters, air and sinker densities in grams per cubic centimeter, surface tensions in dynes per centimeter and weighings in grams, then all terms eq (20) will be in grams per cubic centimeter. If S_N is the numerical value engraved alongside the Nth cardinal point on the stem scale of the hydrometer, then

$$C_N=R_N-S_n \qquad (21)$$

[3] The procedure for obtaining a value of M in eq (19) from the balance observation is explained in section 4.

where C_N is the correction which will convert the Nth cardinal point into grams per cubic centimeter, *provided that* (a) the fluid in which the hydrometer floats is at temperature T and (b) has a surface tension of Γ. Violation of either condition will result in false values in eq (21).

Inasmuch as the ADP equipment is easily instructed to calculate tables of values of $\Delta\rho_N$, eq (19), for a wide selection of T's and Γ's, a correction table which is appropriate to any foreseeable set of conditions is conveniently available.

4. Use of The Balance

Observation of the hydrometer floatation level to 0.1 mm requires an experienced observer working under near-ideal circumstance. Such an observation represents a precision of only 5 in 10^4 of a typical 20-cm stem scale. In order to reduce calibration effort without degrading quality, we have eliminated from the calibration procedure most of these difficult and relatively low-precision measurements, and substituted in their place measurements of other hydrometer properties which can be made to a much higher order of precision with only a fraction of the effort.

The new calibration procedure relies strongly upon weight calculations based on balance observations. On modern single-pan direct-reading balances such determinations are easily made to parts per million. During the calibration it is necessary to determine the apparent weight in air of the hydrometer, $\bar{W}_H$, for use in eq (9), and it is also necessary to determine the apparent weight of the solid-object density standard while immersed in the test bath for calculation of ρ as explained below.

There are two other tasks which are easily performed on such balances which, although important to the hydrometer calibration, are not a part of the calibration procedure. The first task is the determination of the mass of the hats used in the calibration, and the second is the determination of the mass and volume of the solid-object density standard.

Bowman and Schoonover [2] have studied the performance of single-pan direct-reading balances in the above mentioned applications. The brief comments to follow are justified in their paper.

The apparent weight of an object in a medium is a force which is defined as the difference between the *downward* mass force exerted by the object and the *upward* buoyant force exerted on the object by the medium. Thus, in eq (9), the apparent weight in air of the hydrometer, $\bar{W}_H$, is given by

$$\bar{W}_H = M - \rho_A V$$

where M and V are the mass and volume respectively of the hydrometer, and ρ_A the air density at the instant of observation. Since air density is a parameter which is constantly changing with variations in barometric pressure, the temperature of the air, and its relative humidity (in that order of significance), it is necessary to measure these quantities and calculate ρA from

$$\rho_A = \frac{.464554B_A - H_A(.00252T_A - .020582)}{T_A + 273.16} \qquad (22)$$

where B_A, T_A, and H_A are the measured values of barometric pressure (in mm of mercury), temperature of the air (in °C), and relative humidity (in percent).

$\bar{W}_H$ is the force exerted on the balance pan by the hydrometer: however, for reasons explained in the Bowman-Schoonover paper, the balance observation, O_H, must be corrected to obtain $\bar{W}_H$

$$\bar{W}_H = (O_H + C_1)\left(1 - \frac{\rho_A}{\rho_s}\right) \qquad (23)$$

where C_1 is the true mass correction to the balance reading and ρ_s is the density of the built-in balance weights. C_1 and ρ_s may be obtained from the manufacturer, or the experimenter may obtain himself by techniques described by Mrs. Mildred Jones in the appendix to the above paper. The numerical value of $\bar{W}_H$ obtained from eq (23) is the value used in eq (9) in the basic data reduction.

The numerical value of M required in eq (19) may be obtained from this value of $\bar{W}_H$ and an estimate of V, and since $M = \bar{W}_H + \rho_A V$. V is adequately approximated by assuming that the tip volume of the hydrometer stem (fig. 2) is equal to the sum of a right circular cylinder and a hemisphere; thus

$$V = \left[\left(L_T - L_N - \frac{D_N}{2}\right)\left(\frac{\pi D_N^2}{4}\right) + \frac{1}{12}\pi D_N^3\right] + V_0 + V_N$$

where the bracketed term is the tip volume. For minimum error in this approximation, D_N, L_N, and V_N should be taken to refer to the top cardinal point on the stem scale.

If we know the mass and volume of an object by virtue of an independent experiment, we can combine this knowledge with a balance-determination of the object's apparent weight in a medium to obtain the density of the medium itself. This is the technique used to determine the density of the test bath, ρ, in eq (1). By a previous hydrostatic and air weighing we determine the mass, M_s, and volume, V_s, of the solid-object density standard. We now suspend the density standard in the test bath by a fine wire from the balance pan. From the foregoing arguments we know that the apparent weight of the density standard in its medium (that is, the test bath) is

$$\bar{W}_s = M_s - \rho V_s$$

where ρ is the bath density. Also, from (23), we know

$$\bar{W}_s = (O_s + C_2)\left(1 - \frac{\rho_A}{\rho_s}\right)$$

where C_2 is the true mass correction to the balance

reading, O_s. Equating the above two expressions for $\bar{W}_s$ and solving for ρ, we get

$$\rho = \frac{M_s - (O_s + C_2)(1 - \rho_A/\rho_s)}{V_s}. \quad (24)$$

Equation (24) provides a numerical value of ρ for use in the basic data reduction format described in the previous section.

5. The Calibration Report

Except in very unusual cases, a modern instrument calibration must contain more than a table of scale corrections. It should state as precisely as possible the conditions under which the calibration is valid and also the degree of validity. In addition to density, hydrometers are sensitive to the temperature and surface tension of the liquid in which they float, so all three parameters must be examined. Ignoring these two second-order variables results in a calibration of very limited applicability. Under such circumstances the hydrometer can be used only in liquids whose temperatures and surface tensions are equal to those of the test bath. Eq (17) introduce our best estimates of these extraneous effects into the calibration.

One sheet of the calibration printout is shown in figure 3. Each table provides scale corrections to each

SCALE READING	CORRECTIONS AT VARIOUS SURFACE TENSIONS 20 DY/CM	40 DY/CM	60 DY/CM	80 DY/CM
	DENSITY (G/CC)AT 25.2 DEG.C			
1.02	-9.485E-4	-2.479E-4	4.447E-4	1.137E-3
1.015	-7.553E-4	-6.44E-5	6.266E-4	1.318E-3
1.01	-6.686E-4	2.42E-5	7.17E-4	1.41E-3
1.005	-5.8E-4	1.105E-4	8.01E-4	1.492E-3
1	-5.627E-4	1.281E-4	8.19E-4	1.51E-3
.995	-5.473E-4	1.401E-4	8.275E-4	1.515E-3
.99	-5.567E-4	1.269E-4	8.105E-4	1.494E-3
.985	-5.719E-4	1.086E-4	7.89E-4	1.47E-3
.98	-6.017E-4	7.353E-5	7.488E-4	1.424E-3
.975	-6.28E-4	4.356E-5	7.152E-4	1.387E-3
.97	-6.642E-4	5.819E-6	6.759E-4	1.346E-3
.965	-7.116E-4	-4.563E-5	6.204E-4	1.286E-3
.96	-7.479E-4	-8.566E-5	5.765E-4	1.239E-3
.955	-8.059E-4	-1.462E-4	5.135E-4	1.173E-3
.95	-8.564E-4	-2.003E-4	4.557E-4	1.112E-3
	DENSITY (G/CC)AT 25.4 DEG.C			
1.02	-9.452E-4	-2.526E-4	4.4E-4	1.133E-3
1.015	-7.6E-4	-6.907E-5	6.219E-4	1.313E-3
1.01	-6.733E-4	1.955E-5	7.124E-4	1.405E-3
1.005	-5.847E-4	1.059E-4	7.964E-4	1.487E-3
1	-5.673E-4	1.235E-4	8.144E-4	1.505E-3
.995	-5.519E-4	1.355E-4	8.229E-4	1.51E-3
.99	-5.613E-4	1.223E-4	8.059E-4	1.489E-3
.985	-5.765E-4	1.04E-4	7.845E-4	1.465E-3
.98	-6.062E-4	6.902E-5	7.443E-4	1.42E-3
.975	-6.325E-4	3.907E-5	7.107E-4	1.382E-3
.97	-6.687E-4	1.357E-6	6.714E-4	1.341E-3
.965	-7.161E-4	-5.007E-5	6.159E-4	1.282E-3
.96	-7.523E-4	-9.007E-5	5.721E-4	1.234E-3
.955	-8.103E-4	-1.506E-4	5.091E-4	1.169E-3
.95	-8.607E-4	-2.047E-4	4.514E-4	1.107E-3
	DENSITY (G/CC)AT 25.6 DEG.C			
1.02	-9.499E-4	-2.573E-4	4.353E-4	1.128E-3
1.015	-7.647E-4	-7.374E-5	6.172E-4	1.308E-3
1.01	-6.779E-4	1.491E-5	7.077E-4	1.401E-3
1.005	-5.893E-4	1.012E-4	7.918E-4	1.482E-3
1	-5.719E-4	1.189E-4	8.098E-4	1.501E-3
.995	-5.565E-4	1.31E-4	8.184E-4	1.506E-3
.99	-5.658E-4	1.178E-4	8.013E-4	1.485E-3
.985	-5.81E-4	9.949E-5	7.8E-4	1.46E-3
.98	-6.107E-4	6.452E-5	7.398E-4	1.415E-3
.975	-6.37E-4	3.459E-5	7.062E-4	1.378E-3
.97	-6.731E-4	-3.105E-6	6.669E-4	1.337E-3
.965	-7.205E-4	-5.451E-5	6.115E-4	1.278E-3
.96	-7.567E-4	-9.449E-5	5.677E-4	1.23E-3
.955	-8.147E-4	-1.55E-4	5.047E-4	1.164E-3
.95	-8.651E-4	-2.091E-4	4.47E-4	1.103E-3

FIGURE 3. *One page of a multiple-page complete calibration.*

Since hydrometer response to density varies with both temperature and surface tension, a complete hydrometer calibration contains various columns to allow for changes in surface tension, and also it contains different tables for different temperatures.

cardinal point of the stem scale, reducing the observation to density in grams per cubic centimeter. The table is multi-columned in surface tension from 20 to 80 dynes per centimeter. To account for differences in hydrometer performance as a function of temperature, a separate table is given for each 0.2 °C over the temperature range for which calibration is required. This type of calibration report has the widest possible utility.

Occasionally a calibration is called for under very restricted conditions. Such a calibration is shown in figure 4. In this case, the hydrometer is asked to read in terms of one of the numerous specific gravity scales, namely S.G. (25/15.556 °C), which is defined as the quotient of the density of the liquid at 25 °C divided by water density at 15.556 °C. When such a calibration is requested, suitable computer instruction makes $T = 25$ °C and calculated densities divided by suitable water density values in the various data reduction equations. Again the calibration is multi-columned in surface tension inasmuch as the hydrometer user can rarely predict the surface tension of the liquid in which the hydrometer is to be used. As will be pointed out in the appendix, this may be a very unstable factor.

There are two classes of errors in the hydrometer calibration. The systematic errors associated with the test apparatus are assumed to be about equal in all NBS calibrations of this type. We can obtain an estimate of these errors by noting the change in the computed corrections when the various input data items are varied at the computer input by the estimated uncertainty in each. Table 1 shows that the effect of these errors is about 0.00005 S.G.

As previously explained, we believe the random errors in the calibration to be fairly well indicated by the scatter of the five values of L in eq (6). For the calibration shown in figure 4, this amounts to a standard deviation of 0.000075 S.G.

NATIONAL BUREAU OF STANDARDS
MASS AND VOLUME SECTION
9 / 7 / 68

CALIBRATION OF KNEK 260 HYDROMETER AT (25 / 15.556)

SCALE READING	CORRECTIONS AT VARIOUS SURFACE TENSIONS 20 DY/CM	40 DY/CM	60 DY/CM	80 DY/CM
1.02	6.79E-5	7.612E-4	1.454E-3	2.148E-3
1.015	2.483E-4	9.399E-4	1.632E-3	2.323E-3
1.01	3.302E-4	1.024E-3	1.717E-3	2.411E-3
1.005	4.139E-4	1.105E-3	1.796E-3	2.488E-3
1	4.263E-4	1.118E-3	1.809E-3	2.501E-3
.995	4.368E-4	1.125E-3	1.813E-3	2.501E-3
.99	4.224E-4	1.107E-3	1.791E-3	2.475E-3
.985	4.022E-4	1.083E-3	1.765E-3	2.446E-3
.98	3.675E-4	1.043E-3	1.719E-3	2.395E-3
.975	3.362E-4	1.008E-3	1.681E-3	2.353E-3
.97	2.95E-4	9.657E-4	1.636E-3	2.307E-3
.965	2.426E-4	9.093E-4	1.576E-3	2.243E-3
.96	2.014E-4	8.642E-4	1.527E-3	2.19E-3
.955	1.383E-4	7.987E-4	1.459E-3	2.119E-3
.95	8.287E-5	7.396E-4	1.396E-3	2.053E-3

TEST CONDITIONS:
BATH TEMP= 25.63 DEG C
SURFACE TENSION= 30.52 DY/CM
AIR DENSITY= 1.161E-3 GRAMS/CC
BATH DENSITY= 1.01721 GRAMS/CC
CALC.REF.LEVELS: 17.5311 17.5432 17.5141 17.5859 17.5194
AVERAGE VALUE REFERENCE LEVEL= 17.5231
CALCULATED BULB VOLUME= 44.64 CC
CALCULATED STEM VOLUME = 3.29286 CC
ESTIMATED TIP VOLUME= .468146 CC
HYDROMETER MASS= 45.4639 GRAMS

Estimate random error in this particular calibration from standard deviation of these five values.

σ = 0.015 CMS (.000075 S.G.)
3σ = 0.045 CMS (.00022 S.G.)

FIGURE 4. *Calibration (25/15.556 °C), a specific gravity scale which is valid only at 25 °C.*

A partial calibration is adequate if the hydrometer will always be used at some known temperature.

364-586 O - 69 - 2

TABLE 1.

Input Data Item	Estimated uncertainty in input data item**	Calibration error (Spec. Grav.)	Square of calibration error
Air density	1 $\mu g/cm^3$	5×10^{-6}	25×10^{-12}
Bath temperature	0.01 °C	2.3×10^{-6}	6×10^{-12}
Hydrometer weight	100 μg	0	0
Stem diameter	127×10^{-6} cm	19×10^{-6}	361×10^{-12}
Sinker mass*	30 μg	3×10^{-6}	9×10^{-12}
Sinker volume*	0.0001 cm^3	10×10^{-6}	100×10^{-12}
Sinker weight in bath*	100 μg	2×10^{-6}	4×10^{-12}
Hat mass	10 μg	$.15 \times 10^{-6}$	0
Surface tension of bath	1 dyne/cm	35×10^{-6}	1225×10^{-12}
TOTAL			1733×10^{-12}
ESTIMATED UNCERTAINTY			42×10^{-6}

*The sinker is the solid-object density standard referred to in the text.
**These uncertainties are assumed to apply to all NBS calibrations made on this type of equipment.

As a matter of interest, figure 5 shows a graph of a hydrometer calibration in S.G. (15.556/15.556 °C) with the calibration performed by both the old and new techniques. The four parallel curves are the plot of the table of corrections predicted by the new procedure at four levels of surface tension. The data upon which these curves are constructed are based upon a single flotation experiment at point "A" in the lower right-hand corner of the graph. In the upper right corner is a sulfuric acid calibration with a surface tension of about 75 dynes per centimeter, and an oil and gasoline calibration is shown at the 30 dynes per centimeter level. A single-point alcohol flotation is indicated at 45 dynes per centimeter. In these classical calibrations, each open circle represents a complete flotation experiment—equal in experimental effort to the flotation experiment at point "A." In other words, in the situation illustrated here, 22 flotation experiments were required for the old calibration (each open circle), but for the new method, only one such experiment was performed (at point "A").

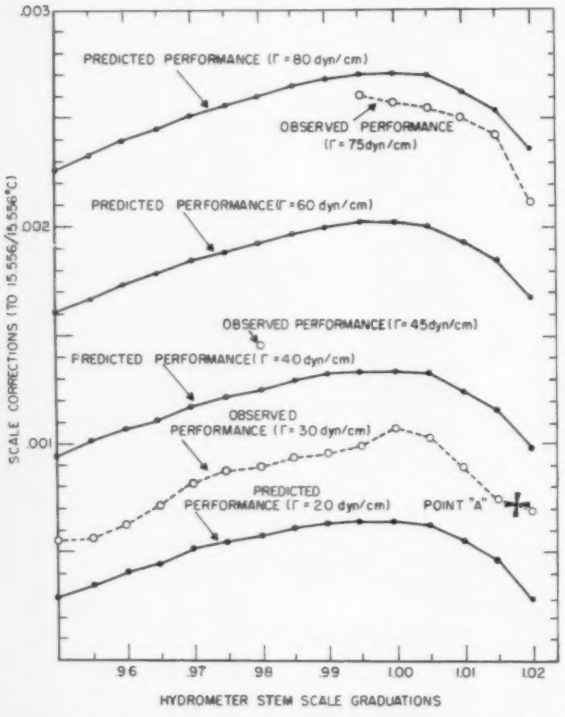

FIGURE 5. *Hydrometer scale corrections obtained by both the old and new calibration procedure.*

The density scale used is SG/60/60 °F). The solid black dots connected by solid lines represent the scale corrections predicted by the computer program at four levels of surface tension. These points are all based upon data taken in the *single* flotation experiment at point "A," the cross in the lower righthand corner. The open circles represent individual flotation experiments taken in liquids of various surface tensions and densitites using the older calibration procedure.

Many Bureau people assisted us in this work. Miss Geraldine Hailes was largely responsible for programming a very awkward data reduction scheme. Roy H. Wampler devised a procedure for converting alcohol densities into other scales. Dr. Daniel P. Johnson checked out the physical validity of the arguments presented.

6. References

[1] Rands, J. B., and Bigg, P. H., Hydrometers and hydrometry, NPL Applied Science Note No. 25 (1961).
[2] Bowman, H. A., and Schoonover, R. M., Procedure for high precision hydrostatic weighing, J. Res. NBS **71C**, No. 3 (1967).

Appendix A. Use of a Reference Standard to Calibrate a Working Instrument

1. Apparatus

One glass cylinder approximately seventeen (17) inches long and two (2) inches in diameter; a suitable test liquid.

2. Test Liquids

Hydrometers should be calibrated in the liquids in which they are to be used; if this is not possible, a liquid should be selected which has the same, or nearly the same, surface tension. The liquids in the following table are suggested as suitable, although any liquid of proper density and surface tension may be substituted. Intermediate densities may be obtained by mixing:

Liquids	*Range*
Mineral oil	0.62 to 1.00
Ammonia	.85 to 1.00
Common salt	1.00 to 1.23
Hydrochloric acid	1.00 to 1.25
Caustic soda	1.00 to 1.55
Nitric acid	1.00 to 1.55
Sulfuric acid	1.00 to 1.85
Thoulet solution (K_2HgI_4)	1.84 to 3.00
Ethanol and water	0.750 to 1.000

3. Preparation

(a) Cleanliness.

The accuracy of hydrometer observations depends upon the cleanliness of the instruments and of the liquids in which the observations are made. Extra care should be taken to keep the liquid surface free of contamination.

In order that readings shall be uniform and reproducible, the surface of the hydrometers, and especially of the stem, must be clean, so that the liquid will rise uniformly and merge into an imperceptible film on the stem.

The readiness with which this condition is fulfilled depends somewhat upon the character of the liquid. Certain liquids, such as mineral oils and strong alcoholic mixtures, adhere to the stem very readily. On the other hand, with weak aqueous solutions of sugar, salts, acids, and alcohol, scrupulous cleaning of the stem is required in order to secure the normal condition.

Before being tested, hydrometers may be thoroughly cleaned by dipping in a mixture of one part concentrated sulfuric acid and two parts fuming sulfuric acid, rinsed with water, and dried by wiping with a clean, lint-free cloth; or they may be washed with soap and water, dried, and wiped with a cloth moistened with alcohol to remove any residual soap film. The stems can usually be kept clean during testing by wiping with alcohol (preferably absolute) and drying before each reading.

In many liquids spontaneous changes in surface tension occur due to the formation of surface films of impurities, which may come from the apparatus, the liquid, or the air. In order to avoid the errors due to these changes, the liquid surface could be cleaned with a vacuum hose or the liquid in the cylinder could be caused to overflow just prior to reading the hydrometer.

The necessity for such special manipulation is confined to the reading of hydrometers in liquids that are subject to surface contamination. Such, in general, are aqueous solutions or mixtures of acids, alkalies, salts, sugars, and weak alcohol mixtures. Oils, alcoholic mixtures of strength above 40 percent by volume, and other liquids of relatively low surface tension are not, in general, liable to surface contamination sufficient to cause appreciable changes in hydrometer readings.

(b) Temperature.

In order that a hydrometer may indicate correctly the density or strength of a specified liquid, it is essential that the liquid be uniform throughout and at the temperature specified on the instrument. If an observation is made at some other temperature than that for which the hydrometer is designed, the reading will be in error. The magnitude of the error will depend upon the thermal expansion of the hydrometer and, in some cases, of the liquid used.

If the latter properties are known, tables of corrections for temperature may be prepared for use with hydrometers at various temperatures. Such tables should be used with caution, and only for approximate results when the temperature differs much from the standard temperature or from the temperature of the surrounding air. (See table 28, NBS Circular C19.)

Publications in which temperature correction tables may be found are listed below.

Liquid	*Publication*
Ethyl alcohol	NBS Circular 19; Gauging Manual, 1938, U.S. Treasury Department, Bureau of Internal Revenue.
Petroleum oils	NBS Circular 19; ASTM–IP Petroleum Measurement Tables.
Sulfuric acid solutions	NBS Circular 19.
Sugar solutions	NBS Circulars 19 and 440.
Vegetable tanning extracts	NBS Circular 449.
Turpentine	NBS Technical Paper 9.

In comparing two hydrometers having the same standard temperature and made of the same type of glass, the temperature of the liquid need not be considered, since the correction required due to variation from standard temperature is the same for both instruments. But the temperatures of the liquid, the hydrometers, and the surrounding atmosphere should be nearly equal during the observation; otherwise, the temperature of the liquid will be changing, causing differences in density. To insure uniformity in the liquid, thorough mixing is required shortly before making the observation. This may be accomplished with a perforated disk or spiral at the end of a rod long enough to reach the bottom of the cylinder. Motion of this stirrer from top to bottom serves to disperse layers of the liquid of different density.

4. Test Procedure

(a) Pour into the cylinder a sufficient amount of the appropriate test liquid to float the hydrometer. Pour the liquid slowly down the side of the cylinder to avoid the formation of air bubbles.

(b) Stir the liquid, avoiding the formation of air bubbles. Make sure the liquid is approximately at room temperature.

(c) Immerse the standard hydrometer in the liquid slightly beyond the point where it floats naturally, then allow it to float freely.

(d) Observe a point slightly below the plane of the liquid surface and then raise the line of vision until this surface, seen as an ellipse, becomes a straight line. The point where this very fine line cuts the hydrometer scale is the reading of the instrument. Holding a white card behind the cylinder just below the liquid level will improve the visibility of the surface.

(e) Immerse the hydrometer to be tested as outlined in item (c), read the hydrometer as outlined in item (d).

(f) Again, read the standard hydrometer as outlined in items (c) and (d).

(g) Average the standard readings and apply scale corrections, supplied by NBS, to the average standard reading.

(h) The difference between the average corrected standard reading and the reading of the hydrometer being tested will be its correction at that point on the scale.

(Paper 73C3&4–289)

JOURNAL OF RESEARCH of the National Bureau of Standards—C. Engineering and Instrumentation
Vol. 73C, Nos. 3 & 4, July–December 1969

The Nuclear Quadrupole Resonance Magnetometer: A New Method for the Precision Measurement of the Magnitude and Direction of Magnetic Fields

Melvin Linzer

Institute for Materials Research, National Bureau of Standards, Washington, D.C. 20234

(September 11, 1969)

A theoretical investigation of the feasibility of a magnetometer based on the observation of the Zeeman splitting of a nuclear quadrupole resonance line is presented. With a single crystal of potassium chlorate as the sensor, an nqr magnetometer with center frequency of 28 MHz and bandwidth of 10 MHz could cover a range of 10 nT to greater than 1 T. Precision at specific crystal orientations should approach 10 nT in the magnitude of the field, at flux densities exceeding 100 μT, and (65/B) microradians in the direction of the field where B is the flux density in mT. If circularly polarized rf excitation is employed, a precision of 10 nT could be achieved at flux densities less than 100 μT. Accuracy of the flux density measurements is limited by the uncertainty in the gyromagnetic ratio of ^{35}Cl, which at the present time is approximately 1×10^{-4}. The effect of the small asymmetry parameter which characterizes the ^{35}Cl resonance in $KClO_3$ is analyzed. Various experimental arrangements are proposed to record the magnitude and direction of the field, to obtain high resolution at low fields and good linearity at high fields, to overcome the difficulties due to the presence of a small asymmetry parameter, and to make an instantaneous measurement of the Zeeman splitting frequency.

Key words: Magnetometer; nuclear quadrupole resonance.

1. Basic Theory

This paper presents a theoretical investigation of the feasibility of a magnetometer based on the observation of the Zeeman splitting of a nuclear quadrupole resonance (nqr) line. A detailed treatment of the Zeeman effect can be found in the monograph of Das and Hahn [1],[1] in the papers quoted therein, and in several subsequent publications [2–8]. We shall confine ourselves in this section to a discussion of the theory relevant to Zeeman splittings in single crystals and its application to the measurement of the magnitude and direction of magnetic fields. The nuclei will be assumed to be characterized by an asymmetry parameter, η, equal to zero. Moreover, the quadrupole energy will be considered sufficiently greater than the Zeeman energy such that the Zeeman splitting is essentially linear with respect to the magnetic field.

Special emphasis will be placed on the $|1/2| \leftrightarrow |3/2|$ transitions; these are responsible for the ^{35}Cl nqr spectrum in potassium chlorate ($KClO_3$), which, as will be shown later, is very suitable for magnetic field measurements. The effect of the small asymmetry parameter in $KClO_3$ is discussed in the next section.

Transitions between the $\pm m$ and $\pm(m+1)$ levels, with $m \geq 1$, give rise to two frequencies spaced symmetrically about the pure quadrupole frequency, ν_Q, with separation

$$\Delta\nu = 2\nu_L \cos\theta$$

$$\nu_L = \frac{|\gamma| B_0}{2\pi}$$

where ν_L is the Larmor frequency, $|\gamma|$ is the absolute value of the gyromagnetic ratio, B_0 is the magnetic flux density, and θ is the angle between the magnetic field and the symmetry axis of the electric field gradient [1]. The intensities of the two lines are one-half the intensity of the original line and are independent of the orientation of the magnetic field.

For transitions between $\pm 1/2$ and $\pm 3/2$ levels, two pairs of splittings are in general observed because of the zeroth-order mixing of the $\pm 1/2$ states in the presence of a magnetic field.[2] The energy level diagram is shown in figure 1 for the case applicable to the ^{35}Cl spectrum in $KClO_3$. When $\eta = 0$ and $\nu_L \rightarrow 0$,

[1] Figures in brackets indicate the literature references at the end of this paper.

[2] For convenience, we have labeled the four quantum states as $\pm 1/2$, $\pm 3/2$. The conventional designation of the $\pm 1/2$ levels in the presence of a small magnetic field is "$\pm$"; at flux densities sufficiently great to cause an appreciable admixture of all the levels, a different notation is usually employed [9].

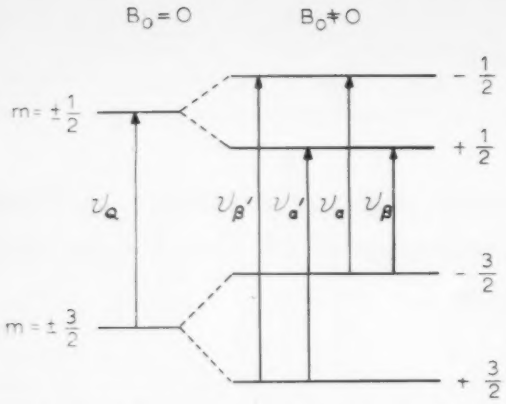

FIGURE 1. *Low-field energy level diagram for the $|1/2| \leftrightarrow |3/2|$ transitions of a nucleus with half-integral spin, negative quadrupole coupling and positive gyromagnetic ratio.*

The use of the quantum numbers $\pm m$ to designate the states in the case $B_0 \neq 0$ is for convenience only.

the splittings are symmetrical about the pure quadrupole frequency, with the inner pair of lines, denoted by $\alpha\alpha'$, always equal to or stronger in intensity than the outer pair of lines, denoted by $\beta\beta'$. The splittings and relative intensities are given by the equations [1]:

$$\Delta\nu_{\alpha\alpha'} = |3-f|\nu_L \cos\theta,\ I_{\alpha\alpha'} = (f+1)/2f$$
$$\Delta\nu_{\beta\beta'} = (3+f)\nu_L \cos\theta,\ I_{\beta\beta'} = (f-1)/2f$$
$$f \equiv [1+(I+1/2)^2 \tan^2\theta]^{1/2}$$

and are shown in figures 2 and 3, respectively. The α components correspond to the transitions $\pm 1/2 \leftrightarrow \pm 3/2$, whereas the β components arise from the transitions $\mp 1/2 \leftrightarrow \pm 3/2$.

Simplified spectra are obtained at three special orientations of the magnetic field. At $\theta = 0°$, only the splitting of the α components is observed with $\Delta\nu_{\alpha\alpha'} = 2\nu_L$. The β components give rise to twice this splitting but have zero intensity at this orientation. At $\theta = 90°$, the α and β components have identical intensities and splittings, with $\Delta\nu_{\alpha\alpha'} = \Delta\nu_{\beta\beta'} = (I+1/2)\nu_L$. At $\theta = \tan^{-1}[2\sqrt{2}/(I+1/2)]$, the splittings are given by

$$\Delta\nu_{\alpha\alpha'} = 0$$
$$\Delta\nu_{\beta\beta'} = 6(I+1/2)\nu_L/[8+(I+1/2)^2]^{1/2}.$$

For $I = 3/2$, θ and $\Delta\nu_{\beta\beta'}$ are equal to 54°44′ (one-half of the tetrahedral angle) and $2\sqrt{3}\ \nu_L$, respectively. The separation between α and β components is therefore $\sqrt{3}\ \nu_L$ at this orientation.

Because of their simplified spectral patterns, these special orientations are easily obtained experimentally. All three alinements give comparable line separations, with maximum splittings between adjacent lines appearing at $\theta = 0°$ and 90°.

Deviations from linearity with respect to the magnitude of the magnetic field depend very strongly on the orientation of the symmetry axis. These deviations may be expressed in terms of a power series [9] in ξ, where $\xi = \nu_L/\nu_Q$ is the ratio of the Larmor frequency to the pure quadrupole frequency and is considered to be much less than one. At $\theta = 0°$, both the α and (vanishing) β component splittings are exactly linear with the field. For the $\theta = 54°44'$ configuration, the β splitting is approximately equal to $2\sqrt{3}\ (1-\xi^2/3)$ but the composite α line is merely broadened by $\sim\xi^4$. At $\theta = 90°$, the fractional deviation is $-3/2\ \xi^2$ for the α splitting and zero for the β splitting.

The Zeeman splittings of the lines are least sensitive to angle at $\theta = 0°$ and most sensitive at $\theta = 90°$. Inspection of figure 2 reveals several large regions of almost uniform slope for the splittings. Values of $|d\Delta\nu/d\theta|$ as well as other pertinent characteristics of the α and β components are given in table 1 for the three special orientations.

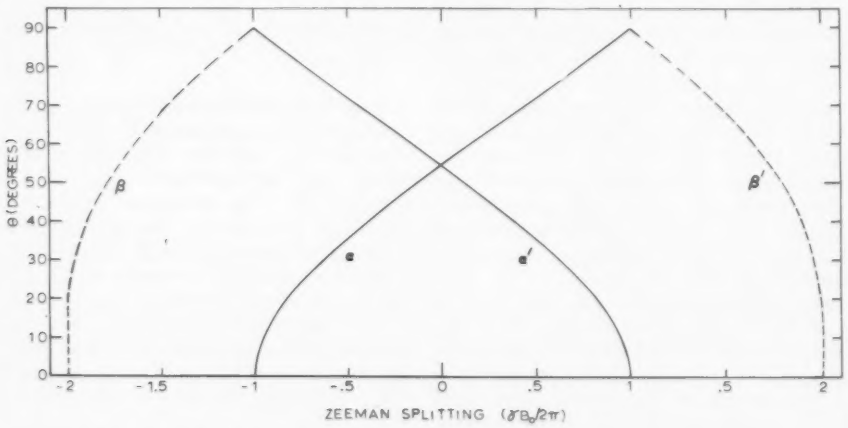

FIGURE 2. *Low-field Zeeman splittings for $|1/2| \leftrightarrow |3/2|$ transitions in the case $\eta = 0$.*

The $\alpha\alpha'\beta\beta'$ notation corresponds to the situation depicted in figure 1.

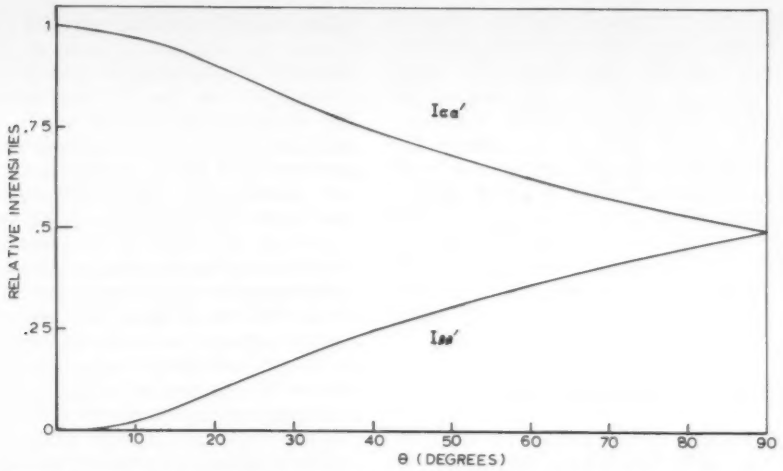

FIGURE 3. *Relative intensities of the low-field Zeeman components for $|1/2| \leftrightarrow |3/2|$ transitions with $\eta = 0$.*

TABLE 1. *Low-field Zeeman parameters of $|1/2| \leftrightarrow |3/2|$ transitions with $\eta = 0$ for three special orientations of the magnetic field with respect to the symmetry axis*

θ	0°		54°44′		90°	
line components	$\alpha\alpha'$	$\beta\beta'$	$\alpha\alpha'$	$\beta\beta'$	$\alpha\alpha'$	$\beta\beta'$
$\Delta\nu(\nu_L)$	2	4	0	$2\sqrt{3}$	2	2
Relative intensity	1	0	2/3	1/3	1/2	1/2
Fractional departure of $\Delta\nu$ from linearity	0	0	$\sim \xi^{4*}$	$-\xi^2/3$	$-3\xi^2/2$	0
$\lvert d\Delta\nu/d\theta\rvert (\nu_L/\text{radian})$	0	0	$\sqrt{3}+1$	$\sqrt{3}-1$	3	3

*Broadening

A measurement of the α and β splittings corresponding to a single orientation of the symmetry axis is sufficient to yield both θ and B_0. The field direction is then determined to be somewhere on the surface of a right circular cone making the angle θ with respect to the field-gradient axis. To ascertain the exact spatial alinement of the field, three non-equivalently oriented symmetry axes are required.

At magnetic fields for which the Zeeman splittings are comparable to or less than the linewidth, the α and β components will overlap each other. When the field direction is known, a measurement of the breadth or shape of the composite line will furnish the flux density. In principle, such a determination could be made to a precision approaching that of a measurement of the splitting frequencies in a resolved spectrum. A major disadvantage, however, is the complex dependence of linewidth and lineshape on flux density and the need to calibrate this dependence for the particular crystal under study. An analogous and perhaps more difficult problem would be encountered in the measurement of field direction at low flux densities.

At low fields, special care must be taken to insure that the amplitude of the oscillating rf field, B_1, is much less than the static field intensity, B_0. Otherwise, the splittings will be increased [10] by a fractional amount $(B_1/2B_0)^2$.

An nqr magnetometer is incapable of determining the polarity of the magnetic field unless circularly polarized excitation is employed. Depending on the sign of the gyromagnetic ratio and the polarity of the field, this type of rf field distribution will eliminate the lines arising from transitions involving either pure $+m$ or $-m$ states [11]. Furthermore, the correction term $(B_1/2B_0)^2$ in the Zeeman splittings will be absent, since it arises from the circularly rotating component of a linearly polarized field which is ineffective in producing transitions to or from a particular m state.

Circular polarization also serves to simplify the observed spectrum. In the case of the $|1/2| \leftrightarrow |3/2|$ transitions, the complex four-line pattern, $\alpha\alpha'\beta\beta'$ is reduced to either α, β or α', β' components. This is due to the fact that although the $\pm 1/2$ states are admixed to zeroth order in the presence of a field, the $\pm 3/2$ states remain relatively pure m states as long as $\xi \ll 1$. Thus, as can be seen from figure 2, the overlap which occurs at angles close to 90° or 54°44′ is eliminated and improved accuracy results.

Because the β components vanish as θ approaches 0°, measurements of the $\alpha\beta$ splittings made with circularly polarized radiation will be limited to those angles at which the β components are sufficiently intense. On the other hand, the α component (and observable β component) splittings may be measured separately by switching the direction of polarization or by subjecting two crystals to counter-rotating rf fields. At low fields, these techniques should also make it possible to obtain the splitting between the composite α, β and α', β'

lines. Thus, the necessity of determining the width or shape of the resonance line, and the corresponding problems associated with the dependence of these parameters on temperature gradients (see below) are avoided. For arbitrary crystal orientation, however, accurate field measurements will still be difficult because the composite lines are in general asymmetrical due to the different intensities of the α and β components. This problem does not exist if θ is equal to 0° or if the transitions $\pm m \leftrightarrow \pm (m+1)$, with $m \geq 1$, are studied. Under these circumstances, only one line will be observed for each direction of polarization, thereby eliminating the overlap and improving the resolution at very low magnetic fields.

2. The Potassium Chlorate Sensor

The foregoing discussion demonstrates that Zeeman splittings in nqr can yield information regarding the magnitude and direction of a magnetic field. Thus, in principle, an nqr spectrometer with a properly chosen sample can function as a magnetometer. To examine the usefulness of this technique, we shall consider the case of a single crystal of potassium chlorate. This compound has several desirable features which make it a suitable sensor for this application. The ClO_3^- ions in the unit cell are completely equivalent with regard to their resonant behavior in an external magnetic field. The unsplit ^{35}Cl resonance line occurs at an experimentally convenient frequency of 28.1 MHz at room temperature and is characterized by an asymmetry parameter close to zero ($\eta \sim 0.005$),[3] and one of the narrowest widths of any quadrupole line yet observed [12]. The first derivative curve in the single crystal was found to have a peak-to-peak linewidth of only 0.29 kHz and exhibited partially resolved Zeeman splittings in fields estimated to be considerably less than earth's field [12].

At $\theta = 0°$, one set of lines is obtained in $KClO_3$ with a splitting parameter of $\frac{2\gamma(^{35}Cl)}{2\pi} = 8.350$ kHz/mT. For this orientation, a linewidth of 0.29 kHz is equivalent to 3.5 μT in field units. Assuming a measurement of the line center to 1/500 of the linewidth, the splitting of two completely resolved lines in a uniform field at $\theta = 0°$ could be determined to a precision of approximately $\sqrt{2}(3.5)/500$ μT, or 10 nT. This precision can be achieved at flux densities exceeding 100 μT and at lower fields if circularly polarized excitation is employed. Similarly, at $\theta = 90°$, the limit of detection of changes in angle can be shown to be approximately $(65/B_0)$ microradians, where B_0 is expressed in mT.

The uncertainty in the absolute value of the flux density will be determined either by the precision of the measurement or by our knowledge of the gyromagnetic ratio of ^{35}Cl in $KClO_3$. The value of $\gamma(^{35}Cl)$ used here is taken from a measurement of the nuclear moment in $NaClO_3$ of 0.8215 ± 0.0001 nuclear magnetons [9]. This is equivalent to a gyromagnetic ratio of $(\gamma/2\pi) = 4.175 \pm 0.0005$ kHz/mT. It is reasonable to assume that the diamagnetic shielding of the chlorine nucleus in the sodium and potassium compounds is identical, at least to the accuracy given above. The chemical shift anisotropy is also expected to be negligible. For the ^{35}Cl nucleus in $NaClO_3$, Kawamori and Itoh [13] report a fractional difference between the shielding at the $\theta = 0°$ and 90° orientations of only $4 \pm 4 \times 10^{-5}$, in good agreement with a calculation neglecting the effect of the cation.

It would be preferable to make a direct measurement of the angular dependence of the gyromagnetic ratio of the ^{35}Cl in $KClO_3$. The ultimate accuracy which can be achieved with the nqr magnetometer will then be determined by the uncertainty in the gyromagnetic ratio of the particular reference sample used to calibrate the magnetic field. At the present time, the primary standard is the gyromagnetic ratio of the proton resonance in liquid water which is known to an accuracy of $\sim 6 \times 10^{-6}$ [14]. This figure also represents the minimum uncertainty attainable with nmr, epr, and Rubidium magnetometers since these too require a measurement of the gyromagnetic ratio of the resonating species used in the sensor.

Next we consider the effect of the small field-gradient asymmetry in $KClO_3$ on the splitting frequencies. Although the value $\eta = 0.005$ is only approximate, it will be used in the following calculation to furnish a rough estimate of the deviations from the equations given in section 1.

At $\theta = 0°$, exact solutions for the energy levels obtain [9]. The corresponding splitting frequencies are

$$\Delta\nu_{\alpha\alpha'} = 2\nu_L$$

$$\Delta\nu_{\beta\beta'} = 2\nu_Q\{[(1+2\xi)^2+\eta^2/3]^{1/2} - [(1-2\xi)^2+\eta^2/3]^{1/2}\}$$

$$\simeq 4\nu_L(1-\eta^2/6) \qquad (\xi, \eta \ll 1).$$

The splitting of the α components is exactly the same as in the case of zero asymmetry and shows no departure from linearity with respect to the magnetic field. The correction term for the zero-intensity β components is $-\eta^2/6$ or 4×10^{-6} for $KClO_3$.

At an arbitrary angle, the frequencies for small η are given by the equations [1]

$$\Delta\nu_{\alpha\alpha} = \nu_L|[\cos^2\theta + \sin^2\theta\ (4+\eta^2-4\eta\cos^2\phi)]^{1/2} - (9\cos^2\theta+\eta^2\sin^2\theta)^{1/2}|$$

$$\Delta\nu_{\beta\beta'} = \nu_L\{[\cos^2\theta + \sin^2\theta\ (4+\eta^2-4\eta\cos^2\phi)]^{1/2} + (9\cos^2\theta+\eta^2\sin^2\theta)^{1/2}\}$$

where ϕ is the azimuthal angle of the magnetic field referenced to the axis in the principal axis system along which the field gradient has its minimum value.

The deviations of the Zeeman splittings from the zero asymmetry case become more pronounced as θ approaches 90°. At this angle, the above equations reduce to

$$\Delta\nu_{\alpha\alpha'} = 2\nu_L[1-\eta/2(\cos 2\phi + 1) + \eta^2/8]$$

[3] This value has been slightly modified from that reported in reference 12 by the use of the correct value of the slope $d\Delta\nu_{\alpha\alpha'}/d\theta$ at $\theta = 54°44'$, rather than the value appropriate to $\theta = 90°$.

$$\Delta\nu_{\beta\beta'} = 2\nu_L[1-\eta/2(\cos 2\phi - 1)+\eta^2/8].$$

Maximum deviation of the α splitting from the zero asymmetry case occurs at $\phi = 0°$ and is equal to $-\eta$ or -0.005 for $KClO_3$. At $\phi = 90°$, the frequency differs from $2\nu_L$ by a negligible amount, $\eta^2/8$. The deviations of the β splittings cover the same range, but the maximum in $+\eta$ and occurs at $\phi = 90°$. Thus if ϕ is unknown, the measured value of the magnetic field can be in error by as much as $|\eta|$.

The cos 2ϕ terms in the above equations may be eliminated by rapidly spinning the crystal about the major axis of the field gradient or by orienting the crystal at $\phi = 45°$. The effect of a non-zero asymmetry parameter is then determined primarily by the terms $\mp(9\cos^2\theta + \eta^2\sin^2\theta)^{1/2}$ and decreases rapidly with θ. For example, at $\theta = 88°$, the deviations are approximately equal to $\mp 5\times10^{-5}$, down from $\mp 2.5\times10^{-3}$ at $\theta = 90°$. The entire term $(9\cos^2\theta + \eta^2\sin^2\theta)^{1/2}$ can be made to vanish if the α, β splittings, $\Delta\nu_{\alpha\beta}$ or $\Delta\nu_{\alpha'\beta'}$, or the average value of the α and β splittings,

$$(\Delta\nu_{\alpha\alpha'} + \Delta\nu_{\beta\beta'})/2,$$

are used to measure the field. Indeed, at angles sufficiently close to 90° to cause appreciable line overlap, it is easier to determine the average than the individual splittings. For the true average to be obtained, however, it is imperative that the composite line be symmetrically split or broadened. This condition implies approximately equal intensities for the α and β components at $\theta \simeq 90°$ and will occur for $\eta \neq 0$ only if the rf field is alined midway between the two minor axes of the field gradient [4] or if the crystal is rotated rapidly about the major axis. These probe configurations are unnecessary, however, if circular polarization is employed. In this case the α, β or α', β' splittings may be observed directly without overlap except at very low fields.

By combining a measurement of $\Delta\nu_{\alpha\beta(\alpha'\beta')}$ or $(\Delta\nu_{\alpha\alpha'} + \Delta\nu_{\beta\beta'})/2$ with sample spinning or a crystal alinement of $\phi = 45°$, the effect of the small asymmetry parameter in $KClO_3$ will be virtually eliminated. The maximum deviation from the zero asymmetry case then occurs at $\theta = 90°$ and is equal to $\eta^2/8$ or 3×10^{-6}.

At high fields, terms in ξ and cross-terms in ξ and η must be included in the expressions for the splittings. When $\xi \gg \eta$, the departures from linearity with respect to the field may be derived from the equations of Ting, Manring, and Williams [9] for the case $\eta = 0$ and have been given in table 1 for the three special orientations. The maximum deviation from linearity is of the order ξ^2 and is approximately 1 percent at 1 T for the $KClO_3$ crystal. In the intermediate region, $\xi \sim \eta$, the field dependence of the splittings can be obtained by numerically diagonalizing the Hamiltonian matrix. Closed-form solutions for any value of ξ have been given [7], however, for the special cases $\theta = 90°$, $\phi = 0°$, 90°.

In conclusion, the simplified equations of section 1 may be applied to the ^{35}Cl spectrum in $KClO_3$ when (1) θ is equal to 0°, or (2) the field is sufficiently low and the procedures described earlier are taken to eliminate the terms in η. If these conditions are not met and if the simple equations do not yield sufficient accuracy, then corrections due to finite η and ξ can be made.

For the $KClO_3$ sensor, departures from linearity with respect to the field are essentially negligible in the region where the nqr magnetometer is expected to have its greatest utility, namely, below 10 mT. At these fields, conventional nmr magnetometers suffer from a very poor signal-to-noise ratio and epr techniques are generally employed for accurate measurements [15]. An nqr magnetometer with $KClO_3$ as the sensor has decided advantages over both the nmr and epr techniques in its ability to sense the direction of the magnetic field and in not requiring major instrumental changes to measure widely different fields. In addition, it can go to much lower fields than is possible with epr magnetometers using currently available sensors, and has much greater accuracy in the low field regime.

3. Experimental Methods

Among the outstanding features of the nqr magnetometer is the wide range of magnetic fields that can be measured with essentially a single-frequency spectrometer and one probe, with all the concomitant advantages of convenience, sensitivity, and compactness. For example, with potassium chlorate as the sensor, a 28-MHz spectrometer with an 8 MHz bandwidth can cover the entire range of roughly 10 nT to 1 T.

Because of the strong temperature dependence of quadrupole frequencies (5.1 kHz/°C for $KClO_3$ at room temperature [16]), an instantaneous recording of the Zeeman splitting to a high degree of precision is desirable. A magnetometer possessing this capability will also make possible the rapid measurement of the direction and magnitude of an unknown field, as well as fast fluctuations in these quantities. One way of accomplishing this is shown schematically in figure 4. An amplitude- or frequency-modulated spectrometer is employed. The center frequency of the spectrometer is swept until it locks to the midpoint of one line and the separation of an AM or FM sideband is simultaneously varied until locking is achieved to the other line. The frequency of the low-frequency oscillator which amplitude or frequency modulates the carrier is then locked to, and exactly equals, the Zeeman splitting. Alternatively, a signal-feedback technique may be employed to yield self-oscillation at the splitting frequency.

At low magnetic fields, a linewidth measurement, rather than a splitting frequency, may be required. The locking technique just described can be used to determine this quantity if the resonance curve has at least two zero crossover points symmetrically situated with respect to the line center. The second-derivative absorption or first-derivative dispersion shape function has this property and is easily observed experimentally.

If the circularly polarized configuration is employed at low fields, the splitting may be determined by rapidly switching the direction of polarization in a

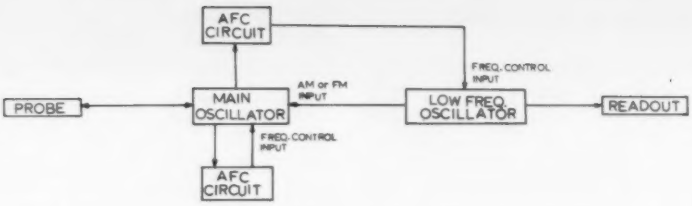

FIGURE 4. *Magnetometer circuit suitable for observation of the instantaneous values of the Zeeman splittings.*

time short compared to the time it takes for the sample temperature to drift or the static field to change. Alternatively, two sensors with oppositely rotating circularly polarized fields will give an instantaneous readout of the splitting frequency.

An instantaneous recording of the Zeeman splitting will obviate the necessity of thermostating the sample to a high degree or of accurately determining the temperature at which the measurement was made. Although the pure quadrupole frequency and asymmetry parameter depend strongly on temperature [1], the splitting will be relatively insensitive to temperature if η and ξ are much less than one. In the case of $KClO_3$, changes in the vibrational frequencies of the ClO_3^- ion with temperature will affect both the field gradient and asymmetry parameter to the order of 10^{-4}/°C at room temperature. From the equations given earlier, the splittings can be seen to be most sensitive to temperature at the $\theta=90°$ orientation. At low fields, the temperature dependence of the α or β splittings is at most $d\eta/dT \simeq 10^{-4}$/°C for the static crystal, $\phi \neq 45°$, configuration and decreases rapidly as θ deviates from 90°. At high fields, the splitting frequencies also exhibit a variation with temperature because of their dependence on ξ^2. For the case $\theta=90°$, and $B_0=$ IT, the change in the α splitting due to this effect is $3\xi^2(d\nu_Q/\nu_Q)dT \simeq 10^{-5}$/°C.

Even if these variations are tolerable, some degree of temperature stabilization is always desirable. In the first place, large temperature instabilities introduce noise in the frequency-locking circuitry and may even cause the system to lose lock. Secondly, a temperature gradient over the sample will broaden the lines and thus adversely affect the precision of the measurement.

Temperature stabilization might also be necessary at low fields when lineshape or linewidth studies are employed for the field measurements. In this case, accuracy as well as precision would suffer from the presence of temperature gradients and changes in the gradients. If the sample is at uniform temperature, however, temperature drifts would have little effect as long as the widths of the individual resonance lines are insensitive to temperature. This condition is satisfied by the ^{35}Cl spectrum in $KClO_3$ [11, 17]; thus, drifts in sample temperature would change the width of the composite line by a mere $d\eta/dT \simeq 10^{-4}$/°C in the worst case ($\theta=90°$, $\phi=0°$ or 90°).

Both the magnitude and direction of a magnetic field can be obtained with a sensor composed of either three orthogonally oriented crystals, one crystal containing at least three nonequivalently oriented symmetry axes with one axis out of the plane of the other two, or variants of these. Alternatively, a single crystal can be mounted on a goniometer assembly and its position adjusted to yield the pattern characteristic of a given orientation.

If changes in field direction are expected to be small, a single crystal configuration with θ set close to 0° may suffice in may applications. In this case, the magnetometer would respond to changes in the magnitude of the field but be relatively insensitive to its direction. For the $|1/2| \leftrightarrow |3/2|$ transitions, this configuration has the additional advantages of furnishing α component signals with maximum intensity and minimum overlap and with splittings which are independent of η, ξ, and temperature.

Time-dependent variations in the magnitude and direction of a magnetic field can be studied by combining the appropriate sample configuration with the instantaneous recording method outlined above. Sophisticated systems can be developed to give separate digital readouts of both these parameters.

Finally, the precision and range of an nqr magnetometer could be considerably improved upon by the use of line-sharpening techniques. In one such method [18], resolution enhancement is achieved by mixing the resonance line with a suitable combination of its higher derivatives.

4. References

[1] Das, J. P., and Hahn, E. L., Nuclear Quadrupole Resonance Spectroscopy, Solid State Physics, Supplement 1 (Academic Press, 1958).
[2] Casabella, P. A., and Bray, P. J., J. Chem. Phys. **28,** 1182 (1958).
[3] Casabella, P. A., and Bray, P. J., J. Chem. Phys. **29,** 1105 (1958).
[4] Toyama, M., J. Phys. Soc. Japan **14,** 1727 (1959).
[5] Morino, Y., and Toyama, M., J. Chem. Phys. **35,** 1289 (1961).
[6] Greschishkin, V. S., and Ainbinder, N. E., Sov. Phys.-Solid State, **3,** 1325 (1961).
[7] Greschishkin, V. S., and Ainbinder, N. E., Sov. Phys.-Solid State, **3,** 2175 (1962).
[8] Negita, H., J. Chem. Phys. **44,** 1734 (1966).
[9] Ting, Y., Manring, E. R., and Williams, D., Phys. Rev. **96,** 408 (1954).

[10] Bloch, F., and Siegert, A., Phys. Rev. **57,** 522 (1940).
[11] Weber, M. J., and Hahn, E. L., Phys. Rev. **120,** 365 (1960).
[12] Zeldes, H., and Livingston, R., J. Chem. Phys. **26,** 5 (1957).
[13] Kawamori, A., and Itoh, J., J. Phys. Soc. Japan **18,** 1614 (1963).
[14] 12th Report of Advisory Committee on Electricity, BIPM, 1968 (unpublished).
[15] Ingram, D. J. E., Spectroscopy at Radio and Microwave Frequencies, pp. 286–289, 2nd Ed. (Plenum Press, 1967).
[16] Utton, D. B., J. Res. Nat. Bur. Stand. (U.S.), **71A** (Phys. and Chem), No. 2, 125 (1967); Utton, D. B., Metrologia **3,** 98 (1967).
[17] Weber, M. J., J. Phys. Chem. Solids **17,** 267 (1961).
[18] Allen, L. C., Gladney, H. M., and Glarum, S. H., J. Chem. Phys. **40,** 3135 (1965); S. H. Glarum, Rev. Sci. Instr. **36,** 771 (1965).

(Paper 73C3&4–290)

JOURNAL OF RESEARCH of the National Bureau of Standards—C. Engineering and Instrumentation
Vol. 73C, Nos. 3 & 4, July–September 1969

Optical FM System for Measuring Mechanical Shock

L. D. Ballard and W. S. Epstein,

Institute for Basic Standards, National Bureau of Standards, Washington, D.C. 20234

E. R. Smith,

Harry Diamond Laboratories, U.S. Army Materiel Command, Washington, D.C., 20438

and

S. Edelman

Institute for Materials Research, National Bureau of Standards, Washington, D.C. 20234

(August 13, 1969)

A technique is described for calibrating shock accelerometers by measuring the Doppler shift in light frequency produced by the change in velocity of a target. The system employs a quadrature laser interferometer and a single-sideband carrier insertion circuit to distinguish between positive and negative velocities.

Key words: Accelerometer; calibration; Doppler; interferometer; laser; shock measuring; single-sideband.

1. Introduction

Shock loading may be one of the most destructive or most beneficial environments encountered by mechanical systems. The damage to structures by sudden loads, such as produced by the collision of objects, is familiar. The forming of materials into desired shapes by forging or explosive forming techniques are examples of desirable effects of controlled impact, or shock loading.

There is a demonstrated need to measure shock loads accurately over a wide range of amplitudes and wave forms. The design of structures to withstand such loads and the efficient use of energy for forming materials are only two of the more obvious benefits of a knowledge of shock loadings and their effects.

One of the problems in measureing mechanical shock has been the inability to calibrate shock measuring systems absolutely except by subjecting them to intense, steady state, sinusoidal motion at a few discrete frequencies. Such calibrations are inherently suspect because they are not characteristic of the environment to be measured, and transducers are frequently damaged during such tests. Sinusoidal calibrations of this nature offer the added difficulty that the tests are very time consuming and expensive.

Shock measuring transducers can also be calibrated by measuring lumped response integrated over the total energy spectrum with no attempt to determine response as a function of frequency. An example of this type of calibration is a peak value calibration where the transducer is subjected to a shock input and calibrated as to the peak reading obtained. The calibration comes from either a reference transducer or computed accelerations via measuring velocity changes over finite time intervals. There is a need for a fast, accurate and absolute method for calibrating shock measuring systems under conditions closely simulating those encountered in actual use [1–7].[1]

2. Shock Measuring System

An interferometer system has been devised to provide an absolute calibration facility for measuring shock induced motion. This system produces an electrical signal that is directly proportional to the velocity of the moving element being studied. This signal can be processed, analyzed and compared to the signal from a transducer that is subjected to the same motion. The system has the following advantages: (1) it is a system completely independent of the transducer, (2) it is based on the Doppler shift of light frequency detected by a moving interferometric fringe pattern, a phenomenon that is known to be linear with velocities

[1] Figures in brackets indicate the literature references at the end of this paper.

in the range of the mechanical shock spectrum, (3) it is capable of measuring actual shock motion having a wide range of amplitudes and rich in frequency content, and (4) the resulting signal can be rapidly and accurately analyzed by known methods and techniques [8].

2.1. Theory

The moving reflector of an optical interferometer is attached to the object whose motion is to be measured. A narrow section of the fringe pattern is viewed by a photodetector; if the interferometer plates are uncoated the photodetector output is [9].

$$E_1 = A + E_0 \sin [k(\delta + 2\xi)] \tag{1}$$

E_1 = output voltage

E_0 = signal out, dependent upon light intensity

A = d-c term

$k = 2\pi/\lambda$

λ = wavelength of monochromatic light

δ = average optical separation between interfering light beams

ξ = displacement of reflector

If we had, instead of eq (1)

$$E_2 = A + E_0 \sin [\omega t + k(\delta + 2\xi)] \tag{2}$$

ω = carrier frequency

which is a frequency modulated wave [10], the velocity of the reflector could be obtained by demodulation. The output of a demodulator is proportional to the instantaneous frequency deviation and the instantaneous frequency in eq (2) is

$$f_1 = \frac{1}{2\pi}\frac{d}{dt}[\omega t + k\delta + 2k\xi] = \frac{\omega}{2\pi} + \frac{2\dot{\xi}}{\lambda} \tag{3}$$

Therefore, the instantaneous frequency will define what the instantaneous velocity is. Equation (3) could have been obtained by direct application of doppler shift equation [11].

If E_1 in eq (1) were demodulated directly, or even after up-conversion of the frequencies, the sign of the output would be ambiguous. The problem is therefore to insert a carrier into E_1 of eq (1) and convert it to E_2 of eq (2).

2.2. Description

The interferometer used in the present work is a commercial model shown schematically in figure 1. It is a modified Michelson type, illuminated by a single-frequency He-Ne laser so that long path differences are possible. The moving retroreflector is a corner cube for the usual reasons. The interfering beams are circularly polarized so that by use of a beam splitter and analyzers, followed by two photodetectors, two electrical outputs in phase quadrature are obtained. The original purpose of this arrangement is for fringe counting [12]. The instrument has internal preamplifiers of bandwidth DC to 500 kHz; for higher velocity external preamplifiers of bandwidth 20 Hz to 60 MHz were used.

If one output is described by eq (1), which we rewrite, dropping the constant A and replacing $k(\delta+2\xi)$

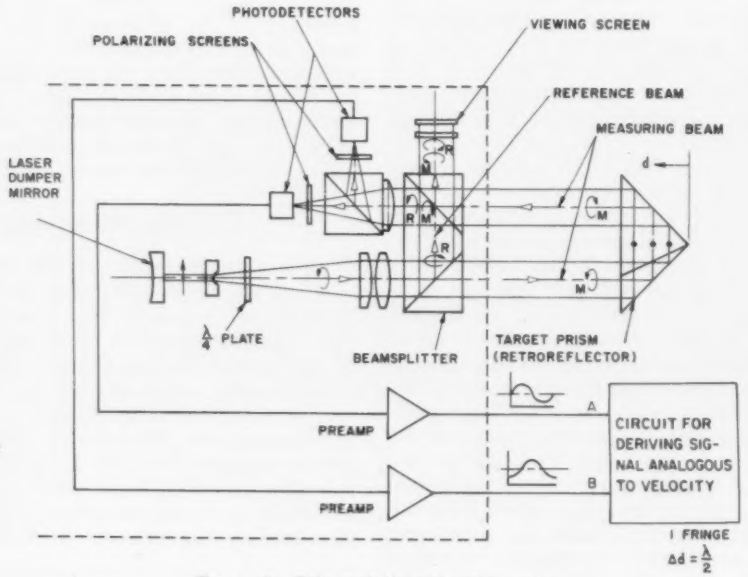

FIGURE 1. *Schematic, laser interferometer.*

by x, as

$$E_A = C \sin x$$

then the other is

$$E_B = C \cos x.$$

The signal E_B is multiplied, in a balanced mixer by the output $D \sin \omega t$ of a local oscillator, giving

$$CD \sin \omega t \cos x, \tag{4}$$

and E_A is multiplied, in another balanced mixer, by $D \cos \omega t$, giving,

$$CD \cos \omega t \sin kt \tag{5}$$

the outputs (4) and (5) are added in a suitable circuit to give

$$CD \sin (\omega t + x) = CD \sin [\omega t + k(\delta + 2\xi)] \tag{6}$$

which is the frequency-modulated wave of eq (2). As already explained, demodulation of this wave yields an output proportional to the velocity of the reflector.

The above method is similar to the phase-shift method of single-sideband generation [13] with the distinct difference that the signal phase shift is produced optically.

The single-sideband circuit was assembled from off-the-shelf hardware of balanced mixers, quadrature hybrid, FM demodulator and carrier oscillator. The carrier used in this case is 60 MHz. The signal is demodulated by a conventional FM discriminator, and the resulting signal can be analyzed by either digital or analog techniques.

The system can be readily calibrated by subjecting the moving element to steady state sinusoidal motion. One technique that has been used involves counting interference fringes over a known time interval. Average and peak velocities can then be computed for the frequency of vibration. Other methods for calibrating the system, such as the Crosby method for determining peak FM swing, could also be used. [14, 15, 16] Inherent in the system is a possible means of checking the calibration factor during the course of each experiment. The calibration factor can be determined by comparison of the average velocity over a known time interval, during which there are no velocity reversals, with the average discriminator output over the same interval. The former is the displacement, determined from a fringe count, divided by the time interval.

3. Performance

To obtain data an accelerometer was attached directly to the face of a corner cube retroreflector. The accelerometer was small enough to fit in a quadrant of the corner cube so as not to interfere with the laser beams. The moving corner cube of the interferometer was mounted on the table of an electrodynamic shaker. The input signal to the shaker was a single sine pulse (301 Hz) repeated at a rate of 75.3 Hz. Qualitative comparisons of signals obtained from various subsystems can be made from figures 2a, b, and c. Figure 2a shows the signals from the discriminator of the interferometer system and from the accelerometer. Figure 2a shows the signals from

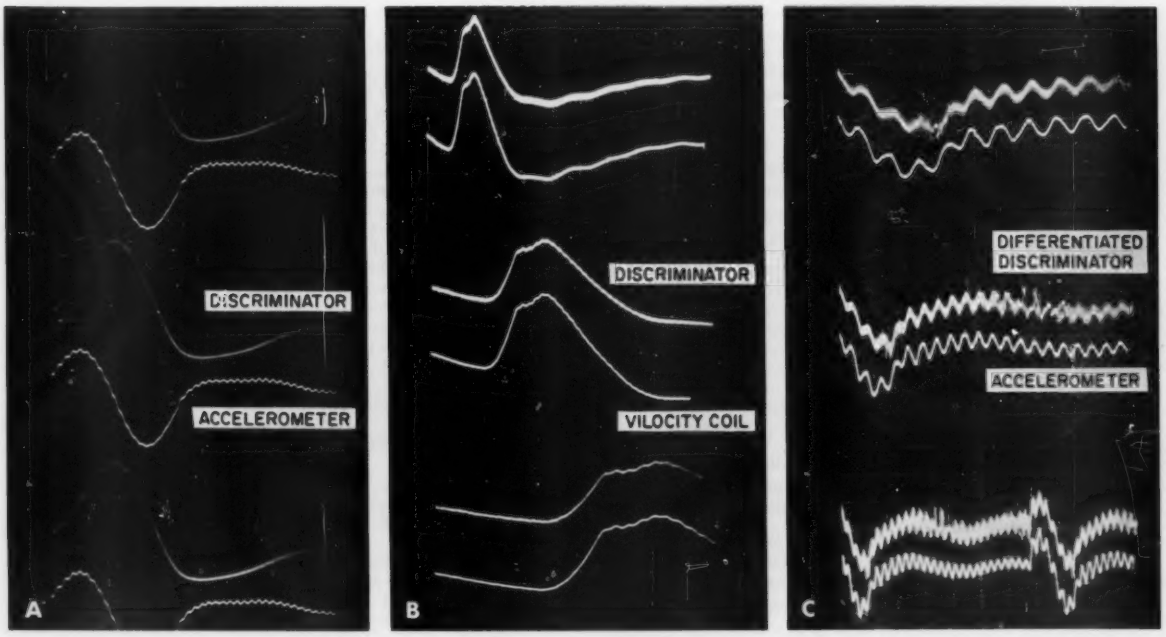

FIGURE 2. *Simultaneous signals from shock motion measuring system.*
a. Discriminator versus accelerometer. b. discriminator versus velocity coil, c. differentiated discriminator versus accelerometer.

the discriminator of the interferometer system and from the accelerometer. Figure 2b shows the signals from the discriminator and from the velocity coil of the shaker. Figure 2c shows the differentiated output of the discriminator and the output of the accelerometer. The two outputs shown in figure 2c were fed to a frequency analyzer and the results plotted on an X-Y plotter. The measured peaks of response are shown in table 1. The calibration factors were arbitrary and the results are only meaningful when compared to each other as shown in the percent deviation column. The differences in harmonic relationships of the frequencies are due to errors in determining the frequency at a point in a logarithmic sweep.

TABLE 1. *Comparison between accelerometer and differentiated discriminator output spectrum due to repetitive sine pulse*

Frequency	Differentiated discriminator[b]	Accelerometer[b]	Accelerometer output deviation from discriminator output[a]
Hz	*Units*	*Units*	*Percent*
76.5	4.50	4.63	+3.6
151	8.23	8.18	0.0
225	7.76	7.75	+.5
301	7.41	7.45	+1.2
376	6.46	6.72	+4.6
2104	6.02	5.75	−3.8

[a] Normalized to maximum discriminator amplitude recoreed at 151 Hz.
[b] Amplitude as measured on a X-Y plotter.

4. Other Applications

The development of this system was oriented towards motion with large velocities and displacements. If the emphasis is changed from detecting frequency to detecting phase modulation, it is feasible to measure fractional parts of a fringe displacement. [17] This approach is not limited to a laser as an electromagnetic radiation source; any coherent source will do, such as radar.

5. Summary

A system has been described that is capable of sensing mechanical shock induced motion and providing a signal that is proportional to the velocity of the motion. The system makes use of the Doppler shift in light frequency, a phenomenon that is known to be linear with amplitude and frequency of motion. The information output is a variable frequency thereby minimizing the linearity requirements for electronic components other than the discriminator. The system can be readily calibrated by use of steady state sinusoidal motion. The information is available in a form that can be analyzed by known methods and techniques.

The authors wish to express their appreciation tor the financial support received from:

U.S. Atomic Energy Commission
Sandia Corporation
Albuquerque, New Mexico AL-67-421,

U.S. Army Missile Command
U.S. Army Metrology and Calibration Center
Redstone Arsenal, Alabama YP-369,

Naval Ordnance System Command
Naval Plant Representative
Metrology Engineering Center
Pomona, California 4355/N1(N69-35).

6. References

[1] Conrad, R. W., and Vigness, Irwin, Calibration of accelerometers by impact techniques, Proc. Inst. Soc. Am. **8,** 166 (1953).
[2] Bouche, R. R., The absolute calibration of pickups on a drop-ball shock machine of the ballistic type, Proc. Inst. Environmental Sci., 115 (1961).
[3] Ramboz, J. D., and Blanchard, C. A., Report No. ESEE08, Endevco 2965 Shock Calibrator, Metrology Engineering Center Naval Plant Representative, Pomona, California; Private Communication.
[4] Burke, R. G., Improved velocity measurement techniques for the shock calibration of accelerometers, Proc. Inst. of Environmental Sci. (1963).
[5] Kelley, R. W., Calibration of shock accelerometers, Proc. 22nd ISA Conf., M18-2-MESTIND-67, Inst. Soc. Am. (1967).
[6] Levy, S., and Kroll, W. D., Response of accelerometers to transient accelerations, J. Res. Nat. Bur. Stand. (U.S.) **45,** No. 4, 303 (1950) RP2138.
[7] Bundy, D. E., The calibration of transducers for use in high intensity shock measurement, Technical Note W.C. 56, Royal Aircraft Establishment, Ministry of Aviation, London W.C. 2, England, March 1964, AD-449463.
[8] IEEE Transactions on Audio and Electroacoustics, **AU-15** No. 2, June 1967, Special Issue on Fast Fourier Transform and Its Application to Digital Filtering and Spectral Analysis.
[9] Schmidt, V. A., Edelman, S., Smith, E. R., and Jones, E., Optical calibration of vibration pickups at small amplitudes, J. Acous. Soc. Am. **33,** 748 (1961).
[10] Hund, A., in the book Frequency Modulation, Eq. 10, p. 16, McGraw-Hill Book Co., New York (1942).
[11] T. P. Gill, in the book The Doppler Effect, Chapter 5 (Academic Press, New York, 1965).
[12] Rowley, W. R. C., Some aspects of fringe counting in laser interferometers, IEEE, Transactions on Instrumentation and Measurement, **Im-15,** No. 4, 146 (1966).
[13] Norgaard, D. E., The Phase-Shift Method of Single-Sideband Signal Generation, Proceedings of the IEEE, **44,** No. 12, 1718 (1956).
[14] Hund, A., ibid., p. 86.
[15] Smith, D. H., Method for Obtaining Small Mechanical Vibrations of Known Amplitude, Proc. Phy. Soc. (London) **57,** 534 (1945).
[16] Ziegler, C. A., Electromechanical Pickup Calibration by the Interferometer Method, J. Acous. Soc. Am. **25,** 135 (1953).
[17] von Willisen, F. K., Time resolved photoelectric interferometry of very high phase resolution, Oral Presentation at 1968 Spring Meeting Optical Soc. Am.

(Paper 73C3&4-291)

JOURNAL OF RESEARCH of the National Bureau of Standards—C. Engineering and Instrumentation
Vol. 73C, Nos. 3 & 4, July–December 1969

Publications of the National Bureau of Standards*

Selected Abstracts

Anderson, G. B., Raybold, R. C., **Studies of calibration procedures for load cells and proving rings as weighing devices,** *Nat. Bur. Stand. (U.S.), Tech. Note 436, 22 pages (Jan. 1969).*

Key words: Calibration; force; load cells; proving rings; transducers; uncertainty; weighing.

Elastic devices such as load cells and proving rings, when used with comparison measurement techniques, yield uncertainties orders of magnitude smaller than generally accepted. Their use, in direct reading application, is affected by numerous characteristics of materials, as well as the techniques of application and interpretation of data. This paper is intended to present progress made in the evaluation of calibration techniques, to the end that such transducers may be used with a predictable uncertainty in direct reading applications. Attempts are being made to formulate calibration procedures which are consistent with application procedures. The confusion existing in the derivation and application of practical force units is considered sufficient justification for a brief discussion of forces derived from mass standards and gravitational acceleration.

Barnes, J. A., **Tables of bias functions, B_1 and B_2 for variances based on finite samples of processes with power law spectral densities,** *Nat. Bur. Stand. (U.S.), Tech. Note 375, 39 pages (Jan. 1969).*

Key words: Spectral density; statistics; unbiased estimate; variance.

D. W. Allan showed that if $y(t)$ is a sample function of a random noise process with a power law spectral density (i.e., $S_y(f)=h|f|^{\alpha}$), then there is generally bias to the estimated variance of y, defined as

$$\sigma_y^2(N, T, \tau)=\frac{1}{N-1}\sum_{n=1}^{N}(\bar{y}_n-\langle\bar{y}\rangle)^2,$$

where N is the number of samples, $\bar{y}_n$ is the average value of $y(t)$ over the nth interval of duration τ, T is the time between the beginnings of any two successive sample intervals, and

$$\langle\bar{y}\rangle\equiv\frac{1}{N}\sum_{n=1}^{N}\bar{y}_n.$$

Allan also showed that, under these conditions, the expectation value of the estimated variance is proportional to τ^{μ} where μ is a constant related to α, the exponent in the spectral density; i.e.,

$$E[\sigma_y^2(N, T, \tau)]\propto\tau^{\mu}.$$

Based on this work one may define the two bias functions

$$B_1(N, r, \mu)\equiv\frac{E[\sigma_y^2(N, T, \tau)]}{E[\sigma_y^2(2, T, \tau)]}$$

and

$$B_2(r, \mu)\equiv\frac{E[\sigma_y^2(2, T, \tau)]}{E[\sigma_y^2(2, \tau, \tau)]}$$

where $r\equiv T/\tau$ and the B's are functions of μ through their dependence on $y(t)$.

If one has a sample variance, $\sigma_y^2(N_1, T_1, \tau_1)$, the bias functions allow one to give an unbiased estimate for $\sigma_y^2(N_2, T_2, \tau_2)$ provided the spectral type is known (i.e., μ is known).

The tables give values of $B_1(N, r, \mu)$ and $B_2(r, \mu)$ accurate to four significant figures for the following values of N, r, μ:

$\mu=-2.0$ to 2.0 in steps of 0.2;

$N=4, 8, 16, 32, 64, 128, 256, 512, 1024, \infty$;

$r=0.001, 0.003, 0.01, 0.03, 0.1, 0.2, 0.4, 0.8, 1, 1.01, 1.1, 2, 4, 8, 16, 32, 64, 128, 256, 512, 1024, 2048, \infty$.

Bean, B. L., Dise, J. R., **Causes of variation in chemical analyses and physical tests of portland cement,** *Nat. Bur. Stand. (U.S.), Bldg. Sci. Ser. 17, 34 pages (Mar. 1969).*

Key words: Portland cement; chemical analyses; physical tests.

Variations in testing that could lead to the rejection of a material fully conforming to specification requirements, or the acceptance of a material with undesirable chemical or physical properties, are apparent in the results reported by laboratories participating in comparative tests of portland cements. Many of the causes for variation in chemical analyses and physical test results are listed in this discussion, and remedies for some of the more frequently encountered deficiencies in apparatus and methods are suggested. Particular consideration is given to problems which do not seem to have been covered in sufficient detail in previous discussions of cement testing procedures. Literature references are given for additional information. (Supersedes NBS Monograph 28.)

Beeghly, H. F., Cali, J. P., Meinke, W. W., Editors, *Nat. Bur. Stand. (U.S.), Spec. Publ. 310, 261 pages (Dec. 1968).*

Key words: Activation analysis standards, isotope reference standards, nuclear fuel burn-up standards, radiation effect standards, radioactivity standards, standards for nuclear chemistry, standards for nuclear technology.

Many diverse organizations are engaged in developing the nuclear standards needed by science, industry, and government for the rapidly growing field of nuclear technology. Often there has been inadequate communication between these groups and insufficient opportunity to get an overall picture of the needs of the country for the many different kinds of standards necessary for this new industry. The Symposium sponsored by the American Chemical Society Division of Nuclear Chemistry and Technology in cooperation with the Committee on Standardization Relations brought together most of the groups with interests in standards for nuclear chemistry and technology to identify the problems, to discuss present programs, and to outline future needs for standards in this broad field. Standards for purposes of the symposium were defined very broadly to include standard materials, standard procedures, standard specifications, standard data, and engineering standards. The mechanisms available for standardization, the "state of the art" in standardization in many areas of the nuclear field, some indications of unmet needs, and estimates of future needs were discussed in a series of papers and panel discussions which are presented here in either complete or summary form.

364-586 O - 69 - 3

Blaine, R. L., Arni, H. T., Evans, D. N., **Interrelations between cement and concrete properties, Part 4. Shrinkage of neat portland cement pastes and concretes,** *Nat. Bur. Stand. (U.S.), Bldg. Sci. Ser. 15, Part 4, 79 pages (Mar. 1969).* Contains two sections as follows:

Section 9. **Shrinkage of hardened portland cement pastes,** R. L. Blaine, H. T. Arni, and D. N. Evans.

Key words: Chemical composition of portland cements; cracking of portland cements; cracking resistance of cements; portland cement; shrinkage of portland cements; trace elements.

The relationship between cement properties and drying shrinkage of partially hydrated neat cement pastes of normal consistency made of a large number of portland cements of different types and composition were studied by fitting multivariable regression equations with the aid of a digital computer. The time of cracking of annular specimens restrained from shrinking by a steel core varied from 0.1 to more than 40 hours. The principal variables which appeared to have the greatest effect were the fineness and K_2O and C_4AF contents of the cements. The fineness and K_2O contents of the cements appeared to have the greatest effect on the nonrestrained shrinkage of prisms at the time of cracking of the annular specimens. The shrinkage of neat cement bars after 1, 6, 27 days, and 6 months in laboratory air differed greatly with different cements. The principal variables appeared to be the C_3A, SO_3, and C_3A/SO_3 ratios. Other commonly determined variables were associated with each of the above test values. The trace elements, other than Na_2O and K_2O, were not generally associated with the shrinkage or cracking characteristics.

Section 10. **Shrinkage and expansion of concrete,** R. L. Blaine and H. T. Arni.

Key words: Cement composition; expansion-shrinkage ratios; portland cement concrete; shrinkage of concrete; trace elements.

The relationship between the cement characteristics and the drying shrinkages of concretes made of a large number of cements of different types and compositions, as well as the subsequent expansions when the concretes were rewetted, were studied by fitting multivariable regression equations with the aid of a digital computer. Specimens $6 \times 8 \times 16$ inches, were made using 5.5 bags of cement (nominal) per cubic yard with a water/cement ratio of 0.635, as well as with a slump of 5 ± 1 inches. Increases in C_3A, C_4AF, fineness of the cement, and air content of the concrete were associated with increases in both shrinkage on drying and expansion on rewetting of the concretes. Increases in Na_2O, SO_3, and ignition loss of the cements were associated with decreases in the shrinkage values of the concretes. None of the individual trace elements, except possibly Rb and SrO, were associated to a highly significant degree with shrinkage or expansion characteristics of the concretes. The use of trace elements in equations with other more commonly determined variables resulted in a significant reduction in variance. There was no relationship between the shrinkage of concrete specimens moist cured 14 days and then dried in laboratory air for eight weeks, and the shrinkage of neat cements, moist cured only 24 hours and then dried in laboratory air. Higher values for dynamic Young's modulus of elasticity of the concretes were associated with lower shrinkage and expansion values.

Boone, T. H., Skoda, L. F., Cullen, W. C., **Laboratory-field comparison of built-up roofing membranes,** *Nat. Bur. Stand. (U.S.), Tech. 473, 15 pages (Dec. 1968).*

Key words: Bituminous adhesive; bituminous built-up membranes; engineering properties; laboratory-field comparison; strength-thickness.

The values of breaking load, elongation and thermal expansion of nine bituminous built-up membranes prepared by roofing contractors under field conditions and by technicians in the laboratory were measured at sub-freezing temperatures. The data indicated that the field-prepared specimens agreed favorably with laboratory-prepared specimens, although the samples from the field frequently reflected higher values for thermal-shock resistance than did their laboratory-prepared counterparts. The higher values were attributed to the smaller amounts of bitumen used between the plies of the field specimens. The results appeared to support the validity of the application of the "strength-thickness rule" to bituminous built-up membranes.

Braun, W., Carrington, T., **Line emission sources for concentration measurements and photochemistry,** *Nat. Bur. Stand. (U.S.), Tech. Note 476, 23 pages (Mar. 1969).*

Key words: Absorption; analysis; gas; photochemistry; spectroscopy; vacuum ultraviolet.

When a resonance line is absorbed in its own gas, measurements of this absorption can be used to derive a value of the product, nf, of concentration of the absorber and f value of the transition. This line absorption process is also important in the study of fluorescence and photochemistry, where it is possible to produce atoms or molecules in a single quantum state without otherwise disturbing the system. The interpretation and success of these applications of line absorption depend critically on the shape of the line emitted by the light source. This is strongly influenced by the optical depth in the emitting region, and by the inevitable presence of a reversing layer through which the light must travel on its way out of the lamp. This paper presents a simple model which can be used to estimate the effects of these properties of the light source on the threshold and sensitivity of measurements of nf, and on the power which can be delivered to absorbing atoms outside the lamp. Emphasis is on the general principles of lamp design and diagnosis, rather than on accurate description of a particular lamp.

Bryson, J. O., Gross, D., **Techniques for the survey and evaluation of live floor loads and fire loads in modern office buildings,** *Nat. Bur. Stand. (U.S.), Bldg. Sci. Ser. 16, 32 pages (Dec. 1968).*

Key words: Fire loads; live floor loads; loads survey techniques; occupancy loads.

The procedures and techniques developed for measuring and evaluating the live floor loads and fire loads in modern office buildings are summarized. The main features of a computer program for analyzing the data are outlined. This program provides a tabulation of the data, some statistical properties, and selected graphical relationships between the measured loads and the characteristics and usage of the structure. A rationale is developed which is intended to achieve the ultimate goal—easier and less expensive means of surveying live loads in buildings and their combustible content.
Two office buildings have been surveyed in a pilot evaluation of the survey techniques—the National Bureau of Standards Administration Building in Gaithersburg, Maryland, and the U.S. Civil Service Commission Building in downtown Washington, D.C. Typical results are presented to illustrate the computer output.

Bullis, W. M., Editor, **Methods of measurement for semiconductor materials, process control, and devices.** *Quarterly report July 1 to September 30, 1968, Nat. Bur. Stand. (U.S.), Tech. Note 472, 45 pages (Dec. 1968).*

Key words: Carrier lifetime; electrical properties; germanium; methods of measurement; microelectronics; resistivity; semiconductor devices; semiconductor materials; semiconductor process control; silicon; thermal properties; wire bonds.

This quarterly progress report describes NBS activities relating to: measurement of resistivity, carrier lifetime, inhomogeneities, and Hall effect in semiconductor crystals; study of infrared measurement methods, properties of deeplying impurities (in InSb), and high field effects; establishment of a processing facility; evaluation of wire bonds; review of NASA measurement methods; and measurement of second breakdown in transistors, thermal properties of devices, and noise in microwave diodes. Projects on silicon nuclear radiation detectors and specification of germanium are also described. Supplementary data concerning staff, committee activities, technical and information services, and publications are included as appendixes. A list of ASTM Standards relevant to integrated circuit processing is also included.

Bullis, W. M., Editor, **Methods of measurement for semiconductor materials, process control, and devices.** *Quarterly report October 1 to December 31, 1968, Nat. Bur. Stand. (U.S.), Tech. Note 475, 38 pages (Feb. 1969).*

Key words: Carrier lifetime; die attachment; electrical properties; germanium; metallization; methods of measurement; microelectronics; resistivity; semiconductor devices; semiconductor materials; semiconductor process control; silicon; thermal resistance; thermographic measurements; wire bonds.

This second quarterly progress report in this series describes NBS activities relating to: measurement of resistivity, carrier lifetime, inhomogeneities, and Hall effect in semiconductor crystals; study of infrared measurement methods, properties of deep-lying impurities (in InSb), and high field effects; establishment of a processing facility; evaluation of aluminum metallization, wire bonds, and wafer die attachment; review of NASA measurement methods; and measurement of second breakdown in transistors, thermal properties of devices, and noise in microwave diodes. Projects on silicon nuclear radiation detectors and specification of germanium are also described. Supplementary data concerning staff, committee activities, technical services, and publications are included as appendixes.

Bullis, W. M., **Measurement of carrier lifetime in semiconductors, An annotated bibliography covering the period 1949–1967,** *Nat. Bur. Stand. (U.S.), Tech. Note 465, 64 pages (Nov. 1968), 60 cents.*

Key words: Bibliography; diffusion length; diode recovery; excess carrier lifetime; measurement methods; photoconductive decay; photoconductivity; photomagnetoelectric effect; recombination of excess carriers; semiconductors; surface photovoltage.

About 300 papers concerned with the measurement and interpretation of carrier lifetime in semiconductors are listed together with key words and a brief comment for each. Eight types of entries are included: Description of Methods, Analysis of Results, Standard Methods, Experimental Results, Theoretical Models, Auxiliary Procedures and Data, Reviews, and Books. Emphasis is placed on methods of carrying out measurements of carrier lifetime. Hence complete coverage was attempted and nearly two-thirds of the entries appear in the first three categories. A large fraction of the papers listed describe the photoconductivity or photoconductive decay methods. The other most popular methods are based on diode characteristics or the photomagnetoelectric effect. In all, 35 methods for measuring carrier lifetime are represented by entries. In addition, representative papers which describe various models for recombination are included together with a number of papers which discuss the influence of surface recombination and trapping phenomena. Auxiliary procedures such as surface preparation, formation of ohmic contacts, control of temperature, and the like are described in some of the entries. Two indexes, a Key Word Index and an Author Index, are provided together with a classification of the various methods for measuring carrier lifetime.

Cassidy, E. C., Abramowitz, S., Beckett, C. W., **Investigations of the exploding wire process as a source for high temperature studies,** *Nat. Bur. Stand. (U.S.), Monogr. 109, 53 pages (Nov. 1968), 55 cents.*

Key words: Electrical discharges; exploding wire; high current; high speed; high speed photography; high temperature; high voltage; light sources; time-resolved electrical measurements; time-resolved spectroscopy.

Numerous experiments with electrically exploded wires are described. The results include time-resolved measurements of electrical energy, power, voltage, and current during the discharge; periodic still and high-speed photographs of the entire explosion process; integrated and time-resolved measurements of the intensity and spectral distribution of the radiation emitted; and time-resolved absorption spectra from the products of the discharge, with emphasis on observations of the spectrum of the AlO molecule. The apparatus, instrumentation, and fast-measurement techniques developed in order to permit these direct experimental observations and measurements, under the extreme and transient conditions of the explosive discharge, are also described. Results from calculations of the composition, entropy, enthalpy, and density of the explosion mixture are given.

deMaine, P. A. D., **Input/output packages for the systems 360 assembly language processor,** *Nat. Bur. Stand. (U.S.), Tech. Note 433, 14 pages (Sept. 1968), 25 cents.*

Key words: Assembly language; card punch; card read; input/output; on-line print; system 360.

Three input-output (I/O) software packages for use with the Assembly Language Processor (ALP) of the Systems 360 are described. They are for card read, on-line-print and card punch operations. A single pseudo-operation statement, which contains all required formats and addresses, suffices for the execution of each input-output package. Printed error and guide messages aid in program debugging. In addition to the conventional formats (A, I, F and E), Systems 360 column binary (X) and hexadecimal (J and B) are permitted. With a single pseudo-operation these I/O packages can handle up to eight inidivdual items or arrays of any length in a single or mixed format.

Diamond, J. J., Editor, **Bibliography on the high temperature chemistry and physics of materials October, November, December 1968,** *Nat. Bur. Stand. (U.S.), Spec. Publ. 315, 72 pages (Jan. 1969).*

Key words: Bibliography, high-temperature chemistry; chemistry at high temperatures, bibliography; high temperature; high-temperature chemistry, bibliography.

A classified collection of references to scientific research performed at temperatures above 1000 °C and published in the world literature during the fourth quarter of 1968.

Diamond, J. J., Editor, **Bibliography on the high temperature chemistry and physics of materials, January, February, March 1969,** *Nat. Bur. Stand. (U.S.), Spec. Publ. 315–1, 81 pages (Apr. 1969), 75 cents.*

Key words: Bibliography; high temperature; chemistry, high temperature; high temperature chemistry; materials properties; research at high temperatures; thermophysical properties.

The bibliography consists of references to research involving temperatures above 1000 °C, which were noted by the Contributors during the above three-month period. Since this is intended primarily as a current-awareness bibliography, there is no cross-referencing or indexing. This issue contains about 700 references roughly grouped under fifteen subject headings.

Edmonds, D. K., Hord, J., **Incipient and developed cavitation in liquid cryogens,** *Nat. Bur. Stand. (U.S.), Tech. Note 374, 31 pages (Feb. 1969).*

Key words: Cavitation; cryogens; incipience.

Cavitation characteristics of liquid hydrogen and liquid nitrogen flowing in a transparent plastic venturi have been determined and conventional cavitation-inception-parameter curves are given. Representative developed-cavitation data, consisting of pressure and temperature measurements within fully-developed cavities, are also given; measured temperatures and pressures within the cavities were generally not in thermodynamic equilibrium. Existing theory was used to obtain equations which correlate the experimental data for developed cavities in liquid hydrogen or liquid nitrogen. The theory is extended to include the effect of cavity thickness and the experimental data are used to evaluate the results. Some recommendations for future work are given.

Eisele, J. W., Tech. Std. Coordinator, **Fabrics for book covers,** *Nat. Bur. Stand. (U.S.), Prod. Stand. 9–68, 13 pages (Apr. 15, 1968), 10 cents.*

Key words: Book binding; book covers; book cloth; buckrams; starch filled book covers; listing procedures.

This Standard covers the requirements and test procedures for seven groups of plain finished book cloths and buckrams which are impregnated or starch filled and which are used in the bookbinding industry for book covers. Definitions which apply to this standard are also included.

Flynn, D. R., Peavy, B. A., Jr., Eds., **Thermal conductivity,** *Proceedings of Seventh Conference, National Bureau of Standards, Gaithersburg, Md., Nov. 13–16, 1967, Nat. Bur. Stand. (U.S.), Spec. Publ. 302, 820 pages (Sept. 1968),* $6.25.

Key words: Conductance; conductivity; contact conductance; contact resistance; electrical conductivity; electrical resistivity; heat transfer; Lorenz function; resistivity; temperature; thermal conductivity; thermal diffusivity; thermal resistivity; thermophyiscal properties.

The Seventh Conference on Thermal Conductivity was held at the National Bureau of Standards on November 13–16, 1967. This volume contains the texts of the papers presented. Topics covered include surveys of the present state of knowledge regarding the thermal conductivity of different materials, descriptions of different apparatuses for measuring thermal conductivity, new experimental data on the thermal conductivity or diffusivity of a variety of materials, and correlations between experimental results and theoretical predictions.

Gosman, A. L., McCarty, R. D., Hust, J. G., **Thermodynamic properties of argon from the triple point to 300 K at pressures to 1000 atmospheres,** *Nat. Stand. Ref. Data Ser., Nat. Bur. Stand (U.S.), 27, 151 pages (Mar. 1969).*

Key words: Argon; compressibility factor; enthalpy; entropy; equation of state; internal energy; Joule-Thomson coefficient; $P-V-T$; specific heat; vapor pressure; virial coefficient.

Tabular values of density, internal energy, enthalpy, and entropy of liquid and gaseous argon are presented for temperatures from 83.8 to 300 K at pressures of 0.01 to 1000 atmospheres. Diagrams of specific heats, compressibility factor, and entropy are included. The properties presented are calculated from an equation of state which was fitted to experimental $P-\rho-T$ data from the world literature. Extensive comparisons were made between the equation of state and the experimental data, and deviation plots are presented. The second virial coefficient and Joule-Thomson inversion curve were also calculated and comparisons made with values from other sources. A vapor pressure equation which covers the range from the triple point to the critical point is also given.

Greenfeld, S. H., **The performance of roofing made with Asplund felts,** *Nat. Bur. Stand. (U.S.), Tech. Note 477, 27 pages (Mar. 1969).*

Key words: Asphalt, Asplund, felt, mineral-surfaced roll roofing; shingles; wood fibers.

A study of the durability of roofing made with Asplund wood fibers was conducted from 1942 to 1967. Concentrations of 0 to 60 percent wood fibers (oak or pine) prepared by three variations of the Asplund process were evaluated. All the mineral-surfaced roll roofings and shingles were performing well after 25 years, with only four specimens showing more deterioration than the controls (only rags and paper in their felts). No differences in performance could be related to the felt composition.

Gross, D., Loftus, J. J., Lee, T. G., Gray, V. E., **Smoke and gases produced by burning aircraft interior materials,** *Nat. Bur. Stand. (U.S.), Bldg. Sci. Ser. 18, 29 pages (Feb. 1969).*

Key words: Aircraft materials; combustion products; fire tests; interior finish; smoke; toxic gases.

Measurements are reported of the smoke produced during both flaming and smoldering exposures on 141 aircraft interior materials. Smoke is reported in terms of specific optical density, a dimensionless attenuation coefficient which defines the photometric obscuration produced by a quantity of smoke accumulated from a specimen of given thickness and unit surface area within a chamber of unit volume. A very wide range in the maximum specific optical density was observed. For the majority of materials, more smoke was produced during the flaming exposure test. However, certain materials produced significantly more smoke in the absence of open flaming. During the smoke chamber tests, indications of the maximum concentrations of CO, HCl, HCN, and other selected potentially toxic combustion products were obtained using commercial colorimetric detector tubes. A study was made of the operation, accuracy, and limitations of the detector tubes used. Measurements of the concentrations of HCl were also made using specific ion electrode techniques.
Qualitative identification of the major components of the original test materials was accomplished primarily by infrared absorption spectrophotometry.

Heinrich, K. F. J., Ed., **Quantitative electron probe microanalysis,** *Proc. Seminar, National Bureau of Standards, Gaithersburg, Md., June 12–13, 1967, Nat. Bur. Stand. (U.S.), Spec. Publ. 298, 305 pages (Oct. 1968),* $3.00.

Key words: Atomic number effect, biological specimens; electron probe microanalysis; electron scattering, fluorescence by the continuum; quantitative analysis; stereometric analysis; x-ray absorption; x-ray emission.

A seminar was held at the National Bureau of Standards in June 1967 to examine critically the factors involved in quantitative electron-probe microanalysis. Major consideration was given to proposed methods for data evaluation, and to requirements for further work in theory, in measurement, and in the preparation of standards. This volume contains a series of invited papers which formed the basis of discussion at the seminar. Topics covered include corrections for the atomic number effect, for x-ray absorption, and for fluorescence by characteristic lines and the continuum. The various ways to derive a simplified model of the complex electron-target interaction are critically analyzed by several authors, and the accuracy of several proposed methods is compared by error histograms constructed on the basis of hundreds of analyses of materials of known composition. Applications to the analysis of biological specimens and to problems of stereometric analysis are also discussed.

Hermach, F. L., Dziuba, R. F., Editors, **Precision measurement and calibration. Selected NBS papers on electricity-low frequency,** *Nat. Bur. Stand. (U.S.), Spec. Publ. 300, Vol. 3, 498 (Dec. 1968).*

Key words: Electrical units; electrical standards; electrical measurements; electrical calibrations; standard cells; zener diodes; resistors; resistance apparatus; capacitors; inductors; ac-dc transfer standards; current transformers; voltage transformers; inductive voltage dividers; high voltage measurements; dielectric measurements; magnetic measurements.

This volume is one of an extended series which brings together some of the previously published papers, monographs, abstracts and bibliographies by NBS authors dealing with the precision measurement of specific physical quantities and the calibration of the related metrology equipment. The contents have been selected as being useful to the standards laboratories of the United States in tracing to NBS standards the accuracies of measurement needed for research work, factory production, or field evaluation.
Volume 3 contains reprints through 1967 on d-c and low-frequency electrical measurements covering the following topics: Electrical Units, Electrical Standards, Standard Cells, Zener Diodes, Resistors, Resistance Apparatus, Capacitors, Inductors, Instruments, AC-DC Transfer Standards, Transformers, Inductive Voltage Dividers, High Voltage Measurements, Dielectric Measurements, and Magnetic Measurements. A selected list of NBS publications on electrical measurements is also included.

Janz, G. J., Dampier, F. W., Lakshminarayanan, G. R., Lorenz, P. K., Tomkins, R. P. T., **Molten salts: Volume 1, Electrical conductance, density, and viscosity data,** *Nat. Stand. Ref. Data Ser., Nat. Bur. Stand. (U.S.), 15, Vol. 1, 145 pages (Oct. 1968),* $3.00.

Key words: Data compilation; density; electrical conductance; molten salts; standard reference data; viscosity.

Data on the electrical conductance, density and viscosity of single-salt melts were compiled from a comprehensive search of the literature up to December 1966 and a critical assessment made of the compiled data. Recommended values were determined and are presented as functions of temperature in the form of equations and tables.
The results from some 174 compounds as single-salt melts are reported; no attempts was made in the present effort to embrace the results for molten salt mixture. Data are presented for fluorides, chlorides, bromides, iodides, carbonates, nitrites, nitrates, oxides, sulfides, sulfates and a miscellaneous group.

Koeser, R. L., Editor, *Report of the 53d National Conference on Weights and Measures, 1969, Nat. Bur. Stand. (U.S.), Spec. Publ. 311, 182 pages (Mar. 1969), $1.25.*

Key words: Conference; weights and measures—laws; weights and measures—regulations; weights and measures—technical requirements; weights and measures—history; weights and measures.

This is a report of the proceedings (edited) of the Fifty-third National Conference on Weights and Measures, sponsored by the National Bureau of Standards, held in Washington, D.C., June 17–21, 1968 and attended by State, county, and city weights and measures officials and representatives of the Federal Government, business, industry, railroads, and associations.

Kropschot, R. H., Birmingham, B. W., Mann, D. B., Eds., **Technology of liquid helium,** *Mono. 111 (Oct. 1968), Nat. Bur. Stand. (U.S.), Monogr. 111, 380 pages (Oct. 1968), $2.00.*

Key words: Conservation; cryoelectronics; cryogenics; cryopumping; helium; liquefaction; magnets; purification; refrigeration; safety; storage; thermodynamic properties; transportation.

The discovery of the element helium was made just 100 years ago in 1868. Today helium is produced in large quantities and used in many technological applications. This treatise is a source document containing information on helium resources, production, conservation, thermodynamic properties, liquefaction and refrigeration techniques, transportation and storage of liquid and safety requirements. It also contains a discussion of uses for liquid and cold gas in cryoelectronics, superconductivity, bubble chambers, cryopumping and missile and space systems. The book brings together articles by noted authorities in cryogenic technology in which they discuss their specialized field in great depth.

Ku, H. H., Editor, **Precision measurement and calibration. Selected papers on statistical concepts and procedures,** *Nat. Bur. Stand. (U.S.), Spec. Publ. 300, Volume 1, 436 pages (Feb. 1969).*

Key words: Accuracy; analysis of measurement data; design of experiments; functional relationships; interlaboratory tests; measurement process; precision; statistical concepts in measurements; systematic error.

This volume is one of an extended series which brings together the previously published papers, monographs, abstracts, and bibliographies by NBS authors dealing with the precision measurement of specific physical quantities and the calibration of the related metrology equipment. The contents have been selected as being useful to the standards laboratories of the United States in tracing to NBS standards the accuracies of measurement needed for research work, factory production, or field evaluation.
Volume 1 deals with methodology in the generation, analysis, and interpretation of precision measurement data. It contains 40 reprints assembled in 6 sections: (1) The Measurement Process, (2) Design of Experiments in Calibration, (3) Interlaboratory Tests, (4) Functional Relationships, (5) Statistical Treatment of Measurement Data, (6) Miscellaneous. Each section is introduced by an interpretive foreword, and the whole is supplemented by abstracts and selected references.

LaFleur, P. D., Editor, **Activation Analysis Section: Summary of activities July 1967 to June 1968,** *Nat. Bur. Stand. (U.S.), Tech. Note 458, 109 pages (Mar. 1969), $1.00.*

Key words: Activation analysis; Cockcroft-Walton neutron generator; computer literature searching; extraction, group separations, homogeneity testing; hydrogen bis(2-ethylhexyl) phosphate, matrix effect; molybdenum; NBS LINAC; NBS reactor; photon activation analysis sensitivities; Standard Reference Materials; zinc.

The facilities used by the reactor, LINAC and neutron generator groups for activation analysis are described. Proposed installation of four new irradiation terminals and a new pneumatic transfer tube system are outlined.
A new 2.5-mA neutron generator has been installed and the biological shield, pneumatic transfer system and the detector assembly modified. Studies of blank problems for oxygen determination and self-absorption corrections in photopeak analysis have resulted in greatly improved precision for Standard Reference Materials. Halide in photographic emulsions, using 14-MeV and 2.6-MeV neutrons, have been determined.
Considerable emphasis has been placed on the development of group radiochemical separations, SRM steel and high purity zinc sample have been analyzed using this technique.
Eighteen different SRMs were analyzed for a variety of elements and a variety of service analyses were performed.
The self-absorption effects of the matrix on irradiation photons were studied and calculations of sensitivities for photon activation analysis were made. Carbon in sulfur, yttrium in rare-earth oxides and oxygen in sodium were determined by photon activation.
The extraction of metals by bis(2-ethylhexyl) orthophosphoric acid has been studied, and distribution coefficients are given for many of the transition metals. The results indicate enhanced applicability of this reagent for radiochemical separations.
Updated keys for computer literature searching and a sample output are included.

Lee, R. D., **Construction and operation of a simple high-precision copper-point blackbody and furnace,** *Nat. Bur. Stand. (U.S.), Tech. Note 483, 16 pages (May 1969), 30 cents.*

Key words: Blackbody; optical pyrometry; radiometry.

Detailed instructions for the construction and operation of an inexpensive copper-point blackbody and furnace are presented. Such a source may be expected to realize the radiance temperature of 1083.3 °C (Int. 48) with an uncertainty of 0.2 °C and a variation in successive use of less than 0.033 °C. The furnace requires no inert gas or vacuum and utilizes only 225 watts to reach a melt in about an hour after turn on. Melts and freezes last about five minutes each and at least fifty melts and freezes are expected during the lifetime of the furnace.

Little, J. L., **Some evolving conventions and standards for character information coded in six, seven, and eight bits,** *Nat. Bur. Stand. (U.S.), Tech. Note 478, 30 pages (May 1969), 35 cents.*

Key words: ASCII; character codes; code extension; coded character sets; collating sequence; data transmission codes; information code structure; international information code; Russian code standard; standard information codes; USASCII.

This Technical Note describes some of the properties of the USA Standard Code for Information Interchange, widely known as ASCII or USASCII. It also relates this code to similar international codes and presents the national code for Russia as an example of the worldwide acceptance of this code, which is comprised of seven information bits representing 128 coded characters. Some of the conventions which are evolving to relate these seven bit codes to six and eight bit computer codes are given, and conventions for extending the code to represent an unlimited repertoire of concepts is also given. Two alternate arrangements of the code table are shown to facilitate an understanding of its structure and application.

Lovell, W. S., Thiel, L. M., **Interferometric measurements of the complex dielectric constant of liquids,** *Nat. Bur. Stand. (U.S.), Tech. Note 369, 89 pages (Aug. 1968), 50 cents.*

Key words: Approximation errors; complex dielectric constant; contour diagrams; Fresnel equations; interferometric measurements; liquid dielectrics; millimeter waves.

Paper I. Errors in the "perfect square" approximation.

Errors arising from the use of a "perfect square" approximation in treating free-space, interferometric measurements of the complex dielectric constant $\epsilon^* = \epsilon' - i\epsilon''$ of liquids are described. It is shown that such errors (1) are generally positive, (2) often exceed values previously estimated for the measurement technique as a whole, and (3) are not generally predictable without some prior knowledge of the dielectric properties of the material being investigated. In addition, these errors depend upon the dielectric thickness over which data are incorporated into the calculations. Finally, an anomaly in the calculations previously attributed to experimental error is shown to arise from the "perfect square" approximation itself. It is concluded that this approximation may at best provide initial estimates for ϵ' and ϵ'' which may then be used in a more complete mathematical treatment.

Key words: Complex dielectric constant; dielectric liquids; diffraction; experimental apparatus; interferometry; millimeter-waves; quasi-optics.

Paper II. Experimental apparatus.

Design details of a free-space, millimeter-wave interferometer are described. The apparatus radiates at oblique incidence to an air-dielectric-metal configuration placed between dissimilar horns. Errors arising from the quasi-optical nature of this radiation are described, and quantitative data are presented which demonstrate techniques for minimizing such errors. The techniques employed should have general applicability in millimeter-wave measurements. For the particular instrument described, the errors are shown to be of such magnitude that experimental reflection coefficient profiles should conform to an adequate theoretical description. A means for more accurate and absolute measurements of the complex dielectric constant of liquids is then provided.

Key words: Continuous normal distribution; dielectric liquids; imperfect reflections; millimeter waves; multiple reflections; perpendicular polarization; transverse displacement; weighted mean.

Paper III. Derivation of the theoretical reflection coefficients.

For measurements of the complex dielectric constant of liquids by free-space reflection and interference of electromagnetic radiation, a theoretical reflection coefficient for the air-dielectric-metal configuration is derived. The derivation is based on a model which treats multiple reflections within the dielectric explicitly. As an extension of earlier theory, this reflection coefficient incorporates effects of (1) imperfect reflections at the dielectric-metal interface, together with other losses, and (2) radiation sources presenting nonplanar wavefronts and having finite bandwidths. Effects arising from a finite sample or receiving surface are also discussed.

Key words: Complex dielectric constant; confidence interval; dielectric liquid; generalized Newton iteration function; interferometric measurement; least squares iteration function; method of selected points; millimeter waves; perpendicular polarization; reflection coefficient; vector solution.

Paper IV. A numerical method for determining the best complex dielectric constant.

A numerical method is presented for determining the best complex dielectric constant $\epsilon^* = \epsilon' - i\epsilon''$ from an experimental record obtained at millimeter-wavelengths from free-space, interferometric measurements of liquids. The method of selected points is applied to the reflection coefficient expression to obtain a set of simultaneous equations which is solved for an initial vector solution using the generalized Newton iteration function. The principle of least squares is then applied to achieve the best fit between the reflection coefficient expression and experimental record. The desired values of ϵ' and ϵ'' are included as components of a final vector solution of the best fitting theoretical curve.

Lutz, G. J., Boreni, R. J., Maddock, R. S., Meinke, W. W., Ed., **Activation analysis: A bibliography,** *Nat. Bur. Stand. (U.S.), Tech. Note 467, Parts 1, 520 pages and 2, 197 pages (Sept. 1968), $6.50 set.*

Key words: Activation analysis; bibliography; element determined; literature file; matrix analyzed; technique used.

References to activation analysis in the open literature are published from a computer readout. The first part of the two-part series contains references numbered according to their accession to the system. The second part contains an author index and three additional indices for "element determined," "matrix analyzed," and "technique used." The two parts, when used together, permit a literature search defined by the three indices. Part 1 will be updated periodically by addenda containing new references while Part 2 will be periodically revised and replaced by new pages which include cross references to the new accessions.

Mason, H. L., Editor, **Making valuable measurements.** *Proceedings of the 1968 Standards Laboratory Conference, Nat. Bur. Stand. (U.S.), Spec. Publ. 313, 177 pages (May 1969), $1.50.*

Key words: Metrology management; National Conference of Standard Laboratories; physical measurement.

The National Conference of Standards Laboratories is a nonprofit, laboratory-oriented organization whose purpose is to promote cooperative efforts toward solving the common problems faced by standards laboratories in their organization and operation. Established in 1961 under the sponsorship of the National Bureau of Standards, NCSL has a membership of more than 200 organizations. Three biennial national meetings have been held previously as well as a number of specialized regional workshops.

The theme of the 1968 Standards Laboratory Conference is "Making Valuable Measurements." The papers presented will attempt to answer the Who? When? Where? How? and Why? of making valuable measurements. The conference provides an opportunity for discussion of problems confronting laboratory managers and calibration personnel.

Representatives of member organizations of the National Conference of Standards Laboratories met at the Boulder facility of the National Bureau of Standards August 25–29, 1968. Major addresses were given by A. V. Astin and J. L. Sloop. Reports and discussions at eight sessions covered the management of valuable measurements: the management of equipment and data, measurement agreement comparisons, international practices, Defense Department activities, NBS activities, NCSL liaison, and NCSL committee work.

McClenon, R. C. Hilsenrath, J., **REFORM: A general-purpose program for manipulating formatted data files,** *Tech. Note (Aug. 1968), 40 cents.*

Key words: File editor; fixed-field file editor; Fortran program; insert program; packing program; reformatting; report generator; unpacking program.

A program listing and description is given of REFORM, an independent program with which it is possible to manipulate and edit files containing as many as nine different fixed-field card formats. It can select or abridge information from any of the cards and print that information, or reformat new cards in any desired order or arrangement. Provision is made for introducing as many as twenty-six arbitrary strings of characters, each of which may be up to seventy-nine characters in length, thereby permitting the insertion of labels, headings, or comments into the file. The program, which operates on the 1108 computer at NBS, is written in ASA FORTRAN, and care has been taken to reduce to a minimum the program changes required to make the program run on other computers.

Messina, C. G., Hilsenrath, J., **Edpac: utility programs for computer-assisted editing, copy-production, and data retrieval,** *Nat. Bur. Stand. (U.S.), Tech. Note 470, 80 pages (Jan. 1969).*

Key words: alphanumeric data files; computer-assisted text-preparation; data retrieval; FORTRAN programs; free field text files; mechanized text editing.

A description and listings are given of EDPAC, a package of five related utility computer programs: SCRAMBLE, SUBSTITUTE, SEARCH, BLOCKSEARCH, JUSTIFY, and their subroutines. These programs perform transformations on alphanumeric data. The programs have been written in FORTRAN, with care taken to make them as system and machine-independent as possible, permitting their use on many different computers.

SCRAMBLE scans an input file for specified characters, which it replaces by different characters. SUBSTITUTE similarly replaces strings of characters by other strings. SEARCH and BLOCKSEARCH scan for the occurrence of certain strings and list the lines or blocks, respectively, in which they occur. JUSTIFY produces text, for printing on a card-controlled typewriter or on an extended character printer, which has been left and right-justified between specified margins.

Some applications of the EDPAC programs are discussed. Emphasis is placed on computer-assisted text preparation.

Muhlenhaupt, R. C., Strobridge, T. R., **An analysis of the Brayton cycle as a cryogenic refrigerator,** *Nat. Bur. Stand. (U.S.), Tech. Note 366, 116 pages (Aug. 1968), $1.25.*

Key words: Brayton; cryogenics; refrigeration.

The performance of a Brayton-cycle refrigerator has been computed taking into account the efficiencies of the various components. The results are presented in graphical form. These charts give the input power requirements, mass flow rate, pertinent temperatures, and allow selection of the optimum high pressure for a given set of component characteristics.

Key words: Brayton; cryogenics; refrigeration.

Oberholtzer, B. L., **Publications of the National Bureau of Standards 1966–1967,** *Nat. Bur. Stand. (U.S.), Spec. Publ. 305, 220 pages (Apr. 1969), $2.00.*

Key words: Articles; publications.

All published work by National Bureau of Standards authors from the middle of 1966 to the end of 1967, both in the extensive publications issued by NBS itself and in outside publications, is covered in this latest supplement to the NBS catalog. Each title is accompanied by complete bibliographic information, plus a list of keywords and an abstract, both prepared by the authors. In addition, there is information on the NBS publishing program, purchase procedures, publication announcement services, and price lists. Information in the catalog is accessible through two indexes: an author index and a key-word index. In the latter, the group of key words for each catalog entry is permuted so that each key word appears once as the first in the group, and therefore determines the alphabetical order in which the group appears in the index. The user can thus locate papers of interest to him through the subject-related key word.

Rapial, A. S., Daney, D. E., **Preparation and characterization of slush hydrogen and nitrogen gels,** *Nat. Bur. Stand. (U.S.), Tech. Note. 378, 43 pages (May 1969), 50 cents.*

Key words: Gels, liquid hydrogen gels; liquid nitrogen gels; liquid-solid hydrogen mixtures; rocket propellants; slush hydrogen; slush hydrogen gels; slush nitrogen gels.

An experimental apparatus has been developed for the gelation of slush hydrogen, and slush hydrogen was gelled for the first time. Measurements of the weight-bearing capacity of the gel as a function of mass percent gelant were made for liquid and slush nitrogen and hydrogen. These measurements verify the simple models discussed here for gelled liquid and slush within the experimental accuracy; the models predict a reduction in gelant concentration from 38 mass percent to 25 mass percent in going from Normal Boiling Point liquid hydrogen to slush hydrogen of 0.40 solid fraction for the silica gelant used in this work. Reduction in the mass percent gelant for other gelants should be similar.

Roberts, B. W., **Superconductive materials and some of their properties,** *Nat. Bur. Stand. (U.S.), Tech. Note 482, 129 pages (May 1969), $1.25. Supersedes and extends Tech. Note 408.*

Key words: Bibliography; compilation of data; composition; critical field; critical temperature; crystallographic data; low temperature; superconductivity.

This is a noncritical compilation of data on superconductive materials that has been extracted from a portion of the literature published up to early 1968. The properties concerned are composition, critical temperature, critical magnetic field, crystallographic data, and lowest temperature tested for superconductivity. The compilation also includes, bibliography, general reference review articles and a special tabulation of high magnetic field superconductors.

Robinson, D. C., **Misalinement detector for axial loading fatigue machines,** *Nat. Bur. Stand. (U.S.), Tech. Note 480, 15 pages (Apr. 1969), 25 cents.*

Key words: Axial loading; fatigue machine; misalinement; test fixtures.

A strain gage device for measuring changes in alinement between the test fixtures of axial loading fatigue machines is described. Variations in fixture orientation are determined by measurement of the bending induced in a compliant beam clamped in parallel mounts attached to the test fixtures. Changes in bending with applied tension loads are an indication of alterations in the alinement between the load transmitting members of a machine. An approximately linear relationship was found to exist between changes in bending determined by the detector and the fatigue life of high strength fasteners for various levels of misalinement induced in a fatigue machine.

Sindt, C. F., Ludtke, P. R., Daney, D. E., **Slush hydrogen fluid characterization and instrumentation,** *Nat. Bur. Stand. (U.S.), Tech. Note 377, 69 pages (Feb. 1969), 65 cents.*

Key words: Friction angle; cryogenic; flow restrictions; gel; liquid-solid mixtures; particle size; plug flow; slurry flow; slush hydrogen.

Areas of the slush hydrogen fluid characterization program covered are production, transfer, and storage of liquid-solid mixtures. An experiment has been performed in which a second component was added to liquid hydrogen to determine the effect on the size of the solid particles produced by the freeze-thaw method. Also, an experiment performed with 4.4% oxygen in nitrogen resulted in particles an order of magnitude smaller in size than those normally observed in freeze-thaw production of pure nitrogen slush. The friction angle of settled solids of slush hydrogen on several metals was determined for surface finishes ranging from 2 to 110 microinches rms. The angle at which solids slide from the surface was found to be a function of the surface finish.

Data were taken in the flow loop over a range of velocities from 1.5 to 40 ft/sec (0.46 to 12.2 m/s). The friction losses determined from the flow data are compared to losses predicted for Newtonian fluids. Losses with slush of solid fractions from 0.1 to 0.4 were found to be lower than with triple-point liquid hydrogen at the higher Reynolds numbers.

Liquid-solid mixtures of hydrogen with solid fraction of 0.5 were transferred through three types of flow restrictions. The restrictions were a globe valve, an orifice, and a venturi. Losses through the restrictions were essentially the same with the high solid fraction slush as with triple-point liquid.

A brief review of the pumping characteristics of slush hydrogen is presented. A comparison of developed head, efficiency, cavitation constant, and net positive suction head is discussed.

Gelling of slush hydrogen with pyrogenic silica was accomplished with solid fractions from 0 to 0.2. The amount of gelling agent required to gel slush was found to be proportional to the liquid volume of the slush.

Stabler, T. M., Editor, **Specifications and tolerances for reference standards and field standard weights and measures. 1. Specifications and tolerances for field standard weights,** *Nat. Bur. Stand. (U.S.), Handb. 105–1, 10 pages (Apr. 1969), 25 cents.*

Key words: Cooperation for uniformity of measurements; field standard weights; specifications; tolerances; weights and measures inspection.

These specifications and tolerances are intended to set forth minimum requirements for standards used in the field by State and local weights and measures officials in the official examination of weighing and measuring devices used in commerce. They should be considered also as appropriate for device installers and repairmen.

Although the National Bureau of Standards has no regulatory authority in this area, its organic legislation (31 Stat. 1449) specifically authorizes "The custody, maintenance, and development of the national standards of measurement, and the provision of means and methods for making measurements consistent with those standards . . . and cooperation with the States in securing uniformity in weights and measures laws and methods of inspection."

Swindells, J. F., Ed., **Precision measurement and calibration. Selected NBS papers on temperature,** *Nat. Bur. Stand. (U.S.), Spec. Publ. 300, Vol. 2, 520 pages (Aug. 1968), $4.75.*

Key words: Acoustical thermometry; cerous magnesium nitrate thermometer; error analysis; liquid-in-glass thermometry; reprints; resistance thermometry; spectroscopic thermometry; standards; temperature scales; thermoelectric thermometry.

This volume is one of an extended series which brings together the previously published papers, monographs, abstracts, and bibliographies by NBS authors dealing with the precision measurement of specific physical quantities and the calibration of the related metrology equipment. The contents have been selected as being useful to the standards laboratories of the United States in tracing to NBS standards the accuracies of measurement needed for research work, factory production, or field evaluation.
Volume 2 contains reprints through June 1967 covering the general topics: Uncertainties, Temperature Scales, Resistance Thermometry, Thermoelectric Thermometry, Liquid-in-Glass Thermometry, Optical Pyrometry, and Spectroscopic Thermometry. A selected bibliography covering the period from January 1953 through December 1965 is included.

Taggart, H. E., Workman, J. L., **Calibration principles and procedures for field strength meters 30 (Hz to 1 GHz),** *Nat. Bur. Stand. (U.S.), Tech. Note 370, 157 pages (Mar. 1969), $1.25.*

Key words: Calibration procedures; field strength meters; loop antennas; dipole antennas.

The National Bureau of Standards has been calibrating many types of field strength meters and their related antennas at frequencies up to 1000 MHz for several years. Various techniques of measurement have been investigated regarding accuracy, calibration time, ease of operation, and reliability. This report discusses some of these calibration techniques in detail, and in some cases lists step-by-step procedures for performing the complete calibration. Typical calibration data are used to take the reader from the beginning of the calibration to the completed test report. All measurement setups are clearly illustrated, listing the equipment necessary to perform the calibration. Methods of calibrating two basic types of antennas are described: (1) the loop antenna at frequencies from 30 Hz to 30 MHz and (2) half-wavelength dipole antennas from 30 to 1000 MHz. Two methods of calibrating loop antennas are discussed in detail, the standard-field method and the injection method. The standard-antenna method of calibrating dipole antennas is fully described. Measurement uncertainties of various methods are discussed. This report was written to help technical personnel actively participate in antenna calibration work. Hopefully this information will help people to set up new calibration services and to improve existing calibrating facilities.

Wachtman, J. B., Jr. Editor, **Mechanical and thermal properties of ceramics.** *Proceedings of a symposium Gaithersburg, Md., April 1–2, 1968, Nat. Bur. Stand. (U.S.), Spec. Publ. 303, 266 pages (May 1969), $4.25.*

Key words: Ceramics; elasticity; fracture; inelastic deformation; melting point; standards; thermal conductivity; thermal expansion; thermal radiation; viscoelasticity.

The proceedings of the Symposium on Mechanical and Thermal Properties of Ceramics, held at the National Bureau of Standards in Gaithersburg, Maryland, on April 1–2, 1968, are presented. The symposium was cosponsored by the American Ceramic Society, the American Society for Testing and Materials, and the National Bureau of Standards. Attention was concentrated upon properties primarily of structural and/or high temperature use including melting points, thermal expansion, thermal conductivity, thermal radiation properties, elasticity, viscoelasticity, inelastic deformation, and fracture. The dependence of these properties upon composition and microstructure was surveyed and the importance of controlling these features of character to insure reliability of ceramics was emphasized. The procedures by which American ceramists formulate standards and specifications to assist in insuring reliability were summarized.

Wegstein, J. H., **A semi-automated single fingerprint identification system,** *Nat. Bur. Stand. (U.S.), Tech. Note 481, 21 pages (Apr. 1969).*

Key words: Computerized-fingerprint identification; fingerprints, pattern-recognition.

A system is described in which a fingerprint is manually coded by tracing certain ridges and noting events such as ridge endings and ridge beginnings. This code is sent by teleprinter to a central file where a computer identifies the fingerprint by comparing the code with codes previously entered in the file. The scheme for comparing codes is given along with some preliminary test results using typical fingerprints.

White, H. S., Jr., Editor, **Code for information interchange, Hardware standard interchange codes and media,** *Nat. Bur. Stand. (U.S.), Fed. Info. Process. Stand. Publ. (FIPS Pub.) 1, 4 pages (Nov. 1, 1968).*

Key words: Federal Information Processing Standard; code for interchange.

This document provides administrative, policy, and guidance information relative to the implementation and utilization of the standard code for information interchange.
The technical specifications of this standard are available to Federal Government activities from the General Services Administration Specifications Activity at a cost of 40 cents per copy. Refer to FIPS 1. Others may obtain copies from the United States of America Standards Institute for $2.00 per copy. Refer to USA Standard X3.4–1968. The technical specifications define a code and character set for use in Federal information processing systems, communications systems and associated equipments.

White, H. S., Jr., Editor, **Perforated tape code for information interchange, Hardware standard interchange codes and media,** *Nat. Bur. Stand. (U.S.), Fed. Info. Process. Stand. Publ. (FIPS Pub.) 2, 4 pages (Nov. 1, 1968).*

Key words: Federal Information Processing Standard; perforated tape code for information interchange.

This document provides administrative policy, and guidance information pertaining to the implementation and utilization of the standard perforated tape code for information interchange. The technical specifications of this standard are available to Federal Government activities from the GSA Specifications Activity at 45 cents per copy. Refer to FIPS 2. Others may obtain copies from the United States of America Standards Institute for $1.50 per copy. Refer to USA Standard X3.6–1965. The technical specifications of the standard specify the representation of the Federal Standard Code for Information Interchange (FIPS 1) on perforated tape used in Federal information processing systems, communications systems, and associated equipments.

White, H. S., Jr., Editor, **Recorded magnetic tape for information interchange (800 CPI, NRZI), Hardware standard interchange codes and media,** *Nat. Bur. Stand. (U.S.), Fed. Info. Process. Stand. Publ. (FIPS Pub.) 3, 4 pages (Nov. 1, 1968).*

Key words: Federal Information Processing Standard; recorded magnetic tape for information interchange (800 CIP, NRZI).

This FIPS PUB provides administrative, policy, and guidance information relative to the implementation and utilization of the standard recorded magnetic tape (800 characters per inch, NRZI (non-return-to-zero—change to one) method of recording) for information interchange.
The technical specifications of this standard are available to Federal Government activities from the GSA Specifications Activity at the 70 cents per copy. Refer to FIPS 3. Others may get copies from the United States of America Standards Institute for $2.50 per copy. Refer to USA Standard X3.22–1967. The technical specifications of the standard provide a format and recording standard for 1/2 inch, 9-track magnetic tape and reels used in Federal information processing systems and associated equipments. It is one of a series of standards implementing the Federal Standard Code for Information Interchange (FIPS 1) in magnetic tape media.

White, H. S., Jr., Editor, **Calendar date,** *Fed. Info. Process. Std. Pub. (FIPS), 4 (Nov. 1, 1968), 20 cents.*

Key words: Calendar Date; Federal Information Processing Standard.

This publication announces the adoption of a Federal standard for representing calendar dates used in the interchange of formatted machine sensible coded data between and among agencies. The technical specifications (FIPS 4) are affixed to the FIPS PUB.

White, H. S., Jr., Editor, **States of the United States,** *Fed. Info. Process. Std. Pub. (FIPS) 5 (Nov. 1, 1968), 20 cents.*

Key words: Federal Information Processing Standard; States of the United States.

This publication announces a standard identification and code for representing the 50 states, the District of Columbia, and the outlying areas of the U.S., all of which are considered to be "first order subdivisions." These codes are for use in the interchange of formatted machine sensible coded data between and among agencies. The technical specifications of the standard (FIPS 5) are affixed to the FIPS PUB.

White, H. S., Jr., Editor, **Counties of the States of the United States,** *Fed. Info. Process. Std. Pub. (FIPS) 6 (Nov. 1, 1968), 40 cents.*

Key words: Federal Information Processing Standards; States of the United States.

This FIPS PUB announces a standard identification and code for representing the counties of the 50 states of the United States for use in the interchange of formatted machine sensible coded data between and among agencies. Also included are the independent cities of the States of Maryland, Missouri, and Virginia which are treated as county equivalents. The technical specifications of the standard (FIPS 6) are affixed to the FIPS PUB.

White, H. S., Jr., Editor, **Implementation of the code for information interchange and related media standards. Hardware standards interchange codes and media,** *Nat. Bur. Stand. (U.S.), Fed. Info. Process. Stand. Publ. (FIPS Pub.) 7, 12 pages (Mar. 7, 1969), 25 cents. (Supplement to FIPS Pub. 1 through 3).*

Key words: Code for Information interchange; Federal Information Processing Standard; information interchange; perforated tape code for information interchange.

This FIPS PUB provides further details covering the implementation of the Code for Information Interchange (FIPS 1), Perforated Tape Code for Information Interchange (FIPS 2), and Recorded Magnetic Tape Code for Information Interchange (800 CPI, NRZI) (FIPS 3). The publication includes a letter of approval of these standards by the President of the United States and a letter with attachments by the Secretary of Commerce providing details and policy of their implementation.

Yakowitz, H., Michaelis, R. E., Vieth, D. L., **Standard reference materials: homogeneity characterization of NBS spectrometric standards IV: preparation and microprobe characterization of W–20% Mo alloy fabricated by powder metallurgical methods,** *Nat. Bur. Stand. (U.S.), Spec. Publ. 260–16, 30 pages (Jan. 1969).*

Key words: Electron probe analysis; metallography; powder metallurgy; spectrometric standards; Standard Reference Materials; W–Mo alloys.

A significant problem of the National Bureau of Standards Standard Reference Materials program is the provision of standards suitable in homogeneity for use with micro-analytical techniques such as the spark source mass spectrograph and the electron probe microanalyzer. An interim approach to the problem has been the extended homogeneity characterization of selected existing standards. This paper describes the preparation and evaluation of the first NBS standard tested specifically from the beginning for application to electron probe microanalyzers. The standard designated SRM 480 is a tungsten-20 weight percent molybdenum alloy prepared by a powder metallurgy process. Based on the results of about 1500 determinations for both tungsten and molybdenum by electron probe microanalysis, the material was found to be of high homogeneity at about the micrometer level of spatial resolution. The coefficient of variation for molybdenum was 2.5% and that for tungsten 1.5%. Correction of relative intensity ratios to obtain concentrations is discussed in terms of input parameter uncertainties such as mass absorption coefficients, and electron backscatter factors. The result of studies for atomic number correction and effects on operating voltage on the microprobe absorption correction, will be given. It is concluded that SRM 480 should be a valuable addition to any microprobe laboratory doing quantitative analyses.

Youden, W. W., **Computer literature bibliography 1964–1967,** *Nat. Bur. Stand. (U.S.), Spec. Publ. 309, Vol.* **2,** *385 pages (Dec. 1968).*

Key words: Author index; coden; computer bibliography; information retrieval; permuted index; title word index.

This bibliography is a continuation of *Computer Literature Bibliography, 1946 to 1963,* and is intended as a further service to the computer community. It contains approximately 5,200 references to computer literature published during the years 1964 through 1967. The Bibliography Section includes the full title and the names of all of the authors of each item published in 17 journals, 20 books composed of chapters by individual authors, and 43 conference proceedings. In addition, references to all items that were reviewed in the IEEE Transactions on Electronic Computers have been included.
The Title Word Index Section provides the means for locating an item if any part of its title is known. Likewise, it can be used to identify all items whose titles include a particular word or phrase. The Author Index Section lists all authors of each item, but does not indicate whether an individual is its sole author.

Abrams, M. D., **A comparative sampling of the systems for producing computer-drawn flow charts,** *Proc. 1968 ACM National Conf., Las Vegas, Nevada, Aug. 27–29, 1968, pp. 743–750 (Brandon/Systems Press, Inc., Princeton, N.J., 1968).*

Key words: Flowchart; graphics; graphical output; algorithmic languages; computer graphics.

Several programs which produce computer-drawn flowcharts from assembly language and algorithmic compiler language are compared. As a background, the applications, implementation, and information transferral properties of flowcharts are briefly treated. The strengths and restrictions of flowcharts as graphical communications media are also briefly discussed. Three programs to draw flowcharts of compiler language programs are directly compared; sample flowcharts and a tabular summary are provided.

Ambler, E., Schooley, J. F., Colwell, J. H., Pfeiffer, E. R., Frederikse, H. R., Hosler, W. R., Thurber, W. R., **Transition temperatures and critical fields of $SrTiO_3$ and mixed titanates,** *Proc. Xth Intern. Conf. Low Temperature Physics, Moscow, U.S.S.R., Aug. 31–Sept. 6, 1966, Vol.* **2B,** *Superconductivity, Paper S123, 142–148 (1968).*

Key words: $(Ba_xSr_{1-x})TiO_3$; $(Ca_ySr_{1-y})TiO_3$; critical fields; magnetic moment; semiconducting systems; penetration depth; superconducting; $SrTiO_3$; transition temperature.

The experimental investigation of the superconducting properties of the semiconducting systems $SrTiO_3$, $(Ba_xSr_{1-x})TiO_3$, and $(Ca_ySr_{1-y})TiO_3$ is reviewed. The studies of a.c. magnetic susceptibility, which yeilds transition temperature and penetration depth; of heat capacity, which yields the electronic density of states and transition temperature; and of magnetic moment, which yields first and second critical fields and transition temperature, are discussed briefly. Tables of experimental values of the parameters mentioned above are included.

Arp, V. D., Kasen, M. B., Reed, R. P., **Magnetic energy storage and cryogenic aluminum magnets,** *Tech. Rept. AFAPL-TR-68-87, 122 pages (Air Force Systems Command, Wright-Patterson Air Force Base, Ohio, Feb. 1969).*

Key words: Aluminum; cryogenics; magnetic energy storage; magnets.

Factors pertaining to aluminum magnet technology have been investigated. Industrial competence and capacity to produce superpurity aluminum have been improved. Methods of analyzing superpurity aluminum have been studied; in particular, the eddy-current decay technique of measuring electrical resistivity ratios between 4 and 295 K have been improved and used extensively. New devices used to sensitively measure stress, strain, and resistivity at 4 K have been developed.
Two major experimental programs were conducted. One pertains to the effects of internal defects, particularly grain boundaries and impurity elements, on the residual resistance ratio. It was found that no one process can be ascribed to the linear relationship between increasing grain size and decreasing resistance ratio. One significant mechanism proposed is that, in super-purity aluminum, grain boundary motion acts to sweep away impurity elements in solid solution, thus having a purifying effect.
The second program involved the relationships between applied stress, plastic strain, and electrical resistivity changes due to the introduction of dislocations and vacancies at 4 K. It was found that the change in resistivity at 4 K is related to $\epsilon^{1.19}$ where ϵ is the plastic strain.

Bach, R. L., Caswell, R. S., **Energy transfer to matter by neutrons,** *Radiation Res. 35, No. 1, 1-25 (July 1968).*

Key words: Kerma; neutron energy transfer; nuclear reactions; neutron dosimetry; first collision dose; energy transfer coefficient.

Calculations of energy transfer (kerma) for neutrons from thermal to 18 MaV energy have been carried out for hydorgen, carbon, nitrogen, and oxygen and for ten compounds or mixtures including tissue. All pertinent nuclear reaction processes are included. The calculation demonstrates the importance of (n, charged particle) reaction processes which have been neglected in nearly all previous calculations. These processes dominate the energy transfer process in carbon, nitrogen, and oxygen above roughly ten MeV.

Barber, D. J., Tighe, N. J., **Neutron damage in single crystal aluminum oxide,** *J. Am. Ceram. Soc.* **51,** *No. 11, 611-617 (Nov. 1968).*

Key words: Aluminum oxide; defects; electron microscopy; neutron damage dislocations; sapphire.

Synthetic aluminum oxide crystals were irradiated with fast neutrons to a dose of 1.8×10^{20} nvc and examined by transmission electron microscopy. As-irradiated crystals contained damage on a fine scale, revealed by diffraction contrast and showed a 28% increase in Knoop diamond hardness compared with un-irradiated material. Annealing above 600 °C, which decreased the hardness, caused the small defect clusters to grow, forming dislocation loops on {1010} planes, with $< 10\bar{1}0 >$ Burgers vectors. Vacancy and interstitial loops occurred. High temperature annealing caused the loops to interact to give dislocation segments; these tended to align with the $< 10\bar{1}0 >$ and $< 11\bar{2}0 >$ directions. Grown-in dislocations also began to climb at high temperatures but showed evidence of impurity pinning. Isolated platelike precipitates on $\{10\bar{1}0\}$ planes were also observed in samples annealed at high temperatures. Possible effects of the observed damage on physical properties are considered and there is qualitative agreement between predictions and existing data.

Bates, R. G., **Measurement of *p*H,** *Handbook of Biochemistry, Ed. H. A. Sober, pp. J100-J194 (Chemical Rubber Company, Cleveland, Ohio, 1967).*

Key words: *p*H; acidity; standardization; glass electrode; indicators.

The operational definition of *p*H, in the form endorsed by the International Union of Pure and Applied Chemistry, is presented. The preparation of standard reference solutions for *p*H measurements is described and the choice of electrodes and measurement techniques is discussed. The proper interpretation of *p*H numbers is set forth briefly, and procedures for *p*H measurement with indicators are described.

Bay, Z., Luther, G. C., **Locking a laser frequency to the time standard,** *Appl. Phys. Letters* **13,** *No. 9, 303-304 (Nov. 1, 1968).*

Key words: Electrooptic modulation; optical frequencies; velocity of light.

On the basis of high frequency modulation experiments and well known locking techniques, a scheme is described for stabilizing a visible laser frequency and simultaneously determining that frequency in terms of the time standard. The importance of this method for a refined determination of the velocity of light and the possibility of establishment of reference lines for spectroscopy and for length measurements, throughout the spectrum wherever laser lines are available, is discussed.

Beatty, R. W., Fentress, G. H., **An attenuation and phase shift divider circuit,** *Proc. IEEE* **56,** *No. 11, 2063-2064 (Nov. 1968).*

Key words: Attenuation; rotary vane attenuator; circuit.

An attenuation divider circuit is described. The theory is presented for accurate division of small attenuation changes by arbitrarily selected ratios, and the procedure for adjusting the circuit is described. The circuit is useful for accurately producing small attenuation changes such as 0.0001 decibel, which is outside the capability of most attenuators.

Beatty, R. W., **Discussion of effect of realizability conditions upon estimated limits of mismatch error in the calibration of fixed attenuators,** *IEEE Trans. Microwave Theory Tech.* **MTT-16,** *No. 11, 976 (Nov. 1968).*

Key words: Attenuation; microwave; mismatch error; realizability; 2-ports.

The effect of realizability conditions for 2-ports upon the estimation of mismatch error is discussed. Only the case of the insertion of fixed symmetrical, reciprocal 2-ports is considered. It is shown that the effect of realizability conditions needs to be considered only for certain ranges of attenuation and VSWR. Most attenuators encountered in practice do not fall within those ranges so that the conventional method of estimating mismatch error limits is usually satisfactory.

Beckett, C. W., Cezairliyan, A., **High-speed thermodynamic measurements and related techniques,** *chapt. in Book, Experimental Thermodynamics, Eds. J. P. McCullough and D. W. Scott, Vol. I, Calorimetry of Non-reacting Systems, chapt. 14, 551-585 (Butterworth and Co., London, England, 1968).*

Key words: Experimental thermodynamics; high-speed thermodynamic measurements; shock wave techniques; thermodynamic measurements; thermodynamic properties.

The needs and requirements of high-speed measurement of thermodynamic properties and related high-speed techniques in millisecond

and microsecond time domain are presented. High-speed generation of heat by electrical pulse methods is reviewed. The technique of the measurement of heat through the measurement of electrical quantities is discussed and the factors causing error are summarized. High-speed temperature measurement methods, both photoelectric and photographic, are discussed. Other related subjects, such as high-speed photography, dynamic pressure measurements, fast x-ray and interferometry, are reviewed briefly. Applications of high-speed measurements to the determination of properties, such as specific heat, thermal diffusivity, electrical conductivity, are presented. Measurement of thermodynamic properties by shock wave techniques is reviewed. Other applications of high-speed measurement techniques in the areas of exploding conductors and high-temperature sources are also discussed.

Bekkedahl, N., **Crystallization of natural rubber,** *Rev. Gen. Caoutchouc Plastiques* **45,** *No. 3, 341–463–9 (1968).*

Key words: Chain folding; contractility; crystallization; dilatometry; heat engine; melting; polymers; rubber; stark rubber.

This review article presents a resume of the research work that has been done at the National Bureau of Standards during the past thirty-five years in the field of crystallization of polymeris materials, with special emphasis on natural rubber. It contains only information on results of research work that has already been published.

Bender, P. L., Alley, C. O., Currie, D. G., Faller, J. E., **Satellite geodesy using laser range measurements only,** *J. Geophys. Res.* **73,** *No. 16, 5353–5357 (Aug. 15, 1968).*

Key words: Laser; satellite; geodesy; range; worldwide; network.

The potential accuracy of a 12-station worldwide geodetic network based on laser range measurements to an optical retro-reflector package on a high altitude satellite has been investigated. An accuracy of 15 cm in the range (one nanosec in the round-trip transit time) seems achievable with about 10 min of observations. The model used consists of range measurements being made at about the same time from the 4 closest ground stations for each of 30 satellite positions. For the "ideal" case the stations were located at the 12 vertices of a regular icosahedron and the satellite positions were over the centers of the 30 edges. This gave an expected uncertainty of less than 45 cm in the distance between any 2 stations, with little dependence on satellite altitude over the range of 20,000 to 110,000 km. For 12 stations chosen from the Pageos Geometric Satellite Network, the expected accuracy for a satellite altitude of 110,000 km was found to be 60 cm or better for the distance between any 2 stations. The results indicate that the geometry can be "strong" even for high satellite altitudes if the satellite positions observed from a given ground station are well separated.

Bender, P. L., Alley, C. O., Currie, D. G., Faller, J. E., **Satellite geodesy using laser range measurements only,** *J. Geophys. Res.* **73,** *No. 16, 5353–5358 (Aug. 15, 1968).*

Key words: Geodesy; laser; geodetic satellite; distance measurements; worldwide geodetic network; geophysics; continental drift.

We have investigated the potential accuracy with which the distances between 12 observing stations spread fairly uniformly over the earth can be determined by using laser range measurements to a high altitude satellite equipped with optical retro-reflectors. For each of 30 satellite positions, it was assumed that range measurements were made at about the same time from the 4 closest stations. For ideal distribution of the stations, the expected uncertainty in the distance between any two stations was found to be less than 45 cm, with little dependence on satellite altitude over the range of 20,000 to 110,000 km. With 12 stations chosen from the Pageos Worldwide Geometric Satellite Network, the expected accuracy for a satellite altitude of 110,000 km is 60 cm or better between any two stations.

Bennett, L. H., **Nuclear magnetism,** *chapt. in Book, Magnetism and Magnetic Materials 1968 Digest,* Eds. H. Chang and T. R. McGuire, *chapt. 14, pp. 201–221 (Academic Press Inc., New York, N.Y., 1968).*

Key words: Magnetic materials; Mössbauer effect; nuclear magnetic resonance; nuclear magnetism; nuclear specific heat; perturbed angular correlation.

This chapter reviews the 1967 literature that was devoted to the study of magnetism and magnetic materials taking advantage of the atomic nucleus as a probe. The bulk of the experimental papers utilize nuclear magnetic resonance (NMR or FNR) or recoilless x-ray absorption, i.e., the Mössbauer effect (ME), as in previous years. Most of the NMR papers reviewed here are for ferromagnetic materials in the ordered state, for which we use the special abbreviation FNR. Other techniques for determining hyperfine (hf) magnetic fields (H_{hf}) include nuclear specific heat and perturbed angular correlation.

Bennett, J. A., **The initiation of fatigue microcracks under sequential bending and torsional loads,** *Trans. ASM* **61,** *No. 2, 210–218 (June 1968).*

Key words: Fatigue strength; micro-cracks; aluminum alloy; bending; torsion; shear stress.

Specimens of 6061–T6 aluminum alloy were stressed first in alternating torsion, then in reversed bending or vice versa. The development of cracks was observed by microscopic examination of replicas taken of the specimen surfaces at intervals during the tests. The results indicate that fatigue damage under uniaxial stress did not reduce the resistance to crack initiation in pure shear; the reverse was also true. Based on the number of cycles to initiate micro-cracks, the fatigue strength in terms of shear stress amplitude was 14% higher in torsion than in bending. Comparison of these results with earlier studies of environmental effects suggests that moisture influences the fatigue behavior of this alloy only after micro-cracks have formed.

Bennett, L. H., Swartzendruber, L. J., **Some comments on "The corrosion of materials in desalination plants",** *Desalination* **4,** *389–390 (1968).*

Key words: Alloys; corrosion; copper; desalination; nickel; iron.

The implications to testing and use of cupro-nickel alloys for desalination are described.

Birmingham, B. W., Ed., **A Report on the 1967 Applied Superconductivity Conference,** *Cryogenics* **8,** *No. 3, 176–179 (June 1968).*

Key words: Cryogenic refrigeration; superconducting electronics; superconducting magnets; superconducting materials; superconducting phenomena; superconducting power transmission; superconductivity.

The 1967 Applied Superconductivity Conference met at the University of Texas in Austin in response to a growing need for improved communications between researchers in superconductivity and potential users of new knowledge from industry, government, private and national laboratories, and universities. Invited papers presented the U.S. Bureau of Mines helium program, U.S. Government programs in superconductivity, and superconductivity in Europe. Subjects covered in contributed papers included magnets and materials, computer devices, and phenomena and other devices. Two panel discussions highlighted superconducting power transmission and refrigeration. An exhibition of apparatus demonstrated superconducting phenomena and applications in addition to the latest cryogenic refrigerator developments and high field magnet materials and designs.

Boutillon, M., Henry, W. H., Lamperti, P. J., **Comparison of exposure standards in the 10–50 kV X-ray region,** *Metrologia* **5,** *No. 1, 1–11 (Jan. 1969).*

Key words: Analysis of uncertainties; air attenuation; correction factors; direct comparison; exposure standards; low-energy x-rays.

Direct comparisons of the low-energy x-ray exposure standards of the International Bureau of Weights and Measures (BIPM) and

the National Research Council of Canada (NRC), the BIPM) and the National Bureau of Standards of the U.S.A. (NBS), were made, using x-rays generated by 10, 30, and 50 kilovolts. The half-value layers for these qualities of radiation were 0.03_6, 0.17_6, and 2.25_7 mm aluminum respectively. The results indicate that a direct comparison between two free-air chambers, in the low-energy x-ray region, can be precise to better than 0.3 percent. The uncertainties and errors in the geometric and correction factors used for the comparison measurements, as well as other systematic and statistical errors, were examined in detail and are reported. The results of preliminary work on the definition of the quality of radiation, air attenuation correction, diaphragm comparisons and saturation correction are included.

Bowen, R. L., Paffenbarger, G. C., Mullineaux, A. L., **A laboratory and clinical comparison of silicate cements and a direct-filling resin: A progress report,** *J. Prosthetic Dentistry* **20,** *No. 5, 426–437 (Nov. 1968).*

Key words: Silicate cements; reinforced resins; solubility; color stability; composites; clinical research; dental materials.

Two silicate cements showing a difference of about 0.7 percent solubility and disintegration in distilled water for 24 hours, showed approximately the same durability in clinical service during a four-to-six year period. There was more disintegration in the interproximal areas of the silicate restorations than there was in the self-cleansing areas.
An experimental reinforced resin gave sufficiently good results to warrant further clinical investigations of more recent and perhaps better composite formulations. Both unreinforced and reinforced resin materials appear to benefit from the use of a primer or "cavity seal."

Brauer, G. M., McLaughlin, R., Huget, E. F., **Aluminum oxide as a reinforcing agent for zinc oxide-eugenol-o-ethoxybenzoic acid cements,** *J. Dental Res.* **47,** *No. 4, 622–628 (July–Aug. 1968).*

Key words: Zinc oxide-eugenol-EBA cements; EBA cements; dental cements; Al_2O_3 reinforced cements; alumina as a reinforcing agent; crown and bridge cements.

Aluminum oxide is a very effective reinforcing agent for *o*-ethoxybenzoic acid (EBA) cements. Addition of Al_2O_3 increases the amount of powder that can be incorporated into the mix. The compressive strength of the hardened cement is increased up to 1055 kg/cm² (15,000 psi) and the ADA film thickness decreased to 26μ. The materials adhere to tooth structure as well as zinc phosphate cements and are suitable as crown and bridge cements. With higher powder-liquid ratios their high 10-minute compressive strength and excellent tissue tolerance suggests their use as bases under metallic restorations. These materials may also be employed as temporary restoratives. Mixes of Al_2O_3 and eugenol or glycerine may be of interest as a temporary non-hardening crown and bridge cement. Incorporation of Al_2O_3 whiskers did not improve the physical properties of these cements.

Brinckman, F. E., Gordon, G., **Energetic intermediates in inorganic synthesis: characterization of transport species in electric discharge,** *Proc. Intern. Symp. Decomposition of Organometallic Compounds to Refractory Ceramics, Metals, and Metal Alloys, Dayton, Ohio, Nov. 1967, pp. 29–46 (Univ. Dayton Press, Dayton, Ohio, Oct. 1968).*

Key words: Electric discharge; reactive intermediates; transport species; oxyfluorides; silicon; boron; germanium; time-of-flight; mass spectrometry.

Commercial processes involving energetic chemical transport and deposition reactions are poorly understood with respect to the identity and mechanistic behavior of their intermediates. Work is presented resulting from recent development of a facility for *in situ* sampling of electric discharge reactions by time-of-flight mass spectrometry. With use of single or mixed reactant gases to sustain a microwave discharge plasma, both homogeneous and heterogeneous reactions have been examined for synthetic potential under conditions of optimized energy input. A number of new compounds thereby have been identified with aid of computerized polyisotopic mass spectral analyses, but also by independent syntheses where known. Several important cases are presented with emphasis on oxyfluorides since both hereto- and homo-μ-oxy-metalloid products form. These systems include Si-O-Si, Si-O-B, B-O-B, Si-O-Ge, Ge-O-Ge, and Ge-O-B species for which some relative stability data can be derived. Extension of these findings to analogous carbon-containing materials (derived from organometals or organometalloids) is also discussed.

Bullis, W. M., **Measurement problems in microcircuit processing** *(Proc. Government Microcircuit Applications Conf., Gaithersburg, Md., Oct. 1–3, 1968) GOMAC Digest 1, 215–217 (Office of Naval Research, Washington, D.C., Oct. 1968).*

Key words: Microelectronics; monolithic microcircuits; reliability; semiconductor devices; silicon; test methods.

Attempts to meet reliability and interchangeability requirements for microcircuits solely by post-fabrication testing have proven to by extremely expensive and, at the same time, not completely successful. Since variations in materials and processing cause a given type of circuit to have a range of characteristics, both reliability and interchangeability are affected. With suitable measurement procedures, these variations could be better controlled. The first step is the establishment of procedures with adequate sensitivity and reproducibility at all stages of microcircuit fabrication from specification and evaluation of the starting materials through the final processing steps. In many cases this can be accomplished with only incremental improvements in existing procedures although in other cases new methods or even new tests must be developed. Once such procedures are available, tests for relevance can be undertaken and then the specification, evaluation, and process control sequence can be refined. A broad program intended to assist in the development of improved test methods is now in progress at the National Bureau of Standards. This program will be discussed briefly in order to indicate the scope of problems encountered and the approach being employed to solve them.

Bullis, W. M., Brewer, F. H., Kolstad, C. D., Swartzendruber, L. J., **Temperature coefficient of resistivity of silicon and germanium near room temperature,** *Solid-State Electron.* **11,** *No. 7, 639–646 (July 1968).*

Key words: Temperature coefficients; resistivity; *n*-type; *p*-type; germanium; silicon; extrinsic exhaustion region.

Temperature coefficients for the resistivity of *n*- and *p*-type germanium and silicon in the neighborhood of room temperature have been determined over a wide range of resistivity. Linear temperature coefficients have been found for the extrinsic exhaustion region ($< 5\,\Omega \cdot$cm for germanium and $< 5000\,\Omega \cdot$cm for silicon). The results are presented as plots of temperature coefficient against resistivity at 23°C. The plots may be used in connection with measurements of resistivity on extrinsic germanium and silicon doped with the usual shallow impurities such as boron, aluminum, gallium, phosphorus, arsenic, and antimony. Accurate linear coefficients cannot be found for specimens doped with deep-lying impurities in sufficient amounts to affect the carrier density nor for specimens with resistivity in the transition region between extrinsic and intrinsic conduction.

Carter, G. C., **The NBS Alloy Data Center,** *Mater. Res. Bull.* **3,** *919–922 (1968).*

Key words: Automated; alloys; bibliography; data; files; information; indexing computer programs; metals; physical properties; reference books (material).

A summary of the detailed description of the Alloy Data Center will be given in this letter.

Case, W. E., Harrington, R. D., **Hysteresis effects in the slope calibration method for magnetometers,** *Proc. IEEE* **56,** *No. 10, 1733–1734 (Oct. 1968).*

Key words: Magnetometer calibration; vibrating-sample magnetometers; magnetization.

The slope method for calibrating vibrating sample magnetometers requires spherical samples of high permeability such that

$$\frac{\mu+2}{\mu-1}\approx 1.$$

It is shown that the presence of a small remanence in the calibration spheres results in an effective permeability that is as great if not greater than the initial permeability which is often used in the above equation. This even higher permeability further increases the validity of this approximation.

Cassidy, E. C., Abramowitz, S., **Time-resolved emission and absorption studies of exploding wire spectra** (*Proc. 4th Conf. Exploding Wires, Boston, Mass., Oct. 18–21, 1967*), *Book, Exploding Wires* **4,** *109–124 (Plenum Press Inc., New York, N.Y., 1968).*

Key words: Exploding wire; time-resolved spectroscopy; electrical discharges; AlO, TiO.

Emission and absorption studies of the spectra produced by exploding wires in oxygen, nitrogen, hydrogen, or argon atmospheres are described. A drum camera and a rotating shutter are used for continuous and time-resolved recording of the explosion spectra. A high-intensity light source (a second exploding wire or Lyman flash-tube), synchronized with the rotating shutter, is flashed through the explosion vapor for the absorption studies. Results from experiments performed under a variety of controlled conditions are presented. Effects of environment, pressure, and electrical energy on the spectrum are discussed, and conditions found conducive to production of selected features are indicated. The exploding wire is shown to be a rich source for study of the AlO molecule, and observation of a number of new bands (believed to be part of the $B\,^2\Pi_i - X\,^2\Sigma^+$ transition) is reported. Preliminary experiments with titanium wires exploded in oxygen suggest that the exploding wire may also be a desirable source for spectral studies of the TiO molecule. Some results from this work are included.

Cassidy, E. C., Cones, H. N., Wunsch, D. C., Booker, S. R., **Calibration of a Kerr cell system for high-voltage pulse measurements,** *IEEE Trans. Instr. Meas.* **IM-17,** *No. 4, 313–320 (Dec. 1968).*

Key words: Electro-optical measurements; high voltage measurements; Kerr cell; pulse measurements.

Several techniques for calibration of an electro-optical (Kerr cell) high voltage pulse measuring system are described. Independent calibrations, without reference to pulse divider measurements, are achieved by application of a direct bias voltage to the Kerr cell. After calibration, experiments with voltages as high as 100 kV demonstrate reasonable agreement (to within 1%) between simultaneous Kerr cell and calibrated pulse divider measurements.

Christ, B. W., Giles, P. M., **On the detection of retained austenite in high-carbon steels by Fe^{57} Mössbauer spectroscopy, with appendix,** *Trans. Met. Soc. AIME* **242,** *1915–1925 (Sept. 1968).*

Key words: Retained austenite; Fe^{57} Mössbauer effect; high carbon steel; carbides; resolution; hyperfine; martensite.

Mössbauer effect measurements have been made on 1-mil thick foils of commercial 1 w/o carbon steel and Iron 2 w/o carbon alloy. The experimental method requires about 3–5 volume percent of a phase in the multiphase steel sample for detection. Room temperature Mössbauer patterns obtained on austenitized and quenched samples exhibit 15, and possibly 21, lines. A sharp, paramagnetic singlet and a quadrupole doublet, poorly-resolved from the singlet, are attributed to austenite. Remaining lines are due to martensite. Accurate evaluation of austenite line parameters is not feasible if significant amounts of other phases such as carbides or martensite occur simultaneously with austenite. This is demonstrated by comparison of hyperfine interactions determined for austenite in multiphase high carbon samples with those reported for iron-carbon austenite in a nearly 100% austenitic sample. Lines from carbides are incompletely resolved from austenite lines, as demonstrated by comparison of austenite line positions with carbide line positions calculated from published values of hyperfine interactions. One martensite line overlaps an austenite line in the pattern for commercial 1 w/o carbon steel. Results of this study suggest that the usefulness of Fe^{57} Mössbauer spectroscopy for quantitative analysis of austenite in quenched and tempered steels, may be restricted by poor resolution. Use of Mössbauer spectroscopy as a method for identifying components of steels and evaluating their atomic structure is quite feasible, however.

Christ, B. W., Smith, G. V., **Effects of impurities on yield and flow strength of zone refined iron,** *Mem. Sci. Rev. Met.* **LXV,** *208–223 (June 15, 1968).*

Key words: Flow strength; hydrogen-purified iron; iron; zone-purification.

Effects of impurities on yield and flow strength of hydrogen-purified, zone-refined iron and of dilute, binary alloys made from it in the temperature range 77–300° K have been examined. Data from the literature are compared with new data obtained on hydrogen-purified iron and iron–0.01 and 0.026 wt.% nitrogen alloys. In 300° K tensile tests, hydrogen purification causes substantial changes in the shape of the upper yield, the magnitude of yield stress, the grain-size dependence of yield stress and the response to strain aging treatments. However, hydrogen purification decreases total interstitial impurity by only 0.0008 wt.%.

Dilute iron alloys are found to exhibit unusual, but widely documented solution strengthening behavior. The room temperature strength is proportional to impurity concentration. However, low-temperature strength is inversely proportional to impurity concentration. This phenomenon, termed "alloy softening", is more pronounced in poly- than in monocrystals, and for interstitial than substitutional impurities.

It is concluded that hydrogen-purification of zone-refined iron affects mechanical behavior by modifying interstitial impurity distribution, rather than by total removal of interstitial impurity. Alloy softening may be due to an increase in mobile dislocation density related to solute rearrangements during thermal treatments.

Clark, A. F., **Low temperature thermal expansion of some metallic alloys,** *Cryogenics* **8,** *No. 5, 282–289 (Oct. 1968).*

Key words: Alloys; aluminum; copper; expansivity; iron; metals; nickel; thermal expansion.

The low temperature thermal expansion of several aluminum, nickel, copper, and iron base alloys was measured from liquid hydrogen temperature, 20K, to room temperature, 293K. Both the thermal contraction from room temperature $(L_{293}-L_T)/L_{293}$, and the thermal expansion coefficient, $\frac{1}{L_{293}}\frac{dL}{dT}$, are tabulated as a function of temperature. Comparison of similar alloys and alloy conditions led to the general conclusions that relatively large changes in composition are required to produce significant changes in the thermal expansion, thermal treatment or condition has little effect except when it produces a basic structure change, and the thermal expansion coefficient at room temperature is a good indicator of the total length change to a low temperature.

Clark, A. F., Fickett, F. R., **A nonsuperconducting detection system for low level dc voltages,** *Rev. Sci. Instr.* **40,** *No. 3, 465–468 (Mar. 1969).*

Key words: DC voltage; low level; measurement.

A low level DC detection system with an attainable precision of 25 pV is described. The system utilizes only normal metal components and commercially available equipment. Measurements can be made automatically, in the presence of large (microvolt) spurious voltages, with switched inputs, and in a non "null" configuration. A typical application is described in detail.

Clark, A. F., Powell, R. L., **Longitudinal magnetoresistance of pure single-crystal copper,** *Phys. Rev. Letters* **21,** *No. 12, 802–804 (Sept. 16, 1968).*

Key words: Copper; electronic scattering; magnetoresistance.

The longitudinal magnetoresistance was measured along the [100] direction of a pure single crystal of copper. The temperature dependence of the saturation ratio, $\rho(B=\text{sat.})/\rho(B=0)$, is given between 4 and 35 K. A limit is placed on the diffusion approximation for small angle electron scattering and it is suggested that the assumption of a relaxation time or of a mean-free-path parallel to the velocity is not valid for some types of impurity or low temperature phonon scattering.

Corruccini, R. J., **Principles of thermometry (measurement of temperature),** *Book, Treatise on Analytical Chemistry, Ed. I. M. Kolthoff, P. J. Elving, and E. B. Sandell,* **41,** *Part I, Theory and Practice, 8, Chapter 87, 4937–4990 (Interscience Publishers, New York, N.Y., 1968).*

Key words: Temperature; temperature measurement; thermometry.

From fundamental thermodynamic concepts the idea of temperature as a quantitative parameter is developed. It is shown how scales of temperature are defined, and how they are accurately realized in practise and transmitted to lower orders of practical thermometers. The operating principles and characteristics of expansion thermometers, resistance thermometers, thermocouples, and radiometric thermometers are presented in some detail.

Creitz, E. C., **Construction details and measurements of response of a gas density balance,** *J. Chromatog. Sci.* **7,** *137–144 (Mar. 1969).*

Key words: Chromatographic detector; density detector; gas density; gas detector.

The measured response of the Nerheim gas density balance, using hot wire anemometers as sensing elements, was compared with the predicted response for such variables as anemometer match, resistance to flow in the exit branches of the duct system, changes in bridge current and reference gas flow rate. Criteria are given for selection of matched pairs of anemometers and for their calibration in the gas flow system. Proper selection of an operating point in terms of reference gas velocity permitted detection of differences in flow rates as small as 1.4×10^{-3} cm s^{-1}. The measured overall sensitivity for oxygen and for methane, using nitrogen as the reference gas, was 0.534×10^{6} and 0.616×10^{6} millivolts per density unit (g cm^{-3}), respectively.

Danielson, B. L., **An optical Faraday rotation technique for the determination of magnetic relaxation times,** *IEEE Trans. Mag.* **MAG–4,** *No. 2, 176–178 (June 1968).*

Key words: Paramagnetic relaxation; Faraday effects.

A technique is described for the measurement of spin-spin and spin-lattice relaxation times in crystals using the optical Faraday rotation as a monitor of the magnetization. The method is applied to the paramagnetic Eu^{2+} ion in $CaF_2:Eu^{2+}$. In this experiment the crystal is placed between a crossed polarizer and analyzer and subjected to a pulsed magnetic field. The transmitted light from a cw argon-ion laser gives a direct indication of the spin relaxation time. Some possible advantages of this technique for the determination of fast relaxation times in concentrated systems are discussed.

Davis, D. D., Braun, W., **Intense vacuum ultraviolet atomic line sources,** *Appl. Opt.* **7,** *No. 10, 2071–2074 (Oct. 1968).*

Key words: Vacuum ultraviolet; atomic lines; flow lamp; photochemistry; O; C; N; Br.

Intense atomic lines (O, N, S, C, Br, Cl, H, Xe, Kr) have been produced by microwave excitation of mixtures of various gases in helium under flow conditions. The intensities generally obtained are greater than 10^{14} quanta/sec and are suitable for atomic fluorescense studies and as photochemical light sources in the vacuum ultraviolet. Conditions for producing these high purity line sources are discussed.

Davis, G. T., Eby, R. K., Martin, G. M., **Variations of the unit-cell dimensions of polyethylene: effect of crystallization conditions, annealing, and deformation,** *J. Appl. Phys.* **39,** *No. 11, 4973–4981 (Oct. 1968).*

Key words: Annealing; crystallization; deformation; density; fold surface; melt; polyethylene; solvent; temperature; time; unit cell.

It is shown that the orthorhombic unit cell dimensions of a given polyethylene are not unique but depend upon physical and thermal history. For polymer crystallized from a 3/4 percent *p*-xylene solution, the values of *a* and *b* determined by the powder camera technique vary (up to 0.6%) systematically with crystallization temperature (50 °C, 70 °C, 90 °C) and the temperature of annealing (up to 127 °C). For "undeformed" crystals, the changes with annealing appear to accompany the increase in crystal thickness and for deformed crystals, they occur over a wider range of temperatures—even below the crystallization temperature. The dimensions change within the first two minutes of annealing and appear to be independent of time thereafter. The only exception observed is a slow decrease of *b* with time upon annealing at 100 °C. Crystals grown from other solvents exhibit very nearly identical effects and the presence of solvents does not alter the cell dimensions at room temperature. Similar effects are observed for crystals grown from the melt by slow cooling, quenching in ice water, and quenching in a dry ice–acetone suspension. The main difference is that cold working does not appear to alter the effects of annealing. The mechanism of the effects cannot be safely assigned but changes in the fold surface probably play a role and a discussion relevant to this and other mechanisms is presented. Corresponding to the changes in cell dimension are changes in cell density which are, however, too small to account for the frequently reported discrepancy between crystal and unit cell density. The effects of cell variation must be considered in interpreting the variation of physical properties.

Dean, J. W., Richards, R. J., **Hydrostatic pressure effects in carbon and germanium thermometers,** *(Proc. 1967 Cryogenic Engineering Conf., Stanford University, Stanford, Calif., Aug. 21–23, 1967), Book, Advances in Cryogenic Engineering* **13,** *505–508 (Plenum Press Inc., New York, N.Y. 1968).*

Key words: Carbon; germanium; pressure effect; thermometer.

This work describes measurements of the hydrostatic pressure coefficient of electrical resitivity for carbon and germanium thermometers in the range of 4 to 295 °K with experimental pressures up to 1000 psig (7.0×10^{6}N/m^2). Pressure coefficients were found to be independent of pressure but to vary with temperature from -0.65×10^{-5} to -1.1×10^{-5} psi^{-1} (-0.944×10^{-9} to -1.6×10^{-9}m^2/N) for germanium and from -1.2×10^{-5} to -1.5×10^{-5} psi^{-1} (-1.74×10^{-9} to -2.18×10^{-9} m^2/N) for carbon. These pressure coefficients result in resistance changes for a 1000 psig (7.0×10^{6}N/m^2) pressure at 20 °K that may be interpreted as temperature errors of 0.3 °K for carbon and 0.03 °K for germanium.

Deslattes, R. D., **Estimates of X-ray attenuation coefficients for the elements and their compounds,** *Acta Cryst.* **A25,** *Part 1, 89–93 (Jan. 1969).*

Key words: Absorption fine structure; mixture rule; X-ray attenuation.

Some recent developments leading to improved knowledge of the distribution of oscillator strength in the photoionization continua of atoms are briefly reviewed. Selective comparisons between the experiments and calculations are indicated. Estimates for attenuation by compounds and solids, insofar as they depart from the mixture rule, require an understnading of x-ray fine structure or, at least of its limiting form, which is not yet at hand. Some of the mechanism leading to fine structure in solids and molecules are briefly reviewed.

Deslattes, R. D., Paretzkin, B., **A small set of reference crystals for double-crystal topography,** *J. Appl. Cryst.* **1,** *Part 3, 176–178 (Sept. 1968).*

Key words: Crystal perfection; silicon; topography.

A set of six reference crystals of silicon makes possible double crystal topography in the grating space range of 1–2 Å with Cu $K\alpha_1$ radiation.

Dickson, R. W., Spinner, S., **An improved method for the determination of torsional and flexural resonance frequencies of cylindrical specimens,** *J. Mater.* **3,** *No. 3, 716–724 (1968).*

Key words: Cylinders; loop; suspension; torsional mechanical resonance frequency.

A suspension method is described for obtaining torsional as well as flexural mechanical resonance frequencies of cylindrical specimens which overcomes many of the difficulties previously encountered in determining the torsional modes for such specimens. The method is readily adaptable for such measurements as a function of temperature. Also internal friction measurements using this method yield responses having less suspension losses than other suspension systems, resulting in more reliable values of internal friction from the specimen.

Douglas, T. B., King, E. G., **High-temperature drop calorimetry,** *chapt. in Book, Experimental Thermodynamics, Eds. J. P. McCullough and D. W. Scott, Vol* **I,** *Calorimetry of Non-reacting Systems, chapt. 8, 293–331 (Butterworth and Co., London, England, 1968).*

Key words: Calorimetric methods; calorimetry; drop calorimetry; thermodynamic properties.

The principles and techniques of the drop method of determining relative enthalpies of solids and liquids above room temperature are discussed in detail and critically, with particular attention to those features which lead to the most accurate results. Typical precise results are compared with those obtained using other calorimetric methods, and the advantages and disadvantages of the drop method are considered. While alternative accessories are referenced and discussed briefly, two important types of furnace (with and without a good thermal conductor) and two types of calorimeter (the "ice" and "copper-block") are treated in detail with respect to their design, construction, and operation with accuracy and convenience. Numerous sample and container problems peculiar to high temperatures are considered. Finally, various aspects of treating the data are dealt with. These aspects include correcting to standard conditions, correcting for chemical impurities and irrelevant phase changes, smoothing and representing enthalpy values, derivation of other thermodynamic properties from enthalpies, and the evaluation and representation of simple expressions of precision and accuracy.

Dragoo, A. L., **Diffusion rates in solids,** *chap. IV in Atomic Energy Review, O. Kubaschewski, Ed., 2, 187–202 (International Atomic Energy Agency, Vienna, Austria, 1968).*

Key words: Borides; carbides; diffusion rates; nitrides; oxides of nuclear materials.

A discussion of the types of diffusion coefficients and of the experimental techniques for their determination is presented for inclusion in the International Atomic Energy Agency Monograph Series on the Physicochemical Properties of Nuclear Materials. The diffusion coefficients for tracer diffusion, self-diffusion, intrinsic diffusion, chemical inter-diffusion and grain-boundary diffusion are described. Experimental methods and limitations are discussed for (1) metallic and metalloid ion diffusion in borides, carbides, nitrides and oxides of Be, Ti, Zr, Hf, Nb, Ta, Mo, Th and U; (2) diffusion of B, C, N and O in metals; and (3) rare gas diffusion from compounds used as nuclear fuels.

Driver, L. D., Arthur, M. G., **A wideband RF voltmeter-comparator,** *IEEE Trans. Instr. Meas.* **IM–17,** *No. 2, 146–150 (June 1968).*

Key words: Detector networks; differential voltmeter; voltage monitor; voltmeter; voltage comparator.

This paper describes a new, wide-band RF voltmeter/comparator for the frequency range dc to 1 GHz and the voltage range 1 to 15 volts. The device employs matched hot-carrier diodes in a dual channel 50 ohm coaxial configuration. Power extraction from the signal under test is negligible and the coaxial line sections are impedance compensated so that the maximum VSWR is 1.02. Applications include the following:

1) Measurement of RF voltage with 3 percent uncertainty limit.
2) Measurement of differential RF voltage.
3) High resolution RF voltage comparator-monitor.
4) Leveler-detector, with flat response, for swept or fixed frequency operation.

Ehrlich, M., **Thermoluminescence response of LiF to X- and gamma-rays; a study of rate and energy dependence over a wide range of exposures,** *Proc. First Intern. Congress Radiation Protection, Rome, Italy, Sept. 5–10, 1966, pp. 429–434 (Pergamon Press Inc., New York, N.Y., 1968).*

Key words: Bremsstrahlung; Co^{60} photons; energy dependence; *F* centers; impurities; LiF (TLD); rate dependence; superlinearity; thermoluminescence; trap formation.

The total thermoluminescence light emission ("response") of LiF (TLD grade) was studied as a function of exposure and exposure rate, and as a function of photon energy. Co^{60} gamma rays and a broad spectrum of low-energy bremsstrahlung were employed. No rate dependence of the response was detected over the entire range of exposures and exposure rates employed (from about 10^2R to 2×10^7R, and from about $10^2R/h$ to $7\times10^6R/h$, respectively). This represents further evidence that centers other than *F* centers are involved in the thermoluminescence of LiF (TLD grade).
A comparison of the curves of response versus exposure for the two photon spectra confirms Naylor's findings that the superlinearity region is steeper for Co^{60} gamma radiation than for low-energy x rays, and reveals that the effect is indeed dependent on photon energy rather than on exposure rate. These findings are compatible with an explanation of superlinearity as being due to the formation of additional traps by the radiation proper. For exposures above those causing superlinearity, the difference in curve shape again disappears. Also, there is no dependence on energy of the location and height of the response maximum, which suggests that the inhibiting mechanism is independent of photon energy.

Ehrlich, M., Placious, R. C., **Thermoluminescence response of CaF_2:Mn in polytetrafluoroethylene to electrons,** *Health Phys.* **15,** *341–350 (1968).*

Key words: CaF_2:Mn; ^{60}Co gamma radiation; electrons, 20 to 400 keV; energy dependence; fluence response; response per unit electron energy absorbed; sample-thickness dependence; thermoluminescence; thin foils.

Foils of powdered CaF_2:Mn in polytetrafluoroethylene, with thicknesses from 15 to 150 μm, were exposed to monoenergetic electrons having energies in the region between 20 and 400 keV. The thermoluminescence response of the foil was studied as a function of the energy and the fluence of the incident electrons, the foil thickness, and the electron energy absorbed in the foils. The dependence on electron energy of the response per unit fluence was found to change considerably with foil thickness, the maximum response occurring at approximately the energy of the incident electrons whose ranges are equal to the thickness of the foil layers. From the lowest incident-electron energy employed (20 keV) up to this energy (200 keV for the 150 μm layer), response per unit fluence increased linearly with electron energy. Therefore, response per unit energy fluence (in this energy range approximately equal to total energy absorbed in the foils) was independent of the energy of the incident electrons, at least within the large error of the experiment. The response per unit of electron energy absorbed also agreed, within the limits of experimental error, with that obtained for foils exposed to ^{60}Co gamma radiation.

Eick, J. D., Hegdahl, T., **Segregation in dental gold casting alloys,** *J. Dental Res.* **47,** *No. 6, Part 2, 1118–1127 (Nov.–Dec. 1968).*

Key words: Casting gold; composition; dental gold alloys; electron micro probe; grain reduction; grain size; segregation.

The purpose of this investigation was to establish a quantitative method for determining the degree of segregation in dental gold casting alloys. The electron micro-probe was employed to analyze concentration differences. A line scan was used to determine the variations in concentration present in the alloy. The nature of the

segregation was expressed by the coefficient of correlation and the coefficient of variation. Segregation occurred between Ag and Cu in the Type I alloys. In the Type II and III alloys Ag and Pd segregated together and opposed Cu, while Ag, Cu, and Pt opposed Pd in the Type IV alloys. Au and Zn did not appear to segregate to a significant degree with the other elements. The coefficient of variation was used to define the degree of segregation on a quantitative basis. The degree of segregation between the fine grained alloys and coarse grained alloys of the same type was not significantly different. Pd was found to have the highest degree of segregation, while Au and Pt segregated the least. As the concentration of Cu was increased in the alloy, the degree of segregation decreased.

Eisenhart, C., Zelen, M., **Elements of probability,** *chap. 12 in Handbook of Physics, second edition, E. U. Condon and H. Odishaw, Eds., Part 1. Mathematics, pp. 1-163–1-197 (McGraw-Hill Book Co., New York, N.Y., 1967).*

Key words: Bayes' theorem; central limit theorem; characteristic function of a distribution; mathematical probability; mean values of random variables; probability distributions; probability inequalities; probability limit theorems; propagation of error; random variables; statistical distributions; tables of probability distributions; transformation of variables in probability distributions.

This chapter provides a concise exposition of the axiomatic definition of (mathematical) probability; of the theory of random variables and distribution functions in one, two, and n dimensions; of the properties of mean values of random variables and of characteristic functions, generating functions, and moments; of measures of location, dispersion, skewness and kurtosis of probability distributions; of weak and strong convergence in probability; of the central-limit theorem and its applications; and of the special properties of the normal, chi-square, Student's t, Snedecor's F, binomial, negative binomial, hypergeometric and Poisson-exponential distributions. The annotated bibliography of 132 entries serves as a guide not only to the principal textbooks, treatises, and monographs on probability theory and its applications, but also to authoritative individual tables of particular probability distributions as well as to general collections of probability and statistical tables.

Enemark, E. A., Gallagher, A., **A Pockels cell light modulator for wide angle radiation,** *Rev. Sci. Instr.* **40,** *No. 1, 40–41 (Jan. 1969).*

Key words: Isotropic radiation; KDP light modulator; light modulator; radio frequencies.

A Pockels cell light modulator which operates at radio frequencies is described. It transmits more isotropic radiation than other Pockels cell or water cell modulators that operate at these frequencies. In addition, the modulated light has less phase variation between different components of the radiation than do water cell modulators.

Engen, G. F., **A method of calibrating coaxial noise sources in terms of a waveguide standard,** *IEEE Trans. Microwave Theory Tech.* **MTT-16,** *No. 9, 636–639 (Sept. 1968).*

Key words: Noise; noise calibration; radiometer.

The UHF and microwave portion of the radio frequency spectrum is characterized by the use of several different types of transmission lines, the most common being coaxial line and rectangular waveguide. A frequent and recurring problem is that of calibrating an item which is fitted with one type of output (or input) terminals, in terms of a "standard" having a different set of terminals or connector. By an extension of certain techniques which were developed in an earlier paper on power calibration transfer, it is possible to make a similar comparison of noise sources. The procedure requires a suitable adaptor and a pair of measurements which are combined in such a way that the adaptor losses approximately cancel.

Engen, G. F., **A method of determining the mismatch correction in microwave power measurements,** *IEEE Trans. Instr. Meas.* **IM-17,** *No. 4, 392–395 (Dec. 1968).*

Key words: Microwave measurements; mismatch; power measurement.

With the increasing demands for accuracy in microwave measurements, mismatch corrections are assuming an increased importance. In the application of a terminating type power meter, the appropriate mismatch factor involves the *complex* reflection coefficients of the generator, load, and power meter.
Instead of measuring the individual reflection coefficients, which usually calls for the use of a slotted line, this paper describes a directional coupler technique which obtains the mismatch factor directly.

Ensign, T. C., Chang, T. T., **Low temperature optical-EPR sample probe using tunable coaxial coupling,** *Rev. Sci. Instr.* **40,** *No. 2, 268–270 (Feb. 1969).*

Key words: EPR-optical double resonance; low temperature; magnetic resonance (EPR); tunable coaxially-coupled microwave cavity.

An optical EPR sample probe using tunable coaxial coupling, for use at fixed temperatures in the range 1–300 K, has been designed and constructed. It allows both critical coupling of the resonant cavity to the microwave system and good sample illumination, while minimizing thermal agitation.

Evans, J. P., Sweger, D. M., **Immersion cooler for freezing ice mantles on triple-point-of-water cells,** *Rev. Sci Instr.* **40,** *No. 2, 376–377 (Feb. 1969).*

Key words: Ice mantle; immersion cooler; triple-point cell.

This note describes a simple immersion cooler designed to freeze an ice mantle on the reentrant well of a triple-point-of-water cell. The cooler consists of a thin wall metal tube, closed at one end and connected to a condenser at the other, filled with a liquid of low boiling point. When the cooler is inserted in the well of the triple point cell and the condenser is chilled with dry ice and alcohol, the liquid-vapor phase transition extracts heat from the cell, producing a uniform ice mantle in 30 minutes.

Feldman, A., Horowitz, D., **Dispersion of the piezobirefringence of GaAs,** *J. Appl Phys.* **39,** *No. 12, 5597–5599 (Nov. 1968).*

Key words: Absorption edge; birefringence, dispersion of piezobirefringence; gallium arsenide; nonlinear piezobirefringence; photoelasticity; piezobirefringence; piezo-optical coefficients; resonance-photolasticity; stress-birefringence.

The piezobirefringence of GaAs shows a large anomalous dispersion near the absorption edge and exhibits a nonlinear stress dependence. The coefficient $\pi_{11} - \pi_{12}$ reverses sign. Lowering the temperature from 298 K to 77 K shifts the dispersion curves + 0.088 eV which is approximately equal to the shift of the energy gap with temperature. These effects, which have not been observed previously in GaAs, are related to the stress dependence of transitions associated with the absorption edge and resonance photo-elasticity described by Kaplyanskii and Lozovskaya.

Feldman, A., Horowitz, D., **Stress-induced dichroism at the absorption edge of $SrTiO_3$,** *Solid State Commun.* **6,** *607–612 (1968).*

Key words: Absorption edge; dichroism; rotary transmission method; selection rules; $SrTiO_3$, uniaxial stress.

The stress-induced dichroism at the absorption edge of $SrTiO_3$ has been measured at room temperature by the rotary transmission method. Stress- and strain-absorption coefficients were determined for the range of photon energies 3.15–3.22 eV. Our results, together with the selection rules derived by Casella, cast doubt upon the assignment of the absorption edge of $SrTiO_3$ to the transition $X_5' \rightarrow X_3$.

Foster, B. E., Blaine, R. L., **A comparison of ISO and ASTM tests for cement strength,** *Am. Soc. Testing Mater. Spec. Tech. Publ. 441, 33–60 (1968*

Key words: Cement strength; ISO cement standards; testing sand; sand gradation.

A comparison of compressive strength tests of 6 portland cements shows that the proposed ISO procedure gave results from 25 to 95 percent higher than ASTM Method C109, depending upon strength level, test age, and cement fineness. The testing sand is seen as the major problem in developing a truly international standard for cement strength, and it is concluded that the selection of equivalent sands is complicated by the prescribed mechanical compaction, which causes forced bleeding. ISO tests using Ottawa-type, round-grain sands are described.

Gardner, T. V., Jr. Dickson, G., Kumpula, J. W., **Application of diffraction gratings to measurement of strain of dental materials,** *J. Dental Res.* **47,** *No. 6, Part 2, 1104–1110 (Nov.–Dec. 1968).*

Key words: Dental amalgam; dental materials; diffraction grating; modulus of elasticity; strain gage; stress-strain measurement.

A system for measurement of strain by means of diffraction gratings ruled on small specimens has been applied to dental materials. The method gives a rapid response to stress, is effective over very short gage lengths, and does not require the attachment of a measuring device to the specimens. Gratings with a spacing of approximately 16,000 lines per inch are ruled on polished specimens. When the specimen is stressed, this spacing is changed resulting in a change in the angle of diffraction of a beam of light directed onto the grating. The change in angle of diffraction is measured by means of photomultiplier tubes behind "V" slits, and from the change in angle, the magnitude of the strain is calculated.

Glasgow, A. R., Jr., **High-temperature valve for corrosive gases,** *Anal. Chem.* **38,** *1104 (July 1966).*

Key words: Fluoride; high-temperature; high-vacuum; metal; nickel-Monel; non-corrosive; valve.

Alterations in a commercially available, bellows-type valve are described which extends its usage with fluorides to higher-temperatures (250 °F to 1000 °F). The altered valve of nickel and Monel parts only was tested with a helium-leak detector from room temperature to 1000 °F and found to be high-vacuum tight across the closed valve seat and at its bellows gasket. The valve has performed well in systems where beryllium fluoride vapors, of fluorine gas, or hydrogen fluoride gas have been present.

Glasgow, A. R., Jr., Ross, G. S., **Cryoscopy, Chapter 88 in Treatise on Analytical Chemistry, Part I, Theory and Practice,** I. M. Kolthoff, P. J. Elving, E. B. Sandell, ed., **8,** *4991–5083 (Interscience Pub., New York, N.Y., 1968).*

Key words: Calorimetry; cryoscopy; dilatometry; freezing; heat of fusion; melting; melting point; molecular weight; purity.

The general principles of cryoscopy as applied to purity analysis, molecular weight determination, and phase investigation are described. The phase rule as it applies to both ideal and non-ideal solutions is discussed. The uses and descriptions of various cryoscopic apparatus are described in some detail. The use of resulting data in the calculation of melting point, sample purity, molecular weight, heat of fusion, heat capacity, and phase diagrams is discussed. The chapter primarily centers around the authors' own work in the field, but includes a bibliography of 175 references.

Haber, S., **A combination of Monte Carlo and classical methods for evaluating multiple integrals,** *Bull. Am. Math. Soc.* **74,** *No. 4, 683–686 (July 1968).*

Key words: Integral; multiple integral; integration; quadrature; numerical analysis; numerical integration; Monte Carlo; modified Monte Carlo.

This is a preliminary announcement, stating results without proof. A class of formulas for multiple integration, called "Stochastic Quadrature Formulas", is defined, and an error estimate given. Some constant-coefficient formulas of this class are described.

Hall, J. L., **The laser absolute wavelength standard problem,** *IEEE J. Quantum Elect.* **QE-4,** *No. 10, 638–641 (Oct. 1968).*

Key words: Laser wavelength standards; wavelength stabilization; saturated molecular absorption.

Stabilized lasers usually exhibit systematic frequency shifts larger than their resettability; this phenomenon is illustrated well by the 6328 Å Helium Neon laser. We describe a Lamb-dip stabilized laser which operates at 1.15259 microns in pure, low pressure (0.12 torr) neon. Optical heterodyne experiments indicate an accuracy exceeding 1 part in 10^9; short and medium term precisions of $1 : 10^{10}$ are easily achieved. We also report the successful operation of a wavelength reference based on the saturation of sharp molecular absorption. In the first experiments the P(7) line of the ν_3 band of methane is saturated inside the cavity of a 3.39 micron Helium-neon laser. The saturation maximum at molecular line center produces an "emission" feature whose linewidth is less than 5 parts in 10^9. The pressure-induced offset is expected to be less than 1 part in 10^{10}. Size scaling is expected to improve these first results by at least 1 decade.

Haller, W., Macedo, P. B., **The origin of phase connectivity in microheterogeneous glasses,** *Phys. Chem. Glasses* **9,** *No. 5,* 153–155 *(Oct. 1968).*

Key words: Glass, microheterogeneous glass; spinoidal decomposition theory; connectivity of microphases; intersecting growth theory; fluctuation theory.

Recently published electron micrographic studies have shown that microheterogeneous glasses with interconnected phases can form from early stages which consist of randomly distributed isolated spheres. These observations lend support to the previously postulated Intersecting Growth Theory, and not to the Spinoidal Decomposition Theory. While a classic diffusion model predicts that the terminal growth rate at approaching surfaces of growing spheres becomes infinitely small due to diffusional depletion of the separating matrix, the experimental facts do not show any such limitations since the approaching growth fronts join rapidly. Various mechanisms are discussed by which a finite joining-rate can be achieved. A mechanism is suggested which is based upon the fact that the classic boundary concept of diffusion is not anymore applicable to bodies of small magnitudes and has to be replaced by the concept of a transitional fluctuating boundary. From ultrasonic and electron microscopic evidence it is estimated that the fluctuations in the investigated systems are of the order of 50Å.
It is furthermore shown that for systems having close to equal volume fraction the criterion for the terminal formation of an interconnected network or of isolated spheroids will be the nucleation density.

Hanley, H. J. M., Childs, G. E., **Interim values for the viscosity and thermal conductivity coefficients of fluid He^4 between 2 and 50 K,** *Cryogenics* **9,** *No. 2, 106–111 (Apr. 1969).*

Key words: Corresponding states; Enskog theory; Helium-four; kinetic theory; quantum fluid; thermal conductivity; viscosity.

We discuss the estimation of viscosity and thermal conductivity coefficients of He^4 between 2 and 50 K for densities up to 0.2 g/cm^3. The literature is reviewed and data sources listed. Interim estimates of the coefficients are given based on limited experimental data, dilute gas kinetic theory, the Enskog theory, and corresponding states.

Hanley, H. J. M., McCarty, R. D., Sengers, J. V., **Density dependence of experimental transport coefficients of gases,** *J. Chem. Phys.* **50,** *No. 2, 857–870 (Jan. 15, 1969).*

Key words: Correlation; density dependence; kinetic theory; least squares analysis; logarithmic expansion; thermal conductivity; viscosity.

We analyse experimental transport data for several gases as a function of density and temperature. Necessary conditions are proposed to check if the data are consistent with a given density function at fixed temperature. It is found that the theoretically suggested density function, which involves terms logarithmic in the density, satisfies the conditions for the data examined in the temperature and pressure ranges considered. A power series in the density does not.

364-586 O - 69 - 4

Based on the analyses, first density coefficients of thermal conductivity and viscosity are reported, together with an estimate of their precision, at reduced temperatures up to $T^* \approx 30$.

Heinrich, K. F. J., **Electron probe microanalysis: a review,** *Appl. Spectry.* **22,** *No. 5, Part 1, 395–404 (Sept.–Oct. 1968).*

Key words: Analysis; spectrometry; x-rays; electron probe; microanalysis.

This review covers the development of electron probe microanalysis in the last ten years. After a brief description of the instrument, the following subjects are discussed: progress in instrumentation, progress in the theory of quantitative analysis, and the future development of microprobe analysis.

Heinrich, K. F. J., Yakowitz, H., **Quantitative electron probe microanalysis: fluorescence correction uncertainty,** *Mikrochim. Acta* **5,** *905–916 (1968).*

Key words: Electron probe microanalysis; error analysis; fluorescence corrections; quantitative analysis; x-ray fluorescence.

In order to evaluate the fluorescence correction uncertainty in electron probe microanalysis, effects of two general types were investigated. The effects of uncertainty in (1) microprobe operational variables, including x-ray emergence angle and operating voltage, and (2) errors in model input parameters, such as fluorescence yield factors and mass attenuation coefficients, were evaluated. The major conclusion of this study is, that even in cases requiring large fluorescence corrections, microprobe operation at high ($\geq 30°$) x-ray emergence angles, and at the lowest voltage compatible with a reasonable x-ray output is entirely satisfactory. This conclusion is reached by substituting into existing fluorescence correction models reasonable input parameter errors, x-ray emergence angles, and operating voltages. Results show that absolute compositional errors vary quite slowly with x-ray emergence angle and operating voltage. The chief source of error among input parameters is the fluorescence yield factor. The role of model selection as a source of potential error is also discussed.

Hertelendy, P., **An approximate theory governing symmetric motions of elastic rods of rectangular or square cross section,** *J. Appl. Mech. Paper No. 68–APM–10, pp. 333–341 (June 1968).*

Key words: Longitudinal modes; theory of symmetric deformations of plates; thickness-shear modes; thickness-stretch modes; variational equations frequency as wave numbers; vibrations of square bars.

Variational equations of motion are developed for symmetric motions of linear elastic bars of rectangular cross-section. In the finite term approximation, sufficient terms are retained to allow a longitudinal mode, two thickness-stretch modes, and two thickness-shear modes of vibration in an infinite bar of square cross-section. Modes for complex wave numbers are also investigated. Adjustment factors in the strain energy and kinetic energy potentials are used to match exact and experimental solutions. Experimental frequency vs wave number results for four modes are reduced by Fourier synthesis and compared both to the approximate theory and to the exact solution for circular cylinders. Theory is intended to predict behavior of thick rectangular bars for which the plane stress solution is not accurate.

Hicho, G. E., Meyerson, M. R., Geil, G. W., **Effect of slack-quenched structures on the tensile properties of AISI 5140 steel** *(Proc. Intern. Conf. Strength of Metals and Alloys), Suppl. Trans. Japan Inst. Metals* **9,** *134–142 (1968).*

Key words: AISI 5140 steel; slack-quenched structures; heat treatment; tempering temperature; tensile strength; yield strength; reduction of area; hardness.

Slack-quenched structures in steels are generally believed to be detrimental even though adequate data on the tensile behavior of these structures are not available. Results are reported of an investigation on the tensile behavior of specimens of AISI 5140 steel slack-quenched to different hardness levels and tested in the conditions as (1) slack quenched and stress relieved at 275 °F, (2) slack quenched and tempered at 400, 550, 700, 850 and 1000 °F, and (3) slack quenched and tempered to selected hardness levels. The tempering of the slack-quenched specimens had a very beneficial effect on the yield behavior and ductility; tempering slack-quenched specimens to a reduction of R_c 5 to 7 in hardness generally produced a maximum increase in the yield strength. Moreover, the yield strength and reduction of area of the slack-quenched specimens tempered to a reduction of R_c 5 to 7 or more in hardness were nearly equal to those of fully-hardened specimens tempered to the same hardness level.

Hiza, M. J., Duncan, A. G., **A simple gas recirculation pump for low flow and high pressure applications,** *Rev. Sci. Instr.* **40,** *No. 3, 513–514 (Mar. 1969).*

Key words: High pressure; low flow rate; pump; recirculation.

A simple pump is described which was designed to recirculate the gas phase in vapor-liquid phase equilibrium studies at flow rates approximately 100 SPP cc/min and at pressures up to 200 atmospheres.

Hiza, M. J., Heck, C. K., Kidnay, A. J., **Liquid-vapor and solid-vapor equilibrium in the system hydrogen-ethane** *(Proc. 1967 Cryogenic Engineering Conf., Stanford University, Stanford, Calif., Aug. 21–23, 1967), Book, Advances in Cryogenic Engineering* **13,** *343–356 (Plenum Press Inc., New York, N.Y., 1968); Proc. Symp. Cryogenic Advance in the Space Program, Tampa, Florida, May 19–22, 1968, 64, No. 88, 57–65 (American Institute of Chemical Engineering, New York, N.Y., 1968).*

Key words: Ethane; hydrogen; hydrogen-ethane system; liquid-vapor equilibrium; low temperature phase equilibrium; solid-vapor equilibrium; solubility of hydrogen in liquid ethane.

Equilibrium gas phase compositions in the system hydrogen-ethane were measured for nine isotherms from 83° to 190 °K up to 150 atmospheres; equilibrium liquid phase compositions were measured for six of the isotherms from 108° to 190 °K. Gas phase compositions up to 130 °K were measured in a single-pass solid-vapor apparatus using continuous analysis with a hydrogen flame ionization detector. The remainder of the measurements were made in a vapor-recirculating liquid-vapor apparatus using chromatographic analysis with a thermal conductivity detector.
Isobaric comparison of enhancement factors, $y_1\pi/p_{01}$, shows the gas phase data obtained by the two methods to be in excellent agreement. These data are in excellent agreement with the gas phase data of Williams and Katz at 185.93 °K. However, the only gas phase data of Williams and Katz below the normal boiling point of ethane (184.52 °K) at 144.26 °K appear to be as much as 25% too high in the concentration of ethane. The liquid phase data are generally higher in hydrogen concentration than the data of Williams and Katz by little more than the combined experimental errors. Very poor agreement was found with the older gas and liquid phase data of Levitskaya from 158.15° to 188.15 °K. The present investigation provides the only gas phase data in the region of the ethane triple point, 89.89 °K.

Hubbell, J. H., Berger, M. J., **Photon attenuation. Attenuation coefficients, energy absorption coefficients, and related quantities,** *Chapter 4 in Engineering Compendium on Radiation Shielding,* R. G. Jaeger, E. P. Blizard, A. B. Chilton, M. Grotenhuis, A. Honig, T. A. Jaeger, H. Eisenlohr, ed. *1, 167–202 (International Atomic Energy Agency, Vienna, Austria, 1968).*

Key words: Attenuation coefficient; Compton scattering; cross section; energy absorption coefficient; gamma rays; pair production; photoelectric absorption, photons; X-rays.

This paper consists of two parts. The first part contains tabulations of the photon attenuation coefficient and the energy transfer coefficient. The values of the attenuation coefficient represent a revision which takes into account new theoretical data on the photoelectric effect and on radiative corrections to Compton scattering and pair production. Rayleigh (coherent) scattering and the photonuclear

effect are disregarded, but can be included by use of auxiliary tables. The main tables cover the energy range 10 keV to 100 MeV for 21 elements and four mixtures. This range is extended to 10 GeV for 16 elements by interpolation from experimental data. The energy transfer coefficient data were taken directly from tabulations in the literature, and cover the energy range 10 keV to 100 MeV. In the second part, information is given on the individual processes (photoelectric absorption, Compton scattering, pair production and other interactions of photons with matter) which combine to give the attenuation coefficient. Theoretical and experimental data are reviewed, and numerical tables and approximation formulas are given.

Hudson, R. P., **The delta campaign. An account of the controversy surrounding the temperature scale for CMN,** *Cryogenics* **9,** *No. 2, 76–79 (Apr. 1969).*

Key words: CMN; low temperature; paramagnetic susceptibility; thermometry.

Theory predicts that the susceptibility of cerous magnesium nitrate will closely approximate Curie's law below 1 K and into the millikelvin region. Specifically, $\chi = c(T-\theta)^{-1}$, with $\theta = -0.27$ mK. Single crystal specimens substantiate this prediction down to about 6 mK, below which strong deviations begin to appear and the susceptibility reaches a limiting, maximum value for temperatures below 2 mK. On the other hand, thermometers fashioned (for convenience) from powdered CMN and shaped into cylinders of diameter equal to height, appear—from the properties of ^{3}He and expectations as to their temperature-dependence—to obey Curie's law down to 3 mK and below. Such drastic differences are of considerable importance, inasmuch as CMN is the only practical thermometer currently available for this region of temperature.
At various times, interested parties have expressed strong views that either the single crystal thermometric results or those for powder cylinders were wrong, or speculated that both might be correct. A condensed survey is here presented of the details of the dilemma, recent attempts to resolve it, and the situation at present.

Hudson, R. P., Kaeser, R. S., **Magnetic temperature scale 0.002–5 °K,** *Proc. Xth Intern. Conf. Low Temperature Physics, Moscow, U.S.S.R., Aug. 31–Sept. 6, 1966, Vol.* **1,** *Properties of Helium, Paper H4, 171–173 (1968).*

Key words: Cerous magnesium nitrate; temperature scale; magnetic thermometer; low temperatures; magnetic cooling; paramagnetic salt.

Our previous measurements of the heat capacity of cerous magnesium nitrate (CMN) as a function of susceptibility using gamma-ray heating have been superseded by new data obtained with a new single-crystal sphere following various improvements in apparatus and procedure. The entropy-susceptibility relation is the same for all specimens and is thus independent of ellipsoid axial ratio; the indicated value of b (coefficient of T^{-2} for "high temperature" heat capacity) is 15 percent smaller than calculated by Cooke, Duffus and Wolf. Combining the heat capacity and entropy data led to values of absolute temperature, which fall below 0.002 °K for the lowest entropy obtained, viz. $S/R = 0.25$. In the region between 0.02 °K and 0.2 °K where both dipole-dipole and lattice specific heat are very small, an anomalous and apparently nonmagnetic contribution to the heat capacity was detected. No explanation for this has been found, but its existence undoubtedly accounts for the apparently non-isentropic demagnetizations experienced for "starting conditions" H/T less than 0.37 oasteds deg^{-1}.

Huget, E. F., Brauer, G. M., **Reactivity of the components of tooth structure,** *J. Colloid Interface Sci.* **27,** *No. 4, 714–721 (Aug. 1968).*

Key words: Components of tooth; reactivity of dentin surfaces; reactivity of anorganic whole tooth surfaces; dentin; anorganic whole tooth; heat of reaction.

A restorative material capable of adhering to tooth structure is greatly needed. Bonding is complicated by the complex nature of tooth structure as well as the mechanical, toxicologic and bacteriologic conditions which occur in the oral cavity. Heats of immersion ($-\Delta H_w$) measurements for dentin, enamel and anorganic whole tooth tissue of known specific surface have been used to study the reactivity and degree of surface modification produced by various ions and functional groups in an aqueous environment. A decrease in the $-\Delta H_w$ value of dentin in water from 10.3 cal/g (4100 ergs/cm^2) to 4.0 cal/g (1590 ergs/cm^2) in 2–40 percent aqueous solutions of organic solvents suggests the strengthening of electro static bonds between polar groups of the collagenous matrix of dentin. In absolute ethanol and hexane, dentin absorbs heat indicating the weakening of hydrophobic bonds. $-\Delta H_w$ values for anorganic whole tooth in aqueous solutions of organic solvents are not appreciably different from those obtained in water (109 ergs/cm^2). The presence of NO_3^-, NO_2^-, CNS^-, SO_4^-, and I^-, at pH 5 depressed the $-\Delta H_w$ of dentin to 4.8 cal/g (1910 ergs/cm^2). Other anions (F^- and Cl^-) had no appreciable effect. At pH 8, however, anions did not appreciably alter the $-\Delta H_w$ of dentin. The addition of aldehyde groups to the liquid adsorbate at pH 8 resulted in the lowering of the apparent $-\Delta H_w$ value of dentin. Changes in $-\Delta H_w$ values for anorganic whole tooth in the presence of anions or aldehyde groups were relatively small.

Iverson, W. P., **Mechanisms of microbial corrosion,** (*Proc. First Intern. Biodeterioration Symp., Southampton, England, Sept. 9–14, 1968), chapter in Biodeterioration of Materials. Microbiological and Allied Aspects, pp. 28–43 (Elsevier Publ. Co., Ltd., Essex, England, 1968).*

Key words: Microbial corrosion; corrosion mechanisms; cathodic depolarization; oxygen concentration cells; metabolic products; anaerobic corrosion.

A discussion of the general and specific mechanisms of microbial corrosion with special emphasis on anaerobic corrosion. General mechanisms include the production of corrosive metabolic products, the initiation of oxygen concentration cells and cathodic depolarization. Recent evidence to be presented indicates that the cathodic depolarization theory may at least in part explain the corrosion due to microorganisms in an anaerobic environment.

Iverson, W. P., **Microbiological corrosion,** *Proc. Conf. Corrosion and Protection of Pipes and Pipelines, London, England, June 13, 1968 (Technical Exhibited Ltd., London, England, 1968).*

Key words: Microbial corrosion; cathodic depolarization; sulfate-reducing bacteria; Desulfovibrio; Thiobacilli; anaerobic corrosion; underground pipeline corrosion.

A discussion of the microorganisms associated with microbial corrosion with emphasis on the sulfate reducers. The mechanisms by which these microorganisms can cause corrosion include; (2) the production of corrosive metabolic products; (b) the formation of concentration cells; (c) cathodic depolarization; (d) combinations of (a), (b) and (c); (e) miscellaneous mechanisms. Corrosive metabolic products which are formed include hydrogen sulfide, ammonia and various acids. The formation of concentration cells will be discussed as it relates to the exterior and interior of pipelines. As the mechanism of cathodic depolarization by bacterial action has been so generally postulated to explain anaerobic corrosion of buried structures, recent evidence for and against this mechanism will be elaborated upon. Practical measures to be instituted in preventing microbial corrosion involve placing underground structures, whenever possible, in "non-aggressive" soil or protection of structures in "agressive" soil by cathodic protection, protective coatings, or both.

Jackson, J. L., Coriell, S. R., **Transport coefficients of composite materials,** *J. Appl. Phys.* **39,** *No. 5, 2349–2354 (Apr. 1968).*

Key words: Transport coefficient; composite material; eutectic; heat conductivity; dielectric constant; magnetic permeability; diffusion constant; electrical conductivity.

The problem of the effective electrical conductivity of a composite material whose local conductivity is a function of position is treated. Using the analogy between this problem and the diffusion of ions in a periodic potential, upper and lower bounds are obtained for the effective conductivity. These bounds are shown to be the conductivities obtained in certain commonly used equivalent circuit approximations. Although the discussion in the paper is in terms

of the electrical conductivity, the theory is equally applicable to many transport coefficients, e.g., the heat conductivity, magnetic permeability, dielectric constant, or diffusion constant.

Johnson, V. J., **Development and operation of a specialized technical information and data center** (*The Cryogenic Data Center*), *J. Chem. Doc.* **8,** *No. 4, 219–224 (Nov. 1968).*

Key words: Operations; current awareness; data evaluation; Bibliography Service; Data Center; Technical Information Center; cryogenics; information retrieval; development.

As is typical of many specialized areas of science and technology, cryogenics has had an explosive development in the last decade and a half. The Cryogenic Data Center was established in 1958 to cope with the problem of organizing the world's literature pertinent to the field of cryogenics and furnishing this rapidly developing industry with reliable information and data. The development of this facility over the ten year period of its existence is discussed. Included is a description of the conversion from a manual to an automated bibliographic retrieval system, the development of cataloging and indexing techniques, the development of comprehensive awareness and literature acquisition procedures with public announcement of new literature, procedures for selecting and compiling data, and finally how the needs of the sponsors and the industry are being served. The discussion emphasizes the problems that are typical in facilities of this type and the need to consider standard or generally accepted solutions. The growing trend for a network system of technical information and data centers requires a high order of compatibility among them.

Joiner, B. L., Rosenblatt, J. R., **The mean deviation and range for $n=3$** *Am. Stat.* **22,** *No. 4, 37–38 (Oct. 1968).*

Key words: Range; mean deviation; samples of size 3; statistics.

Although it is well known that the mean deviation from the sample median is identical to one-third the range for samples of size three from *any* distribution, it is not so well known that the mean deviation from the sample mean has the same distribution as $2/\sqrt{27}$ times the range for samples of size three from the *normal* distribution. In this note a simple method of proving the relationship between the distributions is given, based on the fact that linear functions of normal random variables are normally distributed.

Judd, D. B., **1964 CIE supplementary observer applied to the colorimetry of rutile and anatase forms of titanium dioxide,** *J. Opt. Soc. Am.* **58,** *No. 12, 1638–1649 (Dec. 1968).*

Key words: Color difference; colorimetry; color-matching functions; titanium dioxide; whiteness.

The study by White and Jacobsen of the applicability of the 1964 CIE supplementary observer to large-field colorimetry of the rutile and anatase crystal forms of titanium dioxide has been repeated. The six painted panels used by them were remeasured on a Hardy-type spectrophotometer with closely agreeing results. The arrangement of the panels in order of whiteness by north-sky light was made by 24 observers, yielding 45 arrangements, and these too were in good inverse agreement with the 26 yellowness arrangements made by 13 observers by White and Jacobsen. The spectrophotometric data were reduced to values of U^*, V^*, W^* of the 1964 CIE uniform color space, and the sizes of the chromaticity differences between each panel and the magnesium oxide whiteness standard were computed. By substituting, for CIE illuminant C, the newly recommended CIE illuminants D_{6500} and D_{25000}, representative of overcast sky and clear sky, respectively, and by taking account of normal variations of amount of lens pigment from one observer to another, we found that the 1964 CIE supplementary observer yields correct predictions of the frequency of the various whiteness arrangements of the six panels.

Kamper, R. A., **Cryoelectronics,** *Cryogenics* **9,** *No. 1, 20–25 (Feb. 1969).*

Key words: Electronics; low temperature; superconducting devices.

This is a review of the progress to date in applying superconductivity to electronics.

Kidnay, A. J., Hiza, M. J., Dickson, P. F., **The adsorption isotherms of methane, nitrogen, hydrogen and their mixtures on charcoal at 76 °K,** *(Proc. 1967 Cryogenic Engineering Conf., Stanford University, Stanford, Calif., Aug. 21–23, 1967), Book, Advances in Cryogenic Engineering* **13,** *397–408 (Plenum Press Inc., New York, N.Y., 1968).*

Key words: Adsorption; isotherms; charcoal; hydrogen; methane; mixture adsorption; nitrogen.

The pure component adsorption isotherms of nitrogen, methane, and hydrogen were measured at 76 °K and in the pressure range of 0.19 to 13.5 mm Hg, 0.082 to 6.808 mm Hg and 1.45 to 95.00 atm, respectively. Binary adsorption isotherms for mixtures of 340 ppm nitrogen, 1450 ppm nitrogen, 352 ppm methane, and 770 ppm methane in hydrogen were measured at 76 °K and in the pressure range of 5 to 82 atm. A ternary isotherm for a mixture of 415 ppm methane +686 ppm nitrogen in hydrogen was also determined in the pressure range of 6 to 48 atm.
The empirical adsorption enhancement factor may be used in conjunction with the pure component isotherms to predict the adsorption of nitrogen and methane from the binary gas mixtures with an accuracy that should be sufficient for most engineering calculations. The adsorption of nitrogen and methane from the ternary gas mixtures can be predicted quite accurately through the use of the prediction technique proposed by Kidnay and Myers.

King, R. J., Maley, S. W., Wait, J. R., **Experimental and theoretical studies of propagation of ground waves across mixed paths,** *(Proc. URSI Symp. Electromagnetic Wave Theory, Delft. Holland, Sept. 1965), Chapter in Electromagnetic Wave Theory, J. Brown, ed., pp. 217–224 (Pergamon Press Inc., New York, N.Y., 1965).*

Key words: Electromagnetic ground waves; ground waves; nonhomogeneous paths; propagation of ground waves.

The propagation of electromagnetic ground waves along nonhomogeneous paths has received considerable interest in the past three decades. As a result, several empirical and semi-empirical solutions have been developed and proven useful in calculating the portion of a ground wave transmitted across a coast line. These methods generally have been replaced by more rigorous formulations. Experimental results have been rather meager since ground waves are primarily important at low and very low frequencies where the distances involved are large. Furthermore, it is difficult to evaluate the unwanted effects of other nearby terrain and objects. Therefore, the experiments described here have utilized small laboratory models which simulate, as closely as possible, the mathematical model used in the theoretical formulations. In this way, distances and other parameters can be carefully measured and controlled. If the experimental results compare favorably with the theoretical solution, the theory can then be applied to naturally occurring mixed paths with considerably more confidence.

Koidan, W., **Calibration of standard condenser microphones: coupler versus electrostatic actuator,** *J. Acoust. Soc. Am.* **44,** *No. 5, 1451–1453 (Nov. 1968).*

Key words: Calibration of microphones; microphone calibration standards.

The response-frequency characteristic of a "one-inch" condenser microphone measured by an electrostatic actuator is likely to be significantly different from that measured by reciprocity in an acoustic coupler because of the radiation impedance of the microphone diaphragm with the actuator in place. It cannot be assumed, except at low frequencies, that the radiation impedance is negligible and that the actuator calibration yields the pressure response. Such an assumption also is apt to lead to errors in the determination of the free-field response when calculated with the aid of the free-field correction.

Koonce, C. S., Cohen, M. L., **Theory of superconducting semiconductors and semimetals,** *Phys. Rev.* **177,** *No. 2, 707–719 (Jan. 10, 1969).*

Key words: Dielectric Function; Green's Function; Semiconductors; Semimetals; Superconductivity.

A Green's function method is used to derive a superconducting energy gap equation without the assumption that the Fermi energy is much larger than phonon energies. This equation is then approximated using two separate methods. The first method applies when the screened electron-phonon interaction is almost independent of wavevector and the Fermi energy is of the order of, or larger than phonon energies. The gap equation obtained in this way takes account of the variation in the density of electron states with energy. The second approximation method applies when the screened electron-phonon interaction depends strongly on wavelength or when the Fermi energy is small compared to phonon energies. In this case, the gap equation takes account of the wavevector dependence of the interaction, the wavevector and frequency dependence of the electronic screening, the energy dependence of the density of states, and the wavevector dependence of the superconducting energy gap. In addition, the effects of the retardation of the electron-electron interaction are also included.

Kopec, C. S., **Measurement of gears,** *Handbook of Industrial Metrology, Chapt. 15, pp. 424–450 (Prentice-Hall, Inc., Englewood Cliffs, N.J., 1967).*

Key words: Gears; metrology; index; involute; lead; process control; analytical inspection; composite inspection.

This chapter contains 26 pages of information on gear measuring methods, practices and basic definitiors. The data presented cover only those practices and inspection methods which are recognized and accepted throughout the gear industry as being reliable. The methods described provide measurements which are accurate and repeatable to a degree compatible with the specified quality. Experienced personnel, using calibrated instruments in suitable environment, are required. Process control is the method by which gear accuracy is maintained through control of manufacturing equipment, methods, and processes. When analytical inspection of gear elements is required, methods are described for measuring the following tooth elements: runout, pitch, profile, lead, backlash, tooth thickness and composite method of gear inspection.

Kropschot, R. H., **Report on the fourteenth cryogenic engineering conferecne,** *Cryogenics* **8,** *No. 6, 346–348 (Dec. 1968).*

Key words: Cryogenic Engineering Conference; cryogenics.

Delegates from the United States and 6 foreign countries assembled in Cleveland, Ohio, August 19–21, 1968 to discuss new advances in cryogenics. The Case Western Reserve University was host to the 14th Annual Cryogenic Engineering Conference. The technical program was divided into 12 technical sessions and eight seminars. This review presents the highlights of the conference.

Ku, H. H., **Expressions of imprecision, systematic error, and uncertainty associated with a reported value,** *Meas. Data* **2,** *No. 4, 72–77 (July–Aug, 1968).*

Key words: Accuracy; calibrations; expression of uncertainty; measurements; precision; standard error; systematic error; uncertainty.

The work of a calibration laboratory is described in terms of a sequence of operations that results in the collection, storage and transmittal of information. Since the information content of the statements of uncertainty determines the worth of a reported value, these statements deserve to be well formulated. An annotated guide to such commonly used expressions of uncertainties is given in table form for convenient reference.

Kushner, L. M., **The National Bureau of Standards and the Fire Research and Safety Act of 1968,** *Fire J.* **62,** *No. 5, 32 (Sept. 1968).*

Key words: Fire research; fire technology.

The National Bureau of Standards, which has a long history of activity in the fire research field, will have broadened responsibilities under the terms of the Fire Research and Safety Act of 1968. NBS will not only serve as a research resource, but as a center for administration in new areas of work including technical application to reduce fire losses. The Bureau will seek to avoid duplication of activities underway, and views the new program as a cooperative attack of Government and the private sector on the national fire problem. The levels of activity attained will depend on funding provided, and the short term objective will be to initiate projects for using existing technology to the fullest for reducing losses and improving fire services effectiveness. The development of new techniques for reducing fire losses is a longer term objective.

Lang, S. B., Shaw, S. A., Rice, L. H., Timmerhaus, K. D., **Pyroelectric thermometer for use at low temperatures,** *Rev. Sci. Instr.* **40,** *No. 2, 274–284 (Feb. 1969).*

Key words: Calorimetry; cryogenics; dielectric constant; ferroelectric ceramic; pyroelectric coefficient; thermometry; volume resistivity.

The applicability of pyroelectric thermometry to temperature change or temperature rate measurement at cryogenic levels was studied, with particular emphasis on calorimetry. The pyroelectric coefficients, dc dielectric constants, and volume resistivities of three ferroelectric ceramic materials, Clevite Ceramic B, PZT–4 and PZT–5A, were measured over the temperature range 4.2 to 300 °K. The pyroelectric coefficients were found to be reproducible, but large electric fields, thermal shock, and aging affected the pyroelectric coefficient. Expressions are derived for the temperature responsivity (voltage output per unit temperature change), noise equivalent temperature change (temperature change equivalent to the electrical noise in a pyroelectric thermometer), and figure-of-merit (a parameter characterizing the physical properties of a pyroelectric material). Typical temperature responsivities of 8.0 and 165 volts/°K, and values of noise equivalent temperature change of 2.5 and 0.12 microdegrees K, at 5 and 300 °K respectively, are calculated. Recommendations concerning the usage of a pyroelectric thermometer in a cryogenic calorimeter are given.

Lashof, T. W., **Standardization and application of accuracy and precision statements: TAPPI Standards Committee-ASTM Committee D-6 policy,** *Tappi* **4,** *732–739 (Apr. 1969).*

Key words: Accuracy; paper; precision; standards; test methods.

This paper states the present policy for the use of the terms precision and accuracy for TAPPI and ASTM D-6 Standards and Suggested Methods. Several questions involved in establishing the policy are discussed. Brief examples show how to compute precision from available data, how to state the precision of a test method, and how to apply this information in practical cases.

Levin, E. M., **X-ray determination of the thermal expansion of silver nitrate,** *J. Am. Ceramic Soc.* **52,** *No. 1, 53–54 (Jan. 1969).*

Key words: $AgNO_3$, density $AgNO_3$, polymorphism $AgNO_3$, thermal expansion $AgNO_3$, unit cell dimensions $AgNO_3$.

An x-ray diffractometer furnace was used to obtain powder patterns of orthorhombic (low) $AgNO_3$ between 25° and 140°C and of rhombohedral (high) $AgNO_3$ between 25° and 175 °C. Unit cell dimensions are given for selected temperatures and are essentially a linear function of temperature. The values for the coefficient of expansion of low $AgNO_3$ along a, b, and c, respectively, are 126×10^{-6} deg^{-1}, 57×10^{-6} deg^{-1}, -0.4×10^{-6} deg^{-1}. For high $AgNO_3$ the values along a and c, respectively, are 30×10^{-6} deg^{-1} and 134×10^{-6} deg^{-1}. X-ray density of the high form at a given temperature is greater than that of the low form and, in general, does not agree with previous reported results. The value of dT/dP calculated from the Clausius-Clapyeron equation is -6.9×10^{-3} K/bar, at atmospheric pressure, vs Bridgman's experimental value of -7.6×10^{-3} K/bar.

Little, W. E., Patty, O. L., Zanboorie, M. H., **A millimeter wave reflectometer,** *IEEE Trans. Microwave Theory Tech.* **MTT-16,** *No. 2, 121 (Feb. 1968).*

Key words: Reflectometer; WR–12 waveguide; Millimeter Wave.

This paper describes a millimeter wave reflectometer system that has been developed in WR–12 waveguide. A detailed description

of the system circuitry, a discussion of sources of measurement error and some measurement results are presented.

Lloyd, E. C., **Erasable trace recording methods for chart recorders,** *Rev. Sci. Instr.* **39,** *No. 12, 1953–1954 (Dec. 1968).*

Key words: Chart recorders; automatic; erasable.

Citation of methods described in the technical and patent literature, and description of two new methods, for renewing the chart of closed-chart recorders by automatically removing the trace.

Lloyd, E. C., **Standards for improved measurement of pressure and vacuum** *(Proc. 4th Intern. Measurement Conf., Warsaw, Poland, July 2–7, 1967), Acta Imeko, pp. 451–468 (Hungarian Academy of Sciences, Budapest, Hungary, 1967).*

Key words: Accuracy; calibration; measurement; pressure; standards.

Results of NBS developments are outlined in a number of projects relating to standards for improved measurement of pressures throughout the range from vacuum to very-high pressures. In the vacuum range this includes techniques for generation of stable reference pressures, and improved absolute instruments for force per unit area measurement down to 10^{-9} torr. In the range from a few millibars to hundreds of kilobars the use of fixed points, and the performance of improved piston gages and interpolation instruments, are described. Problems presently limiting accuracy of calibration and NBS investigations of possible solutions are mentioned. Two new "accuracy charts" are presented showing present and possible future NBS capabilities.

Lloyd, E. C., Beckett, C. W., Boyd, F. R., Jr., **Measurements in high-pressure environment,** *Science* **164,** *860–861 (May 16, 1969).*

Key words: Accurate characterization; high-pressure environment; measurements in high-pressure environment.

The highlights of the Symposium on Accurate Characterization of the High Pressure Environment are described. The Symposium was attended by 140 participants from the United States and abroad. Thirty-eight papers were presented and four panel sessions held covering current research at high pressures in static systems and in shock wave experiments. In panel sessions five fixed points below 100,000 bars were proposed, and values for these points recommended. The equation of state of sodium chloride was recommended as a standard for the x-ray determination of pressure. The measurement of temperature in high pressure apparatus and the measurement of phase transformations as a function of temperature and pressure using static and dynamic techniques were presented. Dynamic methods included studies of phase transformations ranging from 20,000 bars up to several million bars. Recent developments in the static high pressure techniques were also presented.

Maeda, K., Young, J., **Propagation of the pressure waves produced by auroras,** *J. Geomagnetism Geoelectricity* **18,** *No. 2, 275–299 (1966).*

Key words: Acoustic modes; auroras; gravity (thermobaric) mode; pressure waves; propagation.

It is shown that the traveling pressure waves associated with auroral activity are not necessarily limited to the acoustic mode, but sometimes extend to the gravity (thermobaric) mode. This is partly due to the existence of large positive lapse rate (i.e. very stable) layers such as in the upper part of the stratosphere and in the thermosphere. As a consequence, clear sinusoidal oscillations which appear occasionally with periods of group velocity minimum (around 5 min) can be ascribed to the Airy phase. As an example, the data obtained at the NBS stations in Washington, D.C. on July 15, 1960 are shown with preliminary results of power spectrum analyses.

Macedo, P. B., Simmons, J. H., Haller, W., **Spectrum of relaxation times and fluctuation theory: ultrasonic studies on an alkali-borosilicate melt,** *Phys. Chem. Glasses* **9,** *No. 5, 156–164 (Oct. 1968).*

Key words: Ultrasonic relaxation; composition fluctuations; spectrum of relaxation times; alkali-borosilicate glass; immiscible alkali-borosilicate glass.

Ultrasonic relaxation measurements (3 to 23 MHz and 750 to 1200 °C) were made using shear waves on a molten glass of 6.72% Na_2O, 25.31% B_2O_3 and 67.97% SiO_2 with a solubility temperature of 749 °C. The spectrum of shear relaxation times was determined between 840 and 1200 °C, where it was found to be highly temperature dependent. A model was proposed which predicts the observed temperature dependence of the spectrum in terms of composition fluctuations. The model is based upon the concept that the activation energy of a molecule depends on the environment within a sphere of radius r_0 about the molecule. The value of $r_0 \sim 50$A obtained from the supercritical composition fluctuations is of the same order as sizes of microheterogeneities directly observed with an electron microscope in single oxide glasses by other workers.

Marzetta, L. A., **Noise limitations in signal detectors,** *Instr. Technol.* **16,** *No. 2, 51–53 (Feb. 1969).*

Key words: Low-frequency detector; noise power; noise temperature; thermal noise; operational amplifiers.

A vigorous development program pursued in recent years by industry has resulted in a number of interesting electropotential detectors. The large void in a performance plot of available signal amplifiers of yesteryear has been almost completely occupied by devices that in some cases approach the theoretical thermal-noise limit, over a signal source resistance range from 10^9 to 10^{16} ohms. There is good reason to expect the small remaining area marked for improvement will be filled in the near future.

Mazur, J., McCrackin, F. L., **Monte Carlo studies of configurational and thermodynamic properties of self-interacting linear polymer chains,** *J. Chem. Phys.* **49,** *No. 2, 648–665 (July 15, 1968).*

Key words: Excluded volume; lattice; Monte Carlo; polymers; random walks; thermodynamics.

Non-self-intersecting walks on the simple cubic and face centered cubic lattices are used as a model for the linear polymer chain with excluded volume. The statistical properties of this model with nearest neighbor interactions between the chain elements are investigated by the Monte Carlo technique. The following properties are investigated: the limiting distribution function of chain-end dimensions, the dependence of mean square length of the chain on the number of chain elements, and the thermodynamic properties of the chain. A particular value for the nearest-neighbor interaction parameter was found which uniquely defines the Flory's theta point of the single chain. Evidence for the phase transitions in the infinitely long chain is also presented.

McCaa, W. D., Jr., Nahman, N. S., **Phenomena and devices, frequency and time-domain analysis of a superconductive coaxial line using the two-fluid model,** *J. Appl. Phys.* **39,** *No. 6, 2592–2596 (May 1968).*

Key words: Superconductive coaxial line; Gorter-Casimir two fluid model; frequency response; step response.

A miniature 80-ft superconductive coaxial line (Nb inner conductor 0.01 in. o.d., Pb outer conductor 0.034 in. i.d., polytetrafluoroethylene dielectric) has been analyzed in terms of the Gorger-Casimir two-fluid superconductivity model, considering the anomalous and classical cases (without relaxation effects) for the normal components. The dielectric and the metal flux trapping losses are assumed to be negligible. The $10^6 - 10^{12}$ Hz line attenuation and the 1–100 psec step responses are presented for the temperature range of 2.3–10 °K. Predictions are compared with the experimental results of several independent investigators. It is concluded that if the dielectric and the metal flux-trapping losses are negligible, then

(1) The model provides bounds between which the responses of physically realized lines will fall, and (2) The normal conductivity of the conductors must be very good if the maximum bandwidth and minimum risetime are to be obtained.

McCamy, C. S., **A half century of photographic standardization in the United States,** *Photo. Sci. Engr.* **12,** *No. 6, 308–312 (Nov.–Dec. 1968).*

Key words: Motion picture standards; photographic standards.

Over the past 50 years, photography and cinematography have reached a high level of standardization in the United States of America. This has been accomplished through cooperative efforts of the photographic industry, interested consumers, and the government. These efforts have been organized by societies such as the Society of Motion Picture and Television Engineers, and by the United States of America Standards Institute and its predecessors. The USA program is coordinated with those of other nations by the International Organization for Standardization. Besides the documentary standards which record the consensus of interested parties with regard to specifications and test methods, there are physical standards, from various sources, which serve as the basis of measurement.

McIntyre, D., Mazur, J., Wims, A. M., **Effects of excluded volume on light scattered from flexible macromolecules,** *J. Chem. Phys.* **49,** *No. 7, 2887–2895 (Oct. 1, 1968).*

Key words: Chain-end distribution; excluded volume; light scattering; particle scattering factor; polydispersity.

The effect of the non-Gaussian behavior of the chain segment distribution in flexible polymer coils on the angular distribution of scattered light is discussed. The explicit form of a general spherical segment distribution function,

$$W(r, N)dr = \frac{t}{\Gamma(3/t)}\left[\frac{\Gamma(5/t)}{\Gamma(3/t)\,\langle R_x^2\rangle}\right]^{3/2}\exp-\left[\frac{\Gamma(5/t)\,r^2}{\Gamma(3/t)\,\langle R_x^2\rangle}\right]^{t/2} r^2 dr,$$

with different values of t, is used to evaluate the general scattering equation for the particle scattering factor $P(\theta)$.

$$P(\theta) = \frac{1}{I_e^2}\sum_i\sum_{i>j}\frac{\sin k s r_{ij}}{k s r_{ij}}.$$

In addition, the effects of excluded volume on the mean end-to-end chain separation $\langle r_x^2\rangle$ is taken to be of the form $\langle r_x^2\rangle \approx N^{1+\epsilon}$, where N is the number of chain steps and ϵ is a parameter, which measures the excluded volume effect on the $\langle r_x^2\rangle$. In this paper, an expansion of the $P(\theta)$ function to the first few terms is carried out and numerically evaluated for the dependence of $P(\theta)$ on the variable x, where $x = ks\langle r_{exp}\rangle$, k is the wave number of the incident light, s is related to the scattering angle and $\langle r_{exp}\rangle$ is the radius of gyration determined from experimental data of the scattering cross section. The computations were carried out for the polymer in good solvent, for which data for ϵ and t were adopted, based on the lattice model of non-self intersecting chain, and for polymer in theta solvent, for which Gaussian chain model was adopted. The computations were carried out for various degrees of polydispersity. A comparison was made between the theoretical and the experimental results on a polystyrene sample of molecular weight of 4.10^6 in cyclohexane at 35°, 45°, 55 °C and in benzene at 40 °C.

Mears, T. W., Young, D. S., **Measurement and Standard Reference Materials in clinical chemistry,** *Am. J. Clin. Pathol.* **50,** *No. 4, 411–421 (Oct. 1968).*

Key words: Clinical; medicine; Standard Reference Materials; measurement.

The concept of the measurement system based upon the four parameters—length (meter), mass (kilogram), time (second), and temperature (kelvin)—is developed. The proper daily operation of an analytical laboratory depend on these basic measurements, and several derived from them, e.g., the liter. An additional component of chemical measurement which directly influences accuracy is the purity of the standards and reagents employed. The Standard Reference Materials program of the National Bureau of Standards provides a central source of guaranteed high-purity reference materials which are available to all. The reliability of chemical measurements will increase as new Standard Reference Materials such as cholesterol, uric acid, urea, and creatinine are utilized to standardize methods and instruments in the clinical laboratories of this country.

Meyerson, M. R., Giles, P. M., Newfeld, P. F., **Dimensional stability of gage block materials,** *J. Mater.* **3,** *No. 4, 727–743 (1968).*

Key words: Gage blocks; dimensional stability; through hardening steel; secondary hardening steel; precipitation hardening steel; ceramic; cermets; length standards; tempering.

Gage blocks which are necessary for the production of dimensionally precise items may undergo a change of dimensions with time. These changes are often extensive enough to cause the gage block to lose its value as a standard of length. This paper describes the program carried out at the National Bureau of Standards, Institute of Materials Research over the past eight years which has been successful in producing gage blocks which exhibit dimensional changes of less than $\pm 2 \times 10^{-7}$ in./in./yr.
Studies have been made on the effect on long term dimensional stability of variation of thermal and mechanical processing procedures of gage blocks produced from four general categories of material. These four categories include (1) through hardened steels, (2) steels with hard cases and annealed cores, (3) steels with hard cases and partially hardened cores, and (4) ceramic and cermet materials.

Mielenz, K. D., **Gas lasers and conventional sources in interferometry,** *chapt. in Book, Electron Beam and Laser Beam Technology, pp. 89–137 (Academic Press Inc., New York, N.Y., 1968).*

Key words: Coherence, interferometers; lasers; light sources; multiple-beam; two-beam.

The theory of length interferometers is derived from the point of view of coherence theory. The performance of gas lasers and conventional sources in length interferometry is discussed.

Mielenz, K. D., **Length measurement and laser wavelength stability,** *ISA Trans.* **6,** *No. 4, 293–297 (1967).*

Key words: Coherence; interferometry; lasers; length measurement, length standards; wavelength stability.

The application of gas lasers as light sources for interferometric length metrology, and the limitations imposed by variations of laser wavelengths, are discussed.

Moore, G. A., **Application of computers to quantitative analysis of microstructures,** *(Proc. Third Intern. Materials Symp., Berkeley, Calif., June 13, 1966), Book, Caramic Microstructures, Ed. R. M. Fulrath and J. A. Pask, Chapt. 3, pp. 71–120 (John Wiley & Sons, Inc., New York, N.Y., 1968).*

Key words: Analysis of microstructures; quantitative microscopy; automatic scanning (of micrographs); precision scanning (of micrographs); computer processing (of micrographs); logical modification of pictures.

The problems and methods of quantitative microscopy are basicly identical in all microscopic sciences. Results are limited by the finite resolution of real micrographs and real observations and by the statistical necessity of processing a very large number of observations, thus dictating automatic scanning, and computer processing methods.
The presence or absence of a specific phase can be represented by a two-dimensional binary array which can be rapidly processed to yield the required measurements. Logical modification by the computer is frequently necessary to substitute for some of the logical discriminations normally made by the human analyst and to facilitate the desired measurements.
Using high precision scanning equipment, the inaccuracies of measurement remain comparable to the limits imposed by statistics. Presently attainable precision is, however, an order of magnitude better than can normally be obtained by manual methods.

Moore, G. A., **Automatic scanning and computer processes for the quantitative analysis of micrographs and equivalent subjects,** (*Proc. Symp. on Automatic Photo Interpretation, Washington, D.C., June 1967*), *Book, Pictorial Pattern Recognition, pp. 275–326* (*Thompson Book Co., Washington, D.C., 1968*).

Key words: Analysis of microstructures; automatic scanning (of micrographs); computer processing (of micrographs); logical modification of pictures; precision scanning (of micrographs) quantitative microscopy.

Basically identical measurement problems are treated in the microscopic branches of all material sciences and in microbiology and medical diagnosis. Visual-manual methods, in use over a century, permit determination of the relative volume of a material phase, and of the average size and spacing of particles of this phase. Redefining a phase as the set of all areas having similar nature and a distinctive tone or color in a photograph, these established methods can be extended to several varieties of non-micrographic pictures.
Statistical considerations require the order of one million observations per picture to attain reasonable precision, dictating automatic scanning and computer processing. Treatment of phase images in binary format permits feasible memory capacities and processing time. Production of a valid binary image requires both high precision scanning and a battery of logical processes which can substitute for darkroom operations and logical discriminating normally made by a human analyst. Other logical processes permit dissection and description of individual phase areas. Presently attainable measurement precision is an order of magnitude greater than is normally attained by manual methods.

Moore, G. A., Wyman, L. L., Joseph, H. M., **Comments on the possibilities of performing quantitative metallographic analyses with a digital computer,** *chap. 13 in Quantitative Microscopy, pp. 380–403* (*McGraw-Hill Inc., New York, N.Y., 1968*).

Key words: Computer analysis of micrographs; grain size; micrographic analysis; pictorial analysis; quantitative microscopy; size distribution.

Preliminary experiments in the analysis of photographic information by means of a digital computer have shown that it is entirely feasible to analyze photomicrographs of metals by this means. The computer may be expected to become the quickest and most economical means of analysis whenever complete grain size or particle size distributions are to be obtained from 80 or more square inches of photomicrograph and when these distributions are to be translated into volume and weight terms.

Munis, R. H., Finkel, M. W., **Goniometric measurements of infrared transmitting materials,** *Appl. Opt.* **7,** *No. 10, 2001–2004* (*Oct. 1968*).

Key words: Infrared scattering; angular scattering instrument; polycrystalline scattering.

An angular infrared scattering instrument has been constructed. Measurements at infrared wavelengths have been made on a polycrystalline specimen. A radiative balance equation has been written and an angular scattering function has been defined. The total scattered radiation is calculated by summation of the scattering function over all solid angles.

Norton, R. B., **Aeronomy Encyclopedia of Atmospheric Sciences and Astrogeology,** R. W. Fairbridge, ed., *pp. 3–7* (*Reinhold Publ. Co., New York, N.Y., 1967*).

Key words: Aeronomy; atmosphere; atmospheric structure and theory.

The definition and general scope of aeronomy is indicated and the division of the atmosphere into regions is discussed. Atmospheric structure and theory is briefly reviewed.

Olver, F. W. J., **Error bounds for the Laplace approximation for definite integrals,** *J. Approx. Theory* **1,** *293–313* (*1968*).

Key words: Asymptotic expansions; Bessel functions; definite integrals; error bounds; gamma function; Laplace approximation.

Explicit error bounds are obtained for the well-known asymptotic expansion of integrals of the form

$$\int_a^b e^{-\lambda p(x)} q(x)\,dx$$

in which λ is a large positive parameter, $p(x)$ and $q(x)$ are real differentiable functions, and $p'(x)$ has a simple zero in the finite or infinite range $[a, b]$. The bounds are expressed in terms of the supremum of a certain function taken over $[a, b]$ and are asymptotic to the absolute value of the first neglected term in the expansion as $\lambda \to \infty$. Several illustrative examples are given, including modified Bessel functions and the gamma function.

Paabo, M., Bates, R. G., **Standards for a practical scale of pD in heavy water,** *Anal. Chem.* **41,** *No. 2, 283–285* (*Feb. 1969*).

Key words: Acidity; carbonate; citrate; deuterium oxide; deuterium ion; glass electrode; heavy water; pD; phosphate; standards for pD.

The glass electrode has been found to respond to deuterium ion in heavy water solutions as well as to hydrogen ion in ordinary water. Furthermore, the glass-calomel pH assembly is useful for practical measurements of pD in heavy water. Several standard reference solutions for pD are needed, however, as the response of individual glass electrodes is not constant over the entire useful pD range. A suitable phosphate solution (pD 7.428 at 25 °C) composed of KD_2PO_4 and Na_2DPO_4 (each 0.025 molal) was established in earlier work. This reference has now been supplemented by two other useful buffer solutions, namely 0.05m KD_2 citrate (pD 4.293 at 25 °C) and a mixture of $NaDCO_3$ and Na_2CO_3 (each 0.025 molal) which has a pD of 10.736 at 25 °C. Values have been assigned at 10 temperatures from 5 to 50 °C. The conventional pD scale fixed by these three standards has been shown to have a satisfactory internal consistency.

Potzick, J., **ac-dc Regulator-modulator,** *Rev. Sci. Instr.* **39,** *No. 8, 1219–1220* (*Aug. 1968*).

Key words: Feedback; modulator; regulator.

A general purpose regulator-modulator is described in which the gain of a d-c amplifier is determined by a control voltage derived through an external feedback loop.

Powell, C. J., **Characteristic energy losses of 8-keV electrons in liquid Al, Bi, In, Ga, Hg, and Au,** *Phys. Rev.* **175,** *No. 3, 972–982* (*Nov. 15, 1968*).

Key words: Aluminum; bismuth; electron energy loss; gallium; gold; indium; liquids; mercury; solids.

Characteristic loss spectra have been obtained in a reflection scattering geometry for liquid Al, Bi, In, Ga, Hg and Au and, in the case of Al, Bi and Au, for the same specimens in the solid phase. Peaks due to surface and volume plasmon excitation dominated the loss spectra for all elements except Au. The relative intensity of these peaks varied rapidly with scattering angle for the liquid and frozen specimens but there was little angular variation when Al, Bi, or Au was evaporated onto a frozen substrate of the same element. The Al plasmon losses varied with temperature and changed at the mp as would be expected from the known density variation. Changes in the Bi plasmon energy losses on melting and changes in other structure on melting have been interpreted in terms of band-structure changes. The peaks in the gold loss spectra appeared to become broader and less distinct on melting from which it was concluded that the Au excited states had shorter lifetimes with increased disorder. In general, however, the liquid and solid-state spectra of the same element were similar, thereby showing that for these materials there was not a large change in band structure on melting.

Powell, C. J., **Interaction of electrons with solids,** *chap. 9.2 in Atomic and Electron Physics, Atomic Interactions, Vol.* **7,** *Methods of Experimental Physics, B. Bederson, Ed., Part B, pp. 275–305* (*Academic Press Inc., New York, N.Y., 1968*).

Key words: Cross-sections; elastic scattering; electron detectors; electron energy analyzers; electron guns; electron scattering; electron-solid interactions; experimental techniques; inelastic scattering; multiple scattering; secondary processes; specimen preparation.

A review is given of methods and techniques useful in experiments where electrons of energy between 0 and 100 keV interact with solids. A general discussion is given firstly of common experimental components and procedures: electron guns, energy analyzers, and electron detectors; specimen preparation; and experimental strategy. The interaction of electrons with solids is considered firstly by assuming that the solid can be represented as an assemblage of atoms, thereby simplifying the analysis. Elastic and inelastic scattering measurements are discussed, followed by a survey of methods useful in situations where multiple scattering occurs and where secondary or higher order electrons and photons are generated. Finally, the relevance of angular anisotropies in elastic and inelastic electron scattering by crystalline solids is described.

Quindry, T. L., **Transmissibility measurements for the determination of structural damping,** (*Proc. Vibrations Conf., Philadelphia, Pa., Mar. 30–Apr. 2, 1969*), *Preprint No. 69–VIBR–36, 7 pages* (*American Society of Mechanical Engineers, New York, N.Y., 1969*).

Key words: Air; antiresonances; cantilever beam; damping; mass-loading; resonances; tip rotary inertia; transmissability; vacuum.

A straightforward means of determining the damping coefficient of structural metals by the use of a mass-loaded cantilever beam is described. In order to determine the structural damping coefficient, δ, from the form $E^*=E(1+j\delta)$, experimental data is normalized to fit the non-dimensional equations of transmissability. Only the experimental values of frequency for the first and second resonance and of transmissability for the first antiresonance and second resonance are needed to determine the structural damping coefficient. The boundary conditions account for the effects of mass-loading and tip rotary inertia. For the same alloys, root stress and temperature did not vary appreciably during the conditions of the test.
Good repeatability was obtained for tests in air and in vacuum from specimens of ZK60A T5 magnesium alloy and 2024 T4 aluminum alloy.
Advantages of mass-loading and obtaining the structural damping coefficient from transmissability at the second resonance are cited.

Ray, C. D., Tsukishima, T., Hyland, R. N., McLane, C. K., Carpenter, R. J., **Analysis of a frequency-swept one-bit digital correlator,** *J. Appl. Phys.* **39,** *No. 8, 3534–3542 (July 1968).*

Key words: Correlator; cross-correlator; digital correlator; diffusion coefficient; plasma; frequency-swept.

An instrument for measuring the cross spectra density of two random variables which are correlated is described. It was constructed to study the relationship between electron density fluctuations and the ambipolar diffusion coefficient in a plasma. A stability in the zero correlation level of 10^{-3} is achieved by use of one-bit digital electronics in the multiplier and integrater. An analysis of the design and function of the instrument is given together with a discussion of possible instrumental errors and statistical uncertainties in the measurements.

Rhodes, I., **The importance of the glossary storage in machine translation,** *Book, Machine Translation, Ed., A. D. Booth, pp. 431–449* (*North-Holland Publ. Co., Amsterdam, The Netherlands, 1967*).

Key words: Glossary storage; machine translation; mechanical translation.

It is imperative that the "blueprints" of the entire scheme for Mechanical Translation be completed, before venturing to embark upon the extremely time- and money-consuming task of constructing the accompanying Machine Glossary. Moreover, this gigantic undertaking needs the full cooperation of all competent workers in this field. A brief outline of the NBS scheme, as well as excerpts from the proposed Glossary, are given in order to highlight the reasons for the above assertions.

Robbins, C. R., **Growth of strontium titanate from a silica flux,** *J. Crystal Growth* **2,** *402–404 (1968).*

Key words: Strontium titanate; single crystals; silica flux; high temperature microscopy; flux growth.

A survey of selected compositions in the ternary system SrO-TiO_2-SiO_2 by high-temperature microscopy has shown that single crystals of $SrTiO_3$ may be grown from a silica flux. Crystals up to 2.5 mm in longest dimension were obtained in a small scale experiment by slow cooling of a 20 g melt of mole ratio 1 $SrTiO_3$: 1 SiO_2. The crystals are clear, colorless to pale brown, of good optical quality, free from inclusions and show no evidence of solid solution by X-ray powder diffractometry.

Robbins, R. F., Reed, R. P., **Tensile properties of neoprene below the glass transition temperature** (*Proc. 1967 Cryogenic Engineering Conf., Stanford University, Stanford, Calif., Aug. 21–23, 1967*), *Book, Advances in Cryogenic Engineering 13, 252–258* (*Plenum Press Inc., New York, N.Y., 1968*).

Key words: Tensile strength; neoprene; glassy state; low temperature; mechanical property; ultimate strength; modulus; rubber.

This paper describes tensile tests on two neoprene compounds at low temperatures. The neoprene compounds were chosen to determine the effect of carbon black filler material on the tensile properties below the glass transition temperature. Stress-strain curves were obtained at 4, 76, and 195 °K, and at strain rates between 0.01 and 10 inches per inch per minute. Results include the following: 1) Neoprene was ductile at temperatures 40 °K below the glass transition temperature (T_g); 2) The ultimate strength of the filled neoprene was less than the unfilled below T_g; 3) The ultimate strength of the filled neoprene was lower at 4 °K than at 76 °K; 4) The ultimate strength of neoprene at 195 °K was strain-rate dependent, and the ultimate strength of the filled neoprene showed a maximum at an intermediate strain rate.

Romanoff, M., **Performance of ductile-iron pipe in soils,** *J. Am. Water Works Assoc.* **60,** *No. 6, 645–655 (June 1968).*

Key words: Corrosion; pipe; underground; pipelines; gray iron; ductile iron; cast iron; soil corrosion; exposure sites; ferrous metals.

This is a progress report on the behavior of specimens of ductile cast-iron pipe after exposures for 1, 2, 4 and 8 years at five National Bureau of Standards soil corrosion test sites. It can be concluded from the data that ductile cast-iron and gray cast-iron corrode at nearly the same rate in a given soil environment, and that the pattern of corrosion and nature of the graphitic corrosion products are also similar for the two materials in a given soil.

Ryan, J. V., **Flammable fabrics act and its implementation,** *Mod. Textiles Mag.* **L,** *No. 3, 67–70 (Mar. 1969).*

Key words: Fabrics; flammability; flammable fabrics act; interior furnishings; National Advisory Committee; textile technology; Textiles; wearing apparel.

The provisions of the Amendments to the Flammable Fabrics Act are reviewed against the background of the original Act plus experiences with its effectiveness. Cooperation with the accident investigation efforts of the Public Health Service is described. Acquisition of data from additional sources has been somewhat successful.
The Department's procedures for rulemaking involve several steps with opportunity for comment from interested parties at two different times, followed by consultation with the National Advisory Committie for the Flammable Fabrics Act.
A general program approach is described, but the level of funding for the current fiscal year will place serious limitations on the ability to implement the program fully.

Sanderson, B. T., Romanoff, M., **Performance of commercially pure titanium in corrosive soils,** *Mater. Production* **8,** *No. 4, 29–32 (Apr. 1969).*

Key words: Corrosion; exposure sites; pipe; soil corrosion; steel; titanium; underground.

This is a progress report on the behavior of specimens of titanium tubing with welded seams after exposure in the soils at six National Bureau of Standards corrosion test sites for exposures up to 8 years. The data show that the titanium tubing as well as the weld and heat affected zones are unaffected by corrosion with respect to pitting or metal attack in any of the soil environments to which they were exposed. Weight losses on the specimens were negligible in all soils. Data for carbon steel pipe specimens which were used as a reference material to determine the corrosiveness of the soils are included.

Saunders, J. B., Bruening, R. J., **A new interferometric test and its application to the 84-in. reflecting telescope at Kitt Peak National Observatory,** *Astron. J.* **73,** *No. 6, 415–531 (Aug. 1968).*

Key words: Aberration of telescopes; interferometer; shearing interferometer; telescopes; wavefront shearing interferometer.

The 84 inch aperture, Cassegrainian type telescope at Kitt Peak National Observatory was tested with a wavefront shearing interferometer. This test provided the optical path difference between 538 uniformly spaced rays in the annular beam of light transmitted by the telescope. Independent tests were made from photographs taken on each of two consecutive nights. The following results were obtained from this test: (a), the coordinates of the points of incidence of each of the 538 rays on the focal plane (a spot diagram), (b), a measure of primary astigmatism; and (c), the deviation of the wavefront, at 538 uniformly spaced points, from a sphere that is centered on the ideal image point.
A description of the mathematical operations is given with the results. The results show a measurable change in the waveform during the test periods (approximately 30 minutes) each night and a larger difference from one night to the next.

Scharf, K., **Steady-state response of silicon radiation detectors to X and gamma rays,** *Proc. Symp. Physics and Nondestructive Testing, ITT Research Institute, Chicago, Ill., Sept. 27–30, 1966, 1, 235–298 (Air Force Materials Laboratory, Wright-Patterson Air Force Base, Ohio, 1968).*

Key words: Radiation detection; radiation detectors; silicon; semiconducting devices; dosimetry; x rays; gamma rays; photovoltaic effects; photodiodes.

A review is given of investigations of the steady-state response of silicon radiation detectors to x and gamma rays which were carried out in the Radiation Physics Division of the National Bureau of Standards. Theoretical relations between photocurrents generated in such detectors by x and gamma rays and exposure rate and quality of radiation are explained. Measurements of the dependence of the generated photocurrent on exposure rate, quality of radiation, voltage applied, and detector temperature carried out on different types of detectors are presented, and different modes of operation of silicon radiation detectors are discussed. By using a special electrical compensation method, exposure rates were measured ranging from 100 mR/hr of ^{137}Cs gamma rays to 10^5 R/hr of 30-kV x rays.

Shideler, R. W., **Interfacing a teletypewriter to nuclear instruments used for computer-coupled activation analysis,** *Proc. 1965 Intern. Conf. Modern Trends in Activation Analysis, College Station, Texas, Apr. 1965, pp. 236–242 (1965).*

Key words: Digital instruments; digital multichannel pulse-height analyzer; multichannel analyzers; nuclear instruments; teletypewriter.

In performing activation analysis using modern digital instruments the volumes of numerical data dictate that an expedient data handling system be used.
The primary concern of this paper is to discuss the techniques and actual designs involved in the interfacing of a teletype to a digital multichannel pulse-height analyzer and to an automatic sample changer.
Two separate designs are discussed for interfacing to the multichannel analyzers. The first involves only minor changes to the analyzer. The second provides interfacing with no modification to the standard analyzer, and includes the additional capability of reading precursor data from external units including a time-of-year clock and programmed data groups. These additional data are included in the output format along with the analyzer data and serve to identify the data as well as to instruct the computer in its subsequent analysis.
Of primary importance in this paper is a discussion of the merits and advantages to be found in adopting the use of the teletype machine as an input-output device. As well as providing typed copy, it will punch and read a paper tape coded in the new ASCII code. The automatic inclusion of precursor data and an appropriate readout format brings on-line computer operation to a reality.

Shimizu, A., **Calculations of the penetration of gamma rays through slabs by the method of invariant imbedding,** *Nucl. Sci. Eng.* **32,** *184–194 (May 1968).*

Key words: Invariant imbedding; transport; shielding; energy spectrum; angular distributions; gamma rays.

The method of invariant imbedding has been applied to the penetration problem of gamma rays through slabs. The accuracy of the method was examined by comparison with other reliable calculations and proved to be competitive with other well developed methods. The method has the advantages that it is much more efficient than the Monte Carlo method and that it is readily applicable to the multi-layer problems. An extensive series of calculations on the transmission of gamma rays through homogeneous slabs was carried out. The energy and angular distributions of transmitted photons from mono-energetic and oblique sources were obtained for slab thickness up to fifteen mean free paths and for seven materials. The results of calculations were compared with experiments.

Shimizu, A., **Calculation of the penetration of gamma rays through two-layer slabs,** *Nucl. Sci. Eng.* **32,** *385–391 (June 1968).*

Key words: Gamma-rays; penetration; dose transmission; invariant imbedding; two-layer slabs; transport theory.

The method of invariant imbedding has been applied to the penetration problem of gamma rays through two-layer slabs, and turned out to be accurate and less time consuming than the Monte Carlo method. A series of calculations were made for two-layer slabs of water, iron and lead for plane oblique sources. An approximate formula for synthesizing the buildup factor of a composite slab from those of elementary layers is derived from numerical solutions by modifying the formula originally proposed by Kalos.

Smith, G. W., Becker, D. A., **Preparation of an NBS biological standard reference material for trace elemental analysis,** *Proc. Nuclear Activation Techniques in the Life Sciences, Amsterdam, The Netherlands, May 8–12, 1967, pp. 197–207 (International Atomic Energy Agency, Vienna, Austria, 1967).*

Key words: Biological; trace; tissue; botanical; bone; blood; reference; neutron; activation; analysis; non-destructive; destructive; variance; leaves; liver; homogeneity.

A survey of leading U.S. biological, medical and forensic laboratories confirms the need for well characterized botanical, soft mammalian tissue, bone tissue and blood standards with elemental constituents at the 100 ppm level and below. The only sources of dried and sterilized tissue and blood known to the authors are certain U.S. drug concerns, whereas H. J. M. Bowen's kale has only been available since 1964 as a botanical comparison sample.
Before reliable analytical data can be obtained on a reference material, homogeneity must be established. Examples are given of this procedure, which is carried out routinely by the NBS on Standard Reference Materials. Homogeneity of Bowen's kale for chlorine (~ 4000 ppm), manganese (~ 14 ppm) and copper (~ 6 ppm) as well as for manganese in beef liver (~ 10 ppm) citrus leaf (~ 28 ppm) and oak leaf (~ 1000 ppm) are given. Measurements were made by neutron activation analysis both with and without chemical separa-

tion, using a Ge(Li) semiconductor detector. This technique was also used for the quantitative determination of the trace constituents chlorine and manganese, non-destructively. In addition, a destructive method was used for the elements arsenic and copper. Analyses of variance, using the activation analysis data, indicate that all of the biological materials except the citrus leaves are homogeneous. Therefore, preparation under contract, of large lots of deciduous leaves and beef liver, will begin. Analyses for homogeneity and elemental content certification will be made by NBS activation analysis and other analytical competencies.

Shives, T. R., Bennett, J. A., **The effect of environment on the fatigue properties of selected engineering alloys,** *J. Mater.* **3,** *No. 3, 695–715 (1968).*

Key words: Fatigue; engineering alloys; environment; humidity; oxygen; crack initiation.

Rotating beam fatigue tests were conducted in controlled environments on specimens of free cutting brass, titanium alloy Ti-4A1-4Mn, magnesium alloy AZ61A, and A1S1 4340 steel. The fatigue strengths of all the alloys were lower in a moist atmosphere than in a dry one, although the difference was small for the brass specimens. The effect of oxygen on the fatigue behavior of the titanium alloy and a vacuum-melted 4340 steel was investigated by conducting tests both in air and in an inert gas; the influence of oxygen was found to depend on whether or not moisture was present. In many of the vacuum-melted steel specimens the fatigue crack started below the surface, and the performance of these individual specimens was related to the size of the inclusion at the origin of the crack. A coating of dodecyl alcohol had a beneficial effect on the two materials (magnesium alloy and steel) on which its influence was investigated. An interesting tarnishing effect was observed on the fatigue portion oxygen; crack initiation.

Smith, R. V., **Current developments in cryomedicine,** *Cryogenics* **9,** *No. 2, 84–89 (Apr. 1969).*

Key words: Cryobiology; cryomedicine; cryosurgery; cryopreservation; cryoprotectants; freezing; thawing.

The paper reviews current developments in the field by summarizing papers presented in the Fifth Annual Meeting of the Society for Cryobiology. Cryomedicine is divided into two areas for the purpose of discussion; cryosurgery and cryopreservation of biological material for clinical use.

Smith, R. V., **Review of heat transfer to helium I,** *Cryogenics* **9,** *No. 1, 11–19 (Feb. 1969).*

Key words: Boiling; Convection; critical; heat transfer; helium I; supercritical.

This paper reviews heat transfer to helium I. Recommendations are made for expressions to be used in design studies and for further work required to produce needed information.

Steward, W. G., Smith, R. V., Brennan, J. A., **Cooldown time for simple cryogenic pipelines** *(Proc. Tenth Midwestern Mechanics Conf., Colorado State University, Fort Collins, Colo., Aug. 21–23, 1967), Book, Developments in Mechanics* **4,** *1513–1525 (Johnson Publ. Co., Boulder, Colo., 1968).*

Key words: Chilldown; cooldown time; cryogenic fluids; transfer lines.

An uncooled pipeline which is used to transfer a cryogenic fluid from one point to another, must ordinarily go through a period of cooling down from ambient temperature to near the liquid boiling temperature. During most of this period the liquid boils and the pipe delivers only warm gas. Some effective methods of estimating this cooldown time have been proposed but they are all laborious. This paper offers a quick method by which cooldown time for a simple system can be calculated from a dimensionless parameter read from a graph. To use the method it is necessary to know the fluid and pipe enthalpy, density, and velocity of sound in the warm gas. The idealized model and closed form solution are described, and comparison with experimental results is shown.

Swartzendruber, L. J., Ulmer, F. H., Coleman, J. A., **Direct reading instrument for silicon and germanium four-probe resistivity measurements,** *Rev. Sci. Instr.* **39,** *No. 12, 1858–1863 (Dec. 1968).*

Key words: Four-point probe; germanium; resistivity measurement; silicon.

A direct reading instrument of moderate precision (± 5%) has been developed for the rapid measurement of resistivity, and its uniformity of silicon and germanium samples with a wide variety of shapes and sizes. An in-line, four-point probe and two analog computing circuits to set the required geometrcial correction factors are used in the instrument. The main features of the instrument are the simplicity of its construction and the facility with which the resistivity measurements can be accomplished.

Tauber, S. J., **Imprecision-problems for information processing,** *Am. Doc.* **19,** *No. 4, 413–414 (Oct. 1968).*

Key words: Imprecision; experimental conditions; semantics; mnemotechnics; levels of abstraction; specificity; information system design.

Some of the characteristics of imprecision which affect information storage and retrieval are pointed out and discussed in the areas of numeric values, experimental conditions, and semantics.

Trugel, R. S., **A comparator for thermal ac-dc transfer standards,** *ISA Trans.* **6,** *No. 4, 286–292 (1967).*

Key words: A–C; D–C; calibration; transfer standard; thermoelement; intercomparison.

Thermal transfer standards play an important role in precision a-c measurements. They are calibrated by intercomparison with standards of known ac-dc difference. A comparator is described that simplifies such routine calibrations. A sequence of null balances in the measuring circuit operates a simple analog computer which indicates the result of the inter-comparison directly in parts per million of ac-dc difference.

Thomas, A. M., **Monte Carlo study of vacuum vane gauge design criteria,** *J. Vacuum Sci. Technol.* **5,** *No. 6, 187–193 (Nov.–Dec. 1968).*

Key words: Molecular flow; Monte Carlo; vacuum; vacuum gauge; vane gauge.

A Monte Carlo method is presented by which the effects of molecular motion in free molecular flow systems of various geometries may be studied. The geometry used in this study is that of a straight tube of circular cross section with a circular vane co-axial with and placed at various distances from the end of the tube. Calculations are made of the ratio of the force on the vane to the isotropic pressure at the opposite end of the tube. Parameters which are varied are tube length, tube wall thickness, distance to the vane, and radius of the vane; all of which are measured in terms of one tube radius. This study revealed that, for short, thin walled tubes and for a large vane, the force on the vane is fairly insensitive to the amount of separation between the tube and the vane as long as this separation is less than about one half a tube radius. However, for longer tubes, the force on the vane falls off quite rapidly as the vane is moved away from the tube end. Also, for tubes with thicker walls, the force-to-pressure ratio increases as the vane is first moved away from the tube and reaches a maximum which may be greater than twice the original value.

Travis, J. C., Spijkerman, J. J., **Mössbauer spectroscopy with Ni^{61},** *chap. in Mössbauer Effect Methodology,* **4,** *237–259 (Plenum Press, Inc., New York, N.Y., 1968).*

Key words: Nickel Mössbauer spectroscopy; single line source; chemical shifts; quadrupole splitting; internal magnetic fields; magnetic fields; magnetic moment ratio; nuclear hyperfine interactions; electronic configurations.

The practical application of Mössbauer spectroscopy to the study of nickel compounds has been retarded by two factors: 1) the late discovery of a suitable, single line source, and 2) the short half lives of both possible parent isotopes of ^{61}Ni. A suitable source of 15% Cr in Ni is activated by one hour of exposure to 100 MeV bremsstrahlung in the NBS linear electron accelerator. The source has a fractional effect of 0.1 ± 0.02, and yields an experimental linewidth of 0.097 ± 0.002 cm/s when extrapolated to zero thickness in source and absorber.

Adequate data have been obtained to determine a magnetic moment ratio, $\mu_e/\mu_g = -0.568 \pm 0.055$, and an estimate for the change in the nuclear charge radius, $\delta R/R = -2.5 \times 10^{-4}$. The ground state quadrupole is negligible for Mössbauer spectroscopy. Spectra which illustrate pure magnetic, pure quadrupolar, and mixed (Laves phase) interactions have been obtained.

This paper discusses the preparation of a single line source, the evaluation of nuclear parameters, theoretical studies of the nuclear hyperfine interactions, and theoretical prediction of the electric field gradient tensor.

Trembath, C. L., Wait, D. F., Engen, G. F., Foote, W. J., **A low-temperature microwave noise standard,** *IEEE Trans. Microwave Theory Tech.* **MTT-16,** *No. 9, 709–714 (Sept. 1968).*

Key words: Cryogenic; microwave; noise; standard.

An X-band thermal noise source is described which consists of a waveguide termination, cooled in a cryogenic environment, along with temperature and pressure monitors and controls. With liquid helium as the cryogen, the effective noise output at the room temperature flange can be set to values around the boiling point of helium (4.2° K) with an accuracy of ± 0.03° K. With liquid nitrogen as the cryogen, the output temperature can be set to values around 77° K with an accuracy of ± 0.16° K.

This accuracy is made possible by several unique features. First, the terminating waveguide section is a vapor bulb thermometer with the abosorbing load surrounded with the cryogenic liquid. Second, heat exchangers are used to permit an unusually short waveguide transition section between cryogenic and room temperature. Third, an absolute pressure regulator is used to control the cryogen boil-off rate resulting in a temperature stability of 0.002° K for helium and 0.02° K for nitrogen.

At present, the useful accuracy of the standard is limited to ±0.1° K because of uncertainties in the insertion loss (about 0.001 dB) of mating room temperature flanges.

Tsai, D. H., Beckett, C. W., **Shock wave propagation in a two-dimensional crystalline lattice** *(Proc. Intern. Union of Theoretical and Applied Mechanics: Intern. Symp. Behavior of Dense Media Under High Dynamic Pressure, Paris, France, Sept. 11–15, 1967), chapt. in Book, The Behavior of Dense Media Under High Dynamic Pressure, pp. 99–108 (Gordon and Breach Publ., New York, N.Y., 1968).*

Key words: Shock wave propagation; two-dimensional lattice dynamics; lattice stability; thermal oscillations; energy calculations; Grüneisen parameter.

Lattice dynamics has been applied to the study of the propagation of a strong, one-dimensional shock wave in a two-dimensional face-centered cubic lattice. The shock was generated at the free surface of the lattice by impact, and propagated into the lattice in the longitudinal direction perpendicular to the free surface. The transverse motion of the lattice points allowed the shock wave to be scattered and the compressive energy to be distributed between the longitudinal and transverse degrees of freedom. In our calculation, a Morse type potential function between pairs of lattice point was employed, and the interactions were assumed to extend to the fourth-neighbors. The equations of motion of the lattice points were solved by an approximate numerical method, and from the solutions, the dynamical behavior of the shock wave, the vibrational energy, and the Grüneisen parameter in the shock compressed region were obtained. These results were compared with similar results for a one-dimensional lattice model.

Ugiansky, G. M., Ellinger, G. A., **Corrosion of Monel 400 in high CO_2 well water,** *Corrosion* **24,** *No. 5, 134–136 (May 1968).*

Key words: Dezincification; corrosion; monel; electron probe microanalysis.

The dezincification type corrosion of a Monel well screen in natural water is discussed in detail. The second phase present in the corroded grain boundaries was determined by electron probe micro-analysis to be nearly pure copper with little or no nickel present. It is concluded that Monel may be susceptible to dezincification type corrosion when used in certain environments.

Ugiansky, G. M., Skolnick, L. P., Kruger, J., Stiefel, S. W., **Rate-controlling step in stress corrosion cracking,** *Nature* **218,** *No. 5147, 1156–1157 (June 22, 1968).*

Key words: Stress corrosion; rate-controlling step; crack propagation; crack initiation; aluminum alloys.

Experimental evidence is reported which shows that crack propagation, rather than crack initiation, is the rate limiting step in the intergranular stress corrosion of the high strength aluminum alloy 7075–T651. The directional susceptibility of certain aluminum alloys is explained on the basis of the crack propagation in an elongated grain structure.

Utech, H. P., Parker, R. L., Early, J. G., Coriell, S. R., **The cam equation for a thermal-wave generator,** *J. Appl. Phys.* **38,** *No. 9, 3799–3800 (Aug. 1967).*

Key words: Cam; thermal wave; equation; thermal diffusivity; generator; sine wave.

The cam equation for sinusoidal thermal wave generator is derived, correcting an equation previously reported in the literature by Abeles, Cody, and Beers.

Vieth, D. L., Yakowitz, H., **Tensile loading device for Kossel microdiffraction and metallography,** *Rev. Sci. Instr.* **39,** *No. 12, 1929–1931 (Dec. 1968).*

Key words: Strain measurement; Kossel x-ray method; metallography instrument design; tensile testing; x-ray microdiffraction.

A leading device used primarily in conjunction with Kossel (divergent beam) x-ray diffraction is described. The device is compatible with any standard upright metallograph as well. It is four inches (10.1 cm) in diameter and accommodates specimens one inch in reduced section by 1/4 inch wide. The device utilizes small load cells having ranges of 0 to 10 pounds (445N) and 0 to 100 pounds (445N) respectively. Load cell error is ± 0.5% of the full load capacity. Load changes of 0.2% of load capacity can be observed. The load device is mechanically and electrically stable. Loads are read on a standard commercial universal indicator.

Wait, D. F., Nemoto, T., **Measurement of the noise temperature of a mismatched noise source,** *IEEE Trans. Microwave Theory Tech.* **MTT-16,** *No. 9, 670–675 (Sept. 1968).*

Key words: Measurement; noise; effective temperature; mismatched generators.

A method is suggested which can measure the available power (or the effective temperature) of a noise generator independent of its reflection coefficient. A system utilizing a compensation generator and a tuned three-port circulator, is constructed at X-band and evaluated for a noise generator of about 10,000 °K. The error analysis and the experimental results indicate that the effective temperature of this generator, with a reflection coefficient of 0.5, can be measured within one-half of one percent in addition to the uncertainty of a standard needed to calibrate the system.

Weiss, B-Z., Meyerson, M. R., **The effect of mean stress on fatigue crack propagation in plates under extension and bending,** *J. Basic Eng.* **90,** *Series D, No. 3, 414–417 (Sept. 1968).*

Key words: Crack propagation; fatigue; plastic zone.

This discussion presents comments on a paper by R. Roberts and

F. Erdogan, "The Effect of Mean Stress on Fatigue Crack Propagation in Plates Under Extension and Bending." Some original data are presented to support the views of the discussers.

Weiss, B–Z., Meyerson, M. R., **Localized microstructural changes and fatigue crack propagation,** *Trans. Met. Soc. AIME* **242,** *2515–2518 (1968).*

Key words: Fatigue crack propagation; plastic deformation; temper embrittlement; carbide precipitation; plastic zone size; austenitic steels.

Changes of plastic zone size during fatigue crack propagation in fully reversed cyclic bending at constant load amplitude for conditions of plain strain were investigated by two different techniques. It appears that the rate of fatigue crack propagation cannot be expressed as a continuous simple function of plastic zone size. This was related to the anisotropic conditions of plastic deformation in the plastic zone preceding the crack. A theoretical-mathematical evaluation was formulated for fatigue crack propagation during repeated cyclic bending under conditions of plane strain. The theory is based on an elastic model and the assumption that the plastic deformation at the tip of the propagating crack does not cause drastic redistribution of stresses in the stress field around the tip of the crack. It was found that fatigue crack propagation can be expressed as a function of stress intensity factor.
Experimental results are in good agreement with the presented theoretical evaluation. The effect of localized (heterogenous) structural changes such as selective precipitation of carbides in austenitic steels, temper embrittlement in a low alloy steel, and partial martensitic transformation in a matastable austenitic steel have been investigated and are discussed.

Weissler, P. G., **International standard reference zero for audiometers,** *J. Acoust. Soc. Am.* **44,** *No. 1, 264–275 (July 1968).*

Key words: Earphones; artificial ear; threshold of hearing; international audiometric reference zero; pure-tone audiometers; uncertainty of threshold of hearing standard.

This is a detailed report on the technical activities of ISO's Technical Committee on Acoustics No. 43, Working Group on Threshold of Hearing, which led to the ISO Recommendation R389, "Standard Reference Zero for the Calibration of Pure-Tone Audiometers," November 1964.
The activities described are the determinations of the transfer factors from loudness balancing experiments between the five earphone-coupler combinations in R389, the incorporation of the transfer data into the computation of the reference equivalent threshold sound pressure levels (RETSPL) in R389, and the details of the weighting of the original threshold determinations. A statistical analysis estimates the average standard deviation of the RETSPL in R389 to be 2 dB due in large part to the variance in the transfer factors. The present USASI standards are definitely outside the ISO uncertainty limits at all frequencies. The standard deviation of the differences between columns in R389 (or the equivalence of the RETSPL for the different earphone-coupler combinations) was estimated to be 2.5 dB. To improve accuracy in audiometry it is suggested that the variance due to the transfer factors be eliminated by agreement on one standard earphone type.

Weitzel, D. H., Sindt, C. F., Daney, D. E., **Hydrogen slush density reference system** *(Proc. 1967 Cryogenic Engineering Conf., Stanford University, Stanford, Calif., Aug. 21–23, 1967), Book, Advances in Cryogenic Engineering* **13,** *523–533 (Plenum Press, Inc., New York, N.Y., 1968).*

Key words: Densitometer; density reference system; liquid hydrogen; nuclear radiation attenuation; slush hydrogen.

A hydrogen slush density reference system has been designed for calibration of field-type instruments and/or transfer standards. The device is based on the buoyancy principle of Archimedes. The solids are weighed in a light-weight container so arranged that solids and container are buoyed by triple-point liquid hydrogen during the weighing process. Nuclear radiation attenuation is considered as the most likely candidate for a transfer standard, and preliminary results obtained with a NRA densitometer are presented. The densitometer was used as an aid to determine pressure drop data for various slush hydrogen concentrations.

West, E. D., Churney, K. L., **A two-body model for the calorimeters with constant-temperature environment,** *J. Appl. Phys.* **39,** *No. 9, 4206–4215 (Aug. 1968).*

Key words: Calorimeter, "drop" calorimeter; enthalpy measurements; heat content measurements; isoperibol calorimeter.

Equations are derived describing a model of an isoperibol calorimeter in which the calorimeter proper consists of two parts thermally connected, one surrounding the other and exchanging heat with the constant temperature environment. These solutions provide insights into the behavior of real calorimeters. Inferences are drawn relative to the effect of the locations of the thermometer and heat source on the energy equivalent of the calorimeter and some possible errors are pointed out. Macleod's application of the two-body theory of King and Grover to high temperature enthalpy measurements is discussed and weaknesses in theory and experiment are pointed out. Procedures having a better theoretical basis are outlined.

West, E. D., Westrum, E. F., Jr., **Adiabatic calorimetry from 300 to 800 °K,** *chap. 9 in Experimental Thermodynamics, Vol.* **I,** *Calorimetry of Nonreacting Systems, J. P., McCullough and D. W. Scott, Eds., pp. 333–367 (Butterworth and Co., London, England, 1968).*

Key words: Adiabatic calorimetry; calorimeter; calorimetry; cryoscopy; melting; phase transition; purity; thermodynamics.

Adiabatic heat capacity calorimetry in the range 300 to 800 °K is reviewed with discussions of principles and two particular calorimeters. The general heat flow problem is discussed qualitatively as it pertains to the design of calorimeters of this type. Construction details are included in the examples and related to the principles. The advantages and disadvantages of different methods of operation are discussed.

Westrum, E. F., Jr., Furukawa, G. T., McCullough, J. P., **Adiabatic low-temperature calorimetry,** *chap. 5 in Experimental Thermodynamics, Vol.* **I,** *Calorimetry of Non-reacting Systems, J. P. McCullough and D. W. Scott, Eds., 133–214 (Butterworth and Co., London, England, 1968).*

Key words: Calorimetry; calorimeters; cryostats; phase studies; phase transitions; thermometry; temperature; time; power; heat-leak correction; curvature correction; premelting correction; vaporization correction; purity; cryoscopy; thermodynamics; thermodynamic properties; low temperature calorimetry; adiabatic calorimetry; smoothing of observations.

Adiabatic heat-capacity calorimetry in the range 4 to about 350° K is reviewed with discussions in principles of calorimeter design, measurements, and analysis of data obtained. Measurements of temperature, power, and time are discussed with critical analysis of expected accuracy of circuitry and equipment used. Methods for transferring samples into the calorimeter vessel and various heat treatments in the calorimeter prior to measurements are suggested for substances that undergo phase transitions. Procedures are given for heat-leak, premelting, curvature, and vaporization corrections. Methods for smoothing the observed heat-capacity data and calculation of thermodynamic properties are discussed.

Wiederhorn, S. M., **Fracture surface energy of glass,** *J. Am. Ceramic Soc.* **52,** *No. 2, 99–105 (1969).*

Key words: Cleavage; cracks; cohesive strength technique; fracture; fracture mechanics; glass; stress intensity factor; surface energy.

Fracture surface energies of six different glasses were measured using the double-cantilever cleavage technique. Values obtained ranged from 3.5 to 5.3 J/m² depending on the chemical composition of the glass and the temperature of the test. The fracture surface energy increased with decreasing temperature and increasing Young's modulus, however, exceptions to this behavior were noted.

The magnitude of the values obtained are discussed with respect to the theoretical strength of glass, and possible irreversible effects at the crack tip such as stress corrosion and plastic deformation are considered.

Wiederhorn, S. M., **Moisture assisted crack growth in ceramics,** *Intern. J. Fracture Mech.* **4,** *No. 2, 171–177 (June 1968).*

Key words: Crack growth; ceramics; static fatigue; stress corrosion; fracture; delayed failure; glass; sapphire.

A method is described to study subcritical crack growth in ceramic materials. Large, macroscopic size cracks were used and quantitative crack velocity measurements were made on glass and sapphire as a function of applied force, temperature and environment. The measured crack velocity was a complex function of stress and water vapor concentration in the environment and portions of the data could be adequately explained by the stress corrosion theory of Charles and Hillig.

Wilcox, R. M., **Bounds for the isothermal, adiabatic, and isolated static susceptibility tensors,** *Phys. Rev.* **174,** *No. 2, 624–629 (Oct. 10, 1968).*

Key words: Susceptibilities; dielectric; magnetic; bounds; inequalities.

Quantum statistical proofs are given that: (1) the isolated (or Kubo) susceptibility tensor is positive indefinite and is bounded from above by the adiabatic susceptibility tensor; (2) the isothermal susceptibility tensor is positive definite and is bounded from below by the adiabatic susceptibility tensor. The results apply to either the static dielectric or magnetic cases. Biasing fields and permanent dipole moments may be present if desired. Criteria for equality of the various susceptibilities is established.

Williams, E. S., **A voltage converter for a new era,** *Meas. Data* **2,** *No. 6, 75–79 (Nov.–Dec. 1968).*

Key words: EMF comparator; frequency compensation; temperature compensation thermoelement; transfer voltmeter; voltage converter.

A set of thermal voltage converters recently developed at NBS consists of five series resistor units and two thermoelements, each of which can be used with any one of the resistors. The thermoelements have rated currents of 2.5 and 5 mA. This arrangement permits each resistor to be used for two voltage ranges. The ac-dc difference of frequency influence of each range is less than 20 ppm at 50 kHz from 1 to 600 volts. Adjacent ranges can also be intercompared, so that all ranges can be evaluated relative to any one in only six steps. The thermoelements are compensated for temperature changes to reduce warm-up drift. Difficulties with reversed d-c differences in the thermoelements and power supply instability are minimized by the test procedure used and by the special emf comparators, which are also described.

Wildhack, W. A., Mason, H. L., Powers, R. S., Jr., **Accuracy charts for RF measurements,** *Proc. IEEE* **55,** *No. 6, 1056–1063 (June 1967).*

Key words: Accuracy; calibration; IEEE; measurements; radio; radio frequency.

The general factors involved in the estimation of uncertainties in calibration or measurement are reviewed briefly. Twenty-five accuracy charts are presented showing the estimated uncertainties in National Bureau of Standards calibrations of laboratory standards or measuring instruments for electrical and radio frequency quantities.

Wolfe, W. C., **Field study of floor coverings,** *Fooring* **74,** *No. 11, 52–58 (Nov. 1968).*

Key words: Adhesion; floor coverings; organic coatings; performance characteristics; specifications; wear.

The National Bureau of Standards has made observations of the performance of floor coverings in areas of severe exposure in Department of Defense installations and some civilian applications over a period of 13 years (1955–68). Valuable information on the adhesion of coatings and coverings to their substrates, on wear and other performance characteristics was obtained. This information has been used by Federal agencies in preparing specifications and in selecting materials for specific applications. However it is evident that the incomplete observations were not adequate to properly evaluate the relative performance of the different systems. Therefore recommendations are made for better-controlled field observations leading to laboratory investigations.

Wofgang, R., Zare, R. N., Branscomb, L. M., **Chemical accelerators,** *Science* **162,** *818–822 (Nov. 15, 1968).*

Key words: Chemical accelerators.

This is a brief account of a conference on chemical accelerators held at the University of Colorado March 28–29, 1968, supported by the Advanced Research Projects Agency.

Yakowitz, H., Heinrich, K. F. J., **Inclusion identification by means of electron probe microanalysis,** *Metallography* **1,** *No. 1, 55–78 (1968).*

Key words: Electron probe microanalysis; inclusion analysis; microscopy; quantative data scanning; concentration mapping; experiment design.

Each stage in the analysis of inclusions by electron probe microanalysis is evaluated. These stages include experimental design and instrument operation, specimen preparation, element identification, element distribution mapping and quantitative data scanning. The use of signals other than x-rays for inclusion analysis is considered as well as the analysis of sub-micron inclusions. The approach taken assumes that microprobe analysis will be used in conjunction with careful optical microscopy and that quantitative microscopy may be used to classify the inclusions after microprobe analysis is carried out.

Young, K. F., Forman, R. A., **Use of polystyrene beads for manufacture of low loss coaxial lines for low temperature research,** *Rev. Sci. Instr.* **39,** *No. 12, 1964–1965 (Dec. 1968).*

Key words: Coaxial cable; low-dielectric-loss coaxial lines; low temperature; transmission lines.

A new inexpensive technique is described for the production of experimental coaxial transmission lines for low temperature use. These lines have been tested in both nuclear quadrupole resonance and dielectric loss measurements and have proven to be as good electrically as commercial coaxial cable, with a large decrease in thermal conduction into the experimental system.

Yakowitz, H., Vieth, D. L., Heinrich, F. J., Michaelis, R. E., **Homogeneity characterization of NBS spectrometric standards. II: Cartridge brass and low-allow steel** *(Proc. 14th Annual Conf. Applications of X-ray Analysis, University of Denver, Denver Research Inst., Denver, Colo., Aug. 25–27, 1965), Book, Advances in X-ray Analysis, Ed. G. R. Mallett, M. Fay, and W. M. Mueller, 9, 289–303 (Plenum Press Inc., New York, N.Y., 1966).*

Key words: Standards of composition; solids mass spectrometer; electron probe microanalyzer; homogeneity—standards; NBS cartridge brass; NBS low-alloy steel; optical metallography.

Most modern instrumental methods of analysis depend on the use of known standards of composition for calibration. Newer analytical techniques such as the solids mass spectrometer, laser probe and, especially, the electron probe microanalyzer have reduced the amount of a sample which can be analyzed quantitatively to a range of about 0.1 micrograms to as little as 0.00005 micrograms. Corollary to these microanalytical advances, homogeneity requirements have become severe for the analytical standards. This paper describes a continuation of the NBS effort to more fully characterize existing standards as to suitability for the new microanalytical techniques (1). An NBS cartridge brass sample in both the wrought (NBS–1102) and chill cast forms (NBS–C1102), as well as a low alloy

steel sample (NBS–463), have been investigated by means of electron probe microanalysis and optical metallography. Some seventeen elements are contained in the brass while twenty-five elements are in the steel. Results for ten elements in the steel are presented while results for six elements in the brass are given. In the steel, Fe, Ni, Cu, and Si are essentially distributed homogeneously at micron levels while Mn, Ta, Nb, Zr, S, and Cr are not. In the brass, Cu and Zn are distributed homogeneously at micron levels while Pb, S, Al, and Si are not. Electron probe microanalyzer results indicate that both NBS–1102 and NBS–C1102 brass are suitable for use as a calibration standard for electron probe microanalysis as well as other microanalytical techniques such as the solids mass spectrometer. The results for brass have been corroborated by a number of laboratories using the electron probe analyzer.

Yee, K. W., Deslattes, R. D., **Transistorized current stabilizer for X-ray tubes with directly heated cathodes,** *Rev. Sci. Instr.* **38,** *No. 5, 637–638 (May 1967).*

Key words: Emission; current; regulator; x-ray tube; controlled impedance; stabilizer.

An instrument is described which stabilizes the emission current in x-ray tubes with directly heated cathodes. Transistors are used in the amplifier and loading circuits. Emission currents from 20 mA to 1 A are maintained constant to within 0.1% for periods of about a half-hour.

Young, R. D., Kuyatt, C. E., **Resolution determination in field emission energy analyzers,** *Rev. Sci. Instr.* **39,** *No. 10, 1477–1480 (Oct. 1968).*

Key words: Analyzer resolution; energy analyzer; energy distribution; field emission.

The influence of energy analyzer transmission function on measured field emission energy distributions has been evaluated by folding a Gaussian transmission function into the field emission total-energy distribution. The resulting distributions at 0, 4.2, 20.3, 77, and 300 °K are plotted as a function of the field- and work function-dependent parameter d, and for the special case $\varphi = 4.40$ eV, $F = 3.0 \times 10^7$ V/cm. A criterion is established for determining the width of an analyzer transmission function from distributions measured at the above temperatures. It is shown that the slope of the log of the energy distribution is changed by less than 1% when the analyzer width is changed from 0 to 100 mV.

Other NBS Publications

J. Res. Nat. Bur. Stand. (U.S.), 73A (Phys. and Chem.), No. 2 (Mar.–Apr. 1969), $2.00

Color representation of electron microprobe area-scan images by a color separation process. H. Yakowitz and K. F. J. Heinrich.

Configurations $3d^n4p$ in singly ionized atoms of the iron group. C. Roth.

Configurations $3d^n4p + 3d^{n-1}4s4p$ in Sc II, Ti II, and V II. C. Roth.

Effective interactions in the even configurations of the third spectra of the iron group. Y. Shadmi, E. Caspi, and J. Oreg.

Test of a kinetics scheme: Emission in $H(^2S) + NO(^2\Pi)$. M. Krauss.

A nuclear magnetic resonance and relaxation study of dimethoxyborane. T. C. Farrar and T. Tsang.

The effects of low energy irradiation on organometallics. Organometal halides of group IVA. F. E. Brinckman. G. F. Kokoszka, and N. K. Adams, Jr.

Measurements of gaseous diffusion coefficients by a gas chromatographic technique. S. P. Wasik and K. E. McCulloh.

Phase relations in the Ru-Ir-O_2 system in air. C. L. McDaniel and S. J. Schneider.

Heats of reaction of natural rubber with sulfur. N. Bekkedahl and J. J. Weeks.

A table of rotational constants of symmetric top molecules giving rise to microwave spectra. M. S. Lojko and Y. Beers.

Energy levels, wave functions, dipole and quadrupole transitions of Fe^{+++} ions in sapphire. J. Lewiner and P. H. E. Meijer.

J. Res. Nat. Bur. Stand. (U.S.), 73A (Phys. and Chem.), No. 3 (May–June 1969), $1.50

New even levels and classified lines in the first spectrum of tungsten (W I). C. H. Corliss.

The heat of combustion of beryllium in fluorine. K. L. Churney, and G. T. Armstrong.

Deuterium isotope effect on the dissociation of weak acids in water and deuterium oxide. R. A. Robinson, M. Paabo, and R. G. Bates.

Vortex motions in ideal Bose superfluid. M. J. Cooper.

Franck-Condon factors for the ionization of H_2O and D_2O. R. Botter and H. M. Rosenstock.

Topological features of hot carrier induced anisotropic breakdown on silicon diode surfaces. G. G. Harman.

The third spectrum of praseodymium (Pr III) in the vacuum ultraviolet. J. Sugar.

J. Res. Nat. Bur. Stand. (U.S.), 73A (Phys. and Chem.), No. 4 (July–Aug. 1969), $1.25

Classical path methods in line broadening. I. The classical path approximation. E. W. Smith, C. R. Vidal, and J. Cooper.

Classical path methods in line broadening. II. Application to the Lyman series of hydrogen. E. W. Smith, C. R. Vidal, and J. Cooper.

The second virial coefficient for the realistic pair potential. H. W. Woolley.

Synthesis of barium ferrates in oxygen. T. Negas and R. S. Roth.

The system SrO—"chromium oxide" in air and oxygen. T. Negas and R. S. Roth.

J. Res. Nat. Bur. Stand. (U.S.), 73A (Phys. and Chem.), No. 5 (Sept.–Oct. 1969), $1.50

Conversion of existing calorimetrically determined thermodynamic properties to the basis of the International Practical Temperature Scale of 1968. T. B. Douglas.

Measured enthalpy and derived thermodynamic properties of alpha beryllium nitride, Be_3N_2, from 273 to 1200 K. T. B. Douglas and W. H. Payne.

Measured enthalpy and derived thermodynamic properties of solid and liquid lithium tetrafluoroberyllate, Li_2BeF_4, from 273 to 900 K. T. B. Douglas, and W. H. Payne.

Nonanalytic vapor pressure equation with data for nitrogen and oxygen. R. D. Goodwin.

Some precise measurements of the vapor pressure of water in the range from 25 to 100 °C. H. F. Stimson.

The configurations $(3d+4s)^n4p$ in neutral atoms of calcium, scandium, and titanium. C. Roth.

Absolute isotopic abundance ratio and atomic weight of terrestrial rubidium. E. J. Catanzaro, T. J. Murphy, E. L. Garner, and W. R. Shields.

J. Res. Nat. Bur. Stand. (U.S.), 73A (Phys. and Chem.), No. 6 (Nov.–Dec. 1969), $1.25

Scaling analysis of thermodynamic properties in the critical region of fluids. M. Vicentini-Missoni, J. M. H. Levelt Sengers, and M. S. Green.

Formulation of a nonanalytic equation of state for parahydrogen. R. D. Goodwin.

Dynamical model for Brillouin scattering near the critical point of a fluid. R. D. Mountain.

Odd configurations in singly-ionized copper. C. Roth.

Capillary depressions for nearly planar menisci. M. C. I. Siu.

Phase transformation in barium tetraborate. C. R. Robbins and E. M. Levin.

Crystallography and preparation of some $ABCl_3$ compounds. H. F. McMurdie, J. de Groot, M. Morris, and H. E. Swanson.

J. Res. Nat. Bur. Stand. (U.S.), 73B (Math. Sci.), No. 1 (Jan.–Mar. 1969), 75 cents.

A table of integrals of the error functions. E. W. Ng and M. Geller.

Fourier coefficients of Mathieu functions in stable regions. H. Früchting.

A note on the T-transformation of Lubkin. W. D. Clark, H. L. Gray, and J. E. Adams.

The cylinder problem in thermoviscoelasticity. W. S. Edelstein.

Relations within sequences of congruential pseudo-random numbers. P. H. Verdier.

On the mean dimensions of restricted random walks. P. H. Verdier and E. A. DiMarzio.

The cube on every connected graph is 1-hamiltonian. G. Chartrand and S. F. Kapoor.

Minimum-length covering by intersecting intervals. W. A. Horn.

J. Res. Nat. Bur. Stand. (U.S.), 73B (Math. Sci.), No. 2 (Apr.–June 1969), 75 cents.

An evaluation of linear least squares computer programs. R. H. Wampler.

The traffic assignment problem for a general network. S. C. Dafermos and F. T. Sparrow.

Sufficient conditions for the instability of numerical integration methods. A. I. A. Karim.

The second orthogonality conditions in the theory of proper and improper rotations. II. The intrinsic vector. H. Gelman.

The second orthogonality conditions in the theory of proper and improper rotations. III. The conjugacy theorem. H. Gelman.

Subgroups of $SL(t, z)$. M. Newman.

Cuttable and cut-reducible matrices. R. B. Marimont.

Automorphic integrals with preassigned periods. J. Lehner.

A digital computer technique for calculating the step response of lumped or distributed networks. J. R. Andrews and N. S. Nahman.

Symmetry and the crossing number for complete graphs. T. L. Saaty.

J. Res. Nat. Bur. Stand. (U.S.), 73B (Math. Sci.), No. 3 (July–Sept. 1969), 75 cents.

A table of integrals of the exponential integral. M. Geller and E. W. Ng.

Principal ideals in matrix rings. M. Newman and S. Pierce.

The second orthogonality conditions in the theory of proper and improper rotations. IV. Solution of the trace and secular equations. H. Gelman.

Minimax error selection of a univariate distribution with prescribed componentwise bounds and ranking. A. J. Goldman.

Minimax adjustment of a univariate distribution to satisfy componentwise bounds and/or ranking. A. J. Goldman.

On the application of some interpolating functions in physics. A. J. Jerri.

Commutator groups and algebras. L. Greenberg.

On a class of nonlinear transformations and their applications to the evaluation of infinite series. H. L. Gray and W. D. Clark.

J. Res. Nat. Bur. Stand. (U.S.), 73B (Math. Sci.), No. 4 (Oct.–Dec. 1969), 75 cents.

Temperature renormalization in the non-linear Vlasov problem. W. L. Sadowski and Z. G. Ruthberg.

Selective excitation of harmonics in a collisionless plasma by two counterstreaming electron beams. W. L. Sadowski and Z. G. Ruthberg.

Simultaneous contractification. A. J. Goldman and P. R. Meyers.

A theorem on convex hulls. W. A. Horn.

The partitioning of interaction in analysis of variance. J. Mandel.

Highly restricted partitions. H. Gupta.

Brief history and use of the English and metric systems of measurement with a chart of the modernized metric system, 1/3 the dimensions of actual chart (SP304), Spec. Publ. 304A (1968), 20 cents.

Cord, M. S., Petersen, J. D., Lojko, M. S., Haas, R. H., Microwave spectral tables, Polyatomic molecules without internal rotation, Mono. 70, Vol. IV (Oct. 1968), $5.50.

Davis, M. M., Acid-base behavior in aprotic organic solvents, Mono. 105 (Aug. 1968), $2.25.

Fraction, G. F., Walker, J. C., Tauber, S. J., Connection tables from Wiswesser chemical structure notations—a partial algorithm, Tech. Note 432 (Sept. 1968), 65 cents.

Freeman, D. H., Editor, Separation and Purification Section: Summary of activities July 1967 to June 1968, Tech. Note 459 (Dec. 1968), 60 cents.

Gebbie, K. B., Thomas, R. N., Editors, Wolf-Rayet stars, Proc. Symp. held at Joint Institute for Laboratory Astrophysics, University of Colorado, Boulder, Colorado, June 10–14, 1968, Spec. Publ. 307 (Dec. 1968), $3.00.

Goldman, D. T., Ed., Neutron cross sections and technology, Proc. Conf., Washington, D.C., Mar. 4–7, 1968, Spec. Publ. 299 (Sept. 1968), $10.50 set of 2 volumes.

Johnston, H. S., Gas phase reaction kinetics of neutral oxygen species, NSRDS–NBS20 (Sept. 1968), 45 cents.

LaFleur, P. D., Editor, Activation Analysis Section: Summary of activities July 1967 to June 1968, Nat. Bur. Stand. (U.S.), Tech. Note 458, 109 pages (March 1969), $1.00.

Lederer, P. S., NBS interagency transducer project, Tech. Note 469 (Oct. 1968), 30 cents.

Menis, O., Ed., Analytical Coordination Chemistry Section: Summary of activities July 1967 to June 1968, Tech. Note. 454 (July 1968), 55 cents.

Miles, B. M., Wiese, W. L., Critically evaluated transition probabilities for Ba I and II, Tech. Note 474 (Jan. 1969), 30 cents.

Shields, W. R., Editor, Analytical Mass Spectrometry Section: Summary of activities July 1967 to June 1968, Tech. Note 456 (Nov. 1968), 55 cents.

The modernized metric system, the International System of units (SI) and its relationship to U.S. customary units, illustrated color wall chart 45 × 29 inches, Spec. Publ. 304 (1968), 50 cents. (Supersedes Misc. Publ. 232).

Moiseiwitsch, B. L., Smith, S. J., Electron impact excitation of atoms, NSRDS–NBS 25 (Aug. 1968), $2.00.

Moore, C. E., Bibliography on the analyses of optical spectra. Section $_{1}^{1}H$–$_{23}^{23}V$, Spec. Publ. 306 (Sept. 1968), $1.00.

Schaffer, R., Ed., Organic Chemistry Section: Summary of activities July 1967 to June 1968, Tech. Note 457 (Sept. 1968), $1.25.

Scribner, B. F., Ed., Spectrochemical Analysis Section: Summary of Activities July 1967 to June 1968, Tech. Note 452 (Sept. 1968), $1.00.

Stevens, M. E., Nonnumeric data processing in Europe, A field trip report, August–October 1966, Tech. Note 462 (Nov. 1968), 65 cents.

Taylor, J. K., Ed., Microchemical Analysis Section: Summary of activities July 1967 to June 1968, Tech. Note 455 (Oct. 1968), $1.25.

Technical highlights of the National Bureau of Standards, Annual Report, Fiscal Year 1968, Spec. Publ. 308 (Nov. 1968), $1.00.

White, H. S., Jr., Editor, General description of the Federal Information Processing Standards Register, Fed. Info. Process. Std. Pub. (FIPS) 0 (Nov. 1, 1968), 20 cents.

White, H. S., Jr., Editor, Calendar date, Fed. Info. Process. Std. Pub. (FIPS) 4 (Nov. 1, 1968), 20 cents.

White, H. S., Jr., Editor, States of the United States, Fed. Info. Process. Std. Pub. (FIPS) 5 (Nov. 1, 1968), 20 cents.

White, H. S., Jr., Editor, Counties of the States of the United States, Fed. Info. Process. Std. Pub. (FIPS) 6 (Nov. 1, 1968), 40 cents.

Acquista, N., Abramowitz, S., Lide, D. R., Structure of the alkali hydroxides. II. The infrared spectra of matrix isolated CsOH and CsOD, J. Chem. Phys. **49,** No. 2, 780–782 (July 15, 1968).

Altschuler, H. M., Comments on "An improved method for measuring scattering parameters of nonreciprocal two-ports," IEEE Trans. Microwave Theory Tech. **MTT–16,** No. 4, 261–262 (Apr. 1968).

Amano, T., Saito, S., Hirota, E., Morino, Y., Johnson, D. R., Powell, F. X., Microwave spectrum of the ClO radical, J. Mol. Spectry. **30,** No. 2, 275–289 (May 1969).

Anderson, H. J., Brenner, A., Preparation of rhenium hexafluoroacetylacetonate, J. Electrochem. Soc. **116,** No. 4, 513 (Apr. 1969).

Arenhovel, H., General formulas for describing the absorption of polarized photons by oriented nuclei, Phys. Rev. **171,** No. 4, 1212–1216 (July 20, 1968).

Arenhovel, H., Danos, M., Baryon resonances in nuclei: Magnetic moment anomaly in ^{3}H and ^{3}He, Physics Letters **28B,** No. 5, 299–301 (Dec. 23, 1968).

Ausloos, P., Lias, S. G., Primary modes of decomposition of superexcited *n*-alkane molecules (Proc. Intern. Conf. Photochemistry, Munchen, Germany, Sept. 6–9, 1967), Ber. deut. Gunsenges. **72,** No. 2, 187–195 (1968).

Ausloos, P., Rebbert, R. E., Lias, S. G., Structure and reactivity of propyl ions in gas-phase radiolysis, J. Am. Chem. Soc. **90,** No. 18, 5031–5033 (Aug. 28, 1968).

Barger, R. L., Hall, J. L., Pressure shift and broadening of methane line at 3.39μ studied by laser-saturated molecular absorption, Phys. Rev. Letters **22,** No. 1, 4–8 (Jan. 6, 1969).

Bates, R. G., Equilibrium properties of acids and bases in amphiprotic mixed solvents (Proc. Symp. Equilibria and Reaction Kinetics in Hydrogen.

Bechtoldt, C. J., Ogburn, F., Smit, J., Structure and morphology of electrodeposited molybdenum dendrites, J. Electrochem. Soc. **115,** No. 8, 814–816 (Aug. 1968).

Bender, P. L., Branscomb, L. M., Credit for gravity apparatus, Phys. Today Letter **20,** No. 10, 17 (Oct. 1967).

Bennett, H. S., Diffuse and propagating modes in the Heisenberg paramagnet, Phys. Rev. **174,** No. 2, 629–639 (Oct. 10, 1968).

Bennett, H. S., Phenomenology of neutron scattering in Heisenberg systems, Phys. Rev. **176,** No. 2, 650–654 (Dec. 10, 1968).

Bennett, L. H., Mebs, R. W., Watson, R. E., Solute Knight shifts in noble metals, Phys. Rev. **171,** No. 3, 611–626 (July 15, 1968).

Berman, H. A., West, E. D., Heat capacity of liquid nitromethane from 35° to 200° C, J. Chem. Eng. Data **14,** No. 1, 107–109 (Jan. 1969).

Birmingham, B. W., Flynn, T. M., National programs and the compressed gas industry (Proc. 55th Annual Meeting of the Compressed Gas Association, New York City, N.Y., Jan. 1968), Chapter in The Future of the Compressed Gas Industry, pp. 39–49 (Compressed Gas Assoc. Inc., New York, N.Y., 1969).

Blandford, J. M., NBS–ARF apparel materials testing and evaluation project, Second Annual Conf. Apparel Research Foundation, Washington, D.C., Oct. 7–9, 1968, 4 pages (Apparel Research Foundation, Washington, D.C., 1968).

Bonded Solvent Systems, University of New Castle, Upon Tyne, England (Jan. 10–12, 1968), Chapter in Hydrogen-Bonded Solvent Systems, A. K. Covington and P. Jones, Eds., pp. 49–86 (Taylor and Francis, London, England, 1968).

Bortner, M. H., A review of rate constants of selected reactions of interest in re-entry flow fields in the atmosphere, Nat. Bur. Stand. (U.S.), Tech. Note 484, 62 pages (May 1969), 60 cents.

Botter, R., Rosenstock, H. M., Franck-Condon factors for NH_2 and H_2O, Chapter in Advances in Mass Spectrometry, **4,** 579–589 (Institute of Petroleum, London, England, 1968).

Branscomb, L. M., Joint Institute for Laboratory Astrophysics of the National Bureau of Standards and the University of Colorado, Boulder, Colorado, observatory report, Bull. Am. Astron. Soc. **1,** No. 1, 27–33 (Jan. 1969).

Branscomb, L. M., Physics and the nation in a crystal ball, Phys. Today **21,** No. 8, 23–28 (Aug. 1968).

Brockman, J. F., Popular science writing, Proc. 1967 Inst. Technical Industrial Communications, Colorado State University, Ft. Collins, Colo., June 12–16, 1967, pp. 96–100 (1967).

Brooks, R., Horton, A. T., Torgesen, J. L., Occlusion of mother liquor in solution-growth crystals, J. Crystal Growth **2,** 279–283 (1968).

Burke, P. G., Cooper, J. W., Ormonde, S., Electron-impact excitation of $n=2$ states in He, Phys. Rev. Letters **17,** No. 7, 345–348 (Aug. 15, 1966).

Campbell, W. H., Aurora, Encyclopedia of Atmospheric Sciences and Astrogeology, R. W. Fairbridge, Ed., pp. 105–106 (Reinhold Publ. Co., New York, N.Y., 1967).

Casella, R. C., Decay modes with coherent resonant-energy transfer between deep impurities in solids, Phys. Rev. **174,** No. 3, 830–834 (Oct. 15, 1968).

Casella, R. C., Time reversal and the K° meson decays, Phys. Rev. Letters **21,** No. 15, 1128–1131 (Oct. 7, 1968).

Clark, H. E., Young, R. D., Field emission through single strontium atoms adsorbed on a tungsten surface, Surface Sci. **12,** 385–389 (1968).

Codling, K., Madden, R. P., Structure in the $L_{II,\ III}$ absorption of aluminum and its oxides, Phys. Rev. **167,** No. 3, 587–591 (Mar. 1968).

Cole, A. R. H., Lafferty, W. J., Thibault, R. J., Rotational fine structure of the perpendicular band, ν_7, of ethane, J. Mol. Spectry. **29,** No. 3, 365–374 (Mar. 1969).

Coriell, S. R., Jackson, J. L., Bounds on transport coefficients of two-phase materials, J. Appl. Phys. **39,** No. 10, 4733–4736 (Sept. 1968).

Crumlish, J. D., Notes on U.S. Government information systems, Law Computer Technol. **1,** No. 11, 15–21 (Nov. 1968).

Cuthill, J. R., Dobbyn, R. C., McAlister, A. J., Williams, M. L., Search for plasmaron structure in the soft x-ray $L_{2,3}$ emission spectrum of Al, Phys. Rev. **174,** No. 2, 515–517 (Oct. 10, 1968).

Cuthill, J. R., McAlister, A. J., Williams, M. L., Dobbyn, R. C., Soft x-ray spectra and comparison with the theoretical density of states (Proc. Conf. Soft X-ray Band Spectra and the Electronic Structure of Metals and Materials, Strathclyde, Scotland, Sept. 18–21, 1967), Chapter in Soft X-ray Band Spectra and the Electronic Structure of Metals and Materisls, Strathclyde, Scotland, Sept. 18–21, 1967), Chapter in Soft X-ray Band Spectra and the Electronic Structure of Metals and Materials. Part II. Heavy Metal and Alloy Spectra and Comparison with other Optical Methods, pp. 151–162 (Academic Press Inc., New York, N.Y., 1968).

Czyz, W., Maximon, L. C., High energy, small angle elastic scattering of strongly interacting composite particles, Ann. Phys. **52,** No. 1, 59–121 (Mar. 1969).

Daniel, A. C., Bevan, A. W., Jr., Mahler, R. J., Nuclear spin-lattice relaxation in the antiferromagnets $CoCl_2 \cdot 2H_2O$, and $FeCl_2 \cdot 2H_2O$, J. Appl. Phys. **39,** No. 2, Part I, 496–497 (Feb. 1, 1968).

Davis, D. D., Okabe, H., Determination of bond dissociation energies in hydrogen cyanide. Cyanogen and cyanogen halides by the photodissociation method, J. Chem. Phys. **49,** No. 12, 5526–5531 (Dec. 15, 1968).

Delaplane, R. G., Ibers, J. A., Ferraro, J. R., Rush, J. J., Diffraction and spectroscopic studies of the cobaltic acid system $HCoO_2$–$DCoO_2$, J. Chem. Phys. **50,** No. 5, 1920–1927 (Mar. 1, 1969).

Dibeler, V. H., Liston, S. K., Mass-spectrometric study of photoionization. IX. Hydrogen cyanide and acetonitrile, J. Chem. Phys. **48,** No. 10, 4765–4768 (May 15, 1968).

Dibeler, V. H., Liston, S. K., Mass spectrometric study of photoionization. XII. Boron trifluoride and diboron tetrafluoride, Inorg. Chem. **7,** No. 9, 1742–1746 (Sept. 1968).

Dibeler, V. H., Walker, J. A., Mass spectrometric study of photoionization. XIII. Boron trichloride and diboron tetrachloride, Inorg. Chem. **8,** No. 1, 50–55 (Jan. 1969).

Dick, C. E., Motz, J. W., Inelastic scattering cross sections for 200- and 400-keV electrons, Phys. Rev. **171,** No. 1, 75–80 (July 5, 1968).

Diller, D. E., Refractive index of gaseous and liquid hydrogen, J. Chem. Phys. **49,** No. 7, 3096–3105 (Oct. 1, 1968).

Drechsel, D., On the model-independent evaluation of inelastic electron scattering data at low momentum transfer, Nucl. Phys. **A113,** No. 3, 665–675 (June 7, 1968).

Drechsel, D., Maximon, L. C., Potential model calculation for coplanar and noncoplanar proton-proton bremsstrahlung, Ann. Phys. **49,** No. 3, 403–444 (Oct. 1968).

Dunn, G. H., Colliding beams (Proc. First Intern. Conf. Atomic Physics, June 3–7, 1968, New York, N.Y.), Chapter in Atomic Physics, B. Bederson, V. W. Cohen, F. M. J. Pichanick, eds., pp. 417–433 (Plenum Press, Inc., New York, N.Y., 1969).

Dunn, G. H., Photodissociation of H_2^+ and D_2^+: Theory, Phys. Rev. **172,** No. 1, 1–7 (Aug. 5, 1968).

Edmiston, C., Krauss, M., Pseudonatural orbitals as a basis for the superposition of configurations. II. Energy surface for linear H_3, J. Chem. Phys. **49,** No. 1, 192–205 (July 1, 1968).

Ehrlich, M., Influence of irradiation rate on the production of F centers in LiF (TLD grade), J. Appl. Phys. **40,** No. 2, 891–892 (Feb. 1969).

Ehrlich, M., Influence of irradiation rate on the production of F centers in LiF (TLD grade), Proc. Second Intern. Conf. Luminescence Dosimetry, Gatlinburg, Tenn., Sept. 23–26, 1968, J. A. Auzier, K. Becker, E. M. Robinson, Ed., Paper No. CONF–680920 Health and Safety (TID–4500), pp. 322–326 (Oak Ridge National Laboratory, Oak Ridge, Tennessee, Sept. 1968).

Ehrlich, M., Lamperti, P. J., Uniformity of high-energy electron-beam calibrations, Phys. Med. Biol. **14,** No. 2, 305–314 (Sept. 1968).

Evenson, K. M., Broida, H. P., Wells, J. S., Mahler, R. J., Mizushima, M., Electron paramagnetic resonance absorption in oxygen with the HCN laser, Phys. Rev. Letters **21,** No. 15, 1038–1040 (Oct. 7, 1968).

Fano, U., Cooper, J. W., Spectral distribution of atomic oscillator strengths, Rev. Mod. Phys. **40,** No. 3, 441–507 (July 1968).

Fatiadi, A. J., Acylation of tetrahydroxy-*p*-benzoquinone, J. Chem. Eng. Data **13,** No. 4, 591–593 (Oct. 1968).

Fatiadi, A. J., Bromine oxidation of inositols for preparation of inosose phenylhydrazones and phenylosazones, Carbohydrate Res. **8,** 135–147 (1968).

Fatiadi, A. J., Esters of benzenepentol (pentahydroxybenzene), J. Chem. Eng. Data **14,** 118–119 (1969).

Fatiadi, A. J., Evidence for a chair conformation of certain osotriazoles of inositols, Chem. Ind. **19,** 617–619 (May 10, 1969).

Fatiadi, A. J., Nature of a colored by-product found in crude inosose phenylosazones, Carbohydrate Res. **9,** 177–185 (1969).

Florin, R. E., Sicilio, F., Wall, L. A., The paramagnetic species from titanous salts and hydrogen peroxide, J. Phys. Chem. **72,** No. 9, 3154–3161 (Sept. 1968).

Folman, M., Klein, R., Second layer migration with trapping on first layer sites: Hydrogen, nitrogen, and carbon monoxide on tungsten, Surface Sci. **11,** 430–442 (1968).

Fowler, H. A., Experiments in electron scattering. 1, Proc. Symp. Quantitative Aspects of Electron Microscopy, Walter Reed Insti-

364-586 O - 69 - 5

tute of Pathology, Washington, D.C., 1965; Lab. Investigations **14,** No. 6, Part 2, 9–16 (1965).

Franklin, A. D., NBS dedicates new laboratory, J. Am. Ceram. Soc. **45,** No. 10, 841–842 (1966).

Franklin, J. L., Dillard, J. G., Rosenstock, H. M., Herron, J. T., Draxl, K., Field, F. H., Ionization potentials, appearance potentials, and heats of formation of gaseous positive ions, Nat. Stand. Ref. Data. Ser., Nat. Bur. Stand. (U.S.), 26, 289 pages (June 1969), $4.00.

Gadsden, M., Airglow, Encyclopedia of Atmospheric Sciences and Astrogeology, R. W. Fairbridge, ed., pp. 8–10 (Reinhold Publ. Co., New York, N.Y. 1967).

Gadsden, M., Airglow motions, International Dictionary of Geophysics 1, 50–56 (1967).

Gallagher, A., Rubidium and cesium excitation transfer in nearly adiabatic collisions with inert gases, Phys. Rev. **172,** No. 1, 88–96 (Aug. 5, 1968).

Gammon, W. H., What educators can expect from the center for Computer Sciences and Technology, Proc. Gen. Conf. Midwestern States Educational Information Project, Des Moines, Iowa, June 20, 1967, P. L. 89–10, Title V, Sect. 505, pp. 30–45 (Department of Public Instruction, State of Iowa, Des Moines, Iowa, 1967).

Gautier, T. N., Zacharisen, D. H., Use of space and time correlations in short-term ionospheric predictions, First Ann. IEEE Commun. Convention, pp. 671–676 (June 1965).

Gebbie, K. B., Thomas, R. N., Non-LTE diagnostic stellar spectroscopy. I. Conceptual and analytical background, Astrophys. J. **154,** 271-283 (Oct. 1968).

Gebbie, K. B., Thomas, R. N., Non-LTE diagnostic stellar spectroscopy. II. On the Schuster mechanism for the production of emission lines, Astrophys. J. **154,** 285–296 (Oct. 1968).

Geltman, S., Topics in atomic collision theory, 30, 247 pages (Academic Press Inc., New York, N.Y., 1969).

Goldman, D. T., Reactor physicsts emphasize need for neutron data, Phys. Today **21,** No. 8, 85–89 (Aug. 21, 1968).

Golub, S., Steiner, B., Photodetachment of $[OH(H_2O)]^-$, J. Chem. Phys. **49,** No. 11, 5191–5192 (Dec. 1, 1968).

Grabner, L., Photoluminescence in $SrTiO_3$, Phys. Rev. **177,** No. 3, 1315–1323 (Jan. 15, 1969).

Green, M. S., Generalized Ornstein-Zernike approach to critical phenomena, J. Math. Phys. **9,** No. 6, 875–890 (June 1968).

Halford, D., Wainwright, A. E., Barnes, J. A., Flicker noise of phase in RF amplifiers and frequency multipliers: characterization, cause, and cure, Proc. 22nd Annual Symp. Frequency Control, Atlantic City, New Jersey, Apr. 22–24, 1968, pp. 340–341 (solid State and Frequency Control Division, Electronic Components Laboratory, U.S. Army Electronics Command, Fort Monmouth, New Jersey, Apr. 1968).

Hardy, S. C., Coriell, S. R., Morphological stability and the ice-water interfacial free energy, J. Crystal Growth **3,** No. 4, 569–573 (1968).

Hardy, S. C., Coreill, S. R., Morphological stability of a growing cylindrical crystal of ice, J. Appl. Phys. **39,** No. 7, 3505–3507 (June 1968).

Hartman, W. J., Feasibility of communication with a satellite by means of tropospheric scatter, IEEE Trans. Commun. Technol. **COM-14,** No. 3, 251 (June 1966).

Herber, R. H., Spijkerman, J. J., Narrow-line source for ^{119}Sn Mössbauer spectroscopy, J. Chem. Phys. **43,** No. 11, 4057–4059 (Dec. 1, 1965).

Herron, J. T., Penzhorn, R. D., Mass spectrometric study of the reactions of atomic oxygen with ethylene and formaldehyde, J. Phys. Chem. **73,** No. 1, 191–196 (Jan. 1969).

Hoover, T. B., The N-methylpropionamide-water system. Densities and dielectric constants at 20–40°, J. Phys. Chem. **73,** No. 1, 57–61 (Jan. 1969).

Hummer, D. G., Non-coherent scattering-IV. Doppler redistribution functions in moving atmospheres, Monthly Notices Roy. Astron. Soc. **141,** 479–488 (Dec. 1968).

Hummer, D. G., Radiative transfer processes in planetary nebulae, (Proc. Intern. Astronomical Union, Symp. No. **34,** Tratranska Lomnica, Czechoslovakia, Sept. 4–8, 1967), Book, Planetary Nebulae, Ed. D. E. Osterbrock and C. R. O'Dell, pp. 166–184 (D. Reidel Publ. Co., Dordrecht, Amsterdam, The Netherlands, 1968).

Hummer, D. G., Rybicki, G. B., Line formation in differentially moving media with temperature gradients, Proc. Natl. Center for Atmospheric Research Conf. Resonance Lines in Astrophysics, Sept. 9–12, 1968, Boulder, Colo., pp. 315–330 (National Center for Atmospheric Research, Boulder, Colo., Dec. 1968).

Hummer, D. G., Rybicki, G. B., Redshifted line profiles from differentially expanding atmospheres, Astrophys. J. **153,** L107–L110 (Aug. 1968).

Hyde, K. E., Gordon, G., Kokoszka, G. F., Magnetic properties of some binuclear copper (II) complexes, J. Inorg. Nucl. Chem. **30,** 2155–2161 (1968).

Ito, J., Silicate apatities and oxyapatities, Am. Mineralogist **53,** 890–907 (May–June 1968).

Ito, J., Johnson, H., Synthesis and study of yttrialite, Am. Mineralogist **53,** 1940–1952 (1968).

Jacox, M. E., Milligan, D. E., Matrix-isolation study of the infrared spectrum of the free radical F_2CN, J. Chem. Phys. **48,** No. 9, 4040–4046 (May 1, 1968).

Jacox, M. E., Milligan, D. E., Matrix-isolation study of the vacuum-ultraviolet photolysis of trichlorosilane. The infrared spectrum of the free radical $SiCl_3$, J. Chem. Phys. **49,** No. 7, 3130–3135 (Oct. 1, 1968).

Jespersen, J. L., Kamas, G., Gatterer, L. E., MacDoran, P. F., Satellite VHF transponder time synchronization, Proc. IEEE **56,** No. 7, 1202–1206 (July 1968).

Johannesen, R. B., Candela, G. A., Tsang, T., Jahn-Teller distortion: magnetic studies of vanadium tetrachloride, J. Chem. Phys. **48,** No. 12, 5544–5549 (June 15, 1968).

Johannesen, R. B., Gordon, C. L., Titanium (IV) bromide (titanium tetrabromide), Book, Inorganic Syntheses IX, Chapt. IV, 46–50 (McGraw-Hill Book Co., New York, N.Y., 1967).

Judd, D. B., Color science and the paint industry, J. Paint Technol. **40,** No. 525, 470–477 (Oct. 1968).

Kahn, A. H., Polarons in anisotropic energy bands, Phys. Rev. **172,** No. 3, 813–815 (Aug. 15, 1968).

Kaufman, V., Radziemski, L. J., Redetermined level values and interaction parameters of S I and Cl II ground configurations, J. Opt. Soc. Am. **59,** No. 2, 227–228 (Feb. 1969).

Keller, R. A., Excited triplet → singlet intersystem crossing, Chem. Phys. Letters **3,** No. 1, 27–29 (Jan. 1969).

Kidnay, A. J., Hiza, M. J., Dickson, P. F., The adsorption isotherms of methane, nitrogen, hydrogen and their mixtures on charcoal at 76° K (Proc. 1967 Cryogenic Engineering Conf., Stanford University, Stanford, Calif., Aug. 21–23, 1967), Book, Advances in Cryogenic Engineering **13,** 397–408 (Plenum Press Inc., New York, N.Y., 1968).

Kim, Y-K., Inokuti, M., Chamberlain, G. E., Mielczarek, S. R., Minima of generalized oscillator strengths, Phys. Rev. Letters **21,** No. 16, 1146–1148 (Oct. 14, 1968).

Kirby, R. K., Rothrock, B. D., Thermal expansion of vitreous selenium from −190° to +30° C, J. Am. Ceram. Soc. **51,** No. 9, 535 (Sept. 1968).

Klein, R., The deposition of hydrogen beams on tungsten, Surface Sci. **11,** 227–241 (1968).

Klein, M., Hanley, H. J. M., Selection of the intermolecular potential. Part 2.—From data of state and transport properties taken in pairs, Trans. Faraday Soc. **64,** Part II, No. 551, 2927–2938 (Nov. 1968).

Klemens, P. G., Jackson, J. L., Diffusion of electrons on the Fermi surface. II. Longitudinal magnetoresistance of Ib metals, Physica **31,** 1421–1427 (1965).

Klose, J. Z., Atomic lifetime measurements with pulsed electron beams, (Proc. Beam-Foil Spectroscopy Conf., Univ. Arizona, Tucson, Arizona, Nov. 20–22, 1967), chapt. in Book, Beam-Foil Spectroscopy, II, 285–304 (Gordon and Breach Publ., New York, N.Y., 1968).

Kokoszka, G. F., Allen, H. C., Jr., Gordon, G., Electron paramagnetic resonance spectra of two zinc-doped and nickel-doped copper chloride pyridine-N-oxide complexes, J. Chem. Phys. **46,** No. 8, 3020–3024 (Apr. 15, 1967).

Kokoszka, G. F., Allen, H. C., Jr., Gordon, G., Electron paramagnetic resonance spectra of polycrystalline dimeric complexes. Copper propionate monohydrate and zinc-doped copper propionate monohydrate, Inorg. Chem. **7,** No. 9, 1730–1735 (1968).

Krause, R. F., Jr., Douglas, T. B., The heats of formation of $AlClF_2$ and $AlCl_2F$ from subliming AlF_3 in the presence of $AlCl_3$ vapor, J. Phys. Chem. **72,** No. 10, 3444–3451 (Oct. 1968).

Kruger, J., The spectrum of corrosion research of the Corrosion Section of the National Bureau of Standards (Proc. 12th Annual

Appalachian Underground Corrosion Short Course, West Virginia University, Morgantown, West Virginia, Oct. 1967), West Virginia University Tech. Bull. **86,** 11–13 (1967).

Kuriyama, M., Theory of x-ray diffraction by a distorted crystal. II. Scattering amplitude for a wave packet of finite size, J. Phys. Soc. Japan **25,** No. 3, 846–856 (Sept. 1968).

Kuyatt, C. E., Measurement of electron scattering from a static gas target, Book, Methods of Experimental Physics, Vol. 7. Atomic and Electron Physics, Chapt. 1. Electron-Atom Interactions, Ed. B. Pederson and W. L. Fite, pp. 1–43 (Academic Press Inc., New York, N.Y., 1968).

Lance, H. W., Metrology and National goals (Proc. 22nd ISA Conf. and Exhibit, Chicago, Ill., Sept. 11–14, 1967) ISA Preprint No. M4-1-MESTIND-67, 1–14 (1967); excerpt in Meas. Data **2,** No. 2, 68–71 (Mar.–Apr. 1968).

Lafferty, W. J., Maki, A. G., Pringle, W. C., Jr., Comments on "Two rotational lines of allene C_3H_4", J. Chem. Phys. **50,** No. 1, 564–565 (Jan. 1, 1969).

Latanision, R. M., Staehle, R. W., Plastic deformation of electrochemically polarized nickel single crystals, Acta Met. **17,** 307–319 (Mar. 1969).

Laufer, A. H., McNesby, J. R., Photolysis of methane at 1236–A: quantum yield of hydrogen formation, J. Chem. Phys. **49,** No. 5, 2272–2278 (Sept. 1, 1968).

Lee, T. G., A system for continuously monitoring hydrogen chloride concentrations in gaseous mixtures using a chloride ion-selective electrode, Anal. Chem. **41,** 391–392 (Feb. 1969).

Lonie, M., A report on body sizing for boys and students, Boys' and Young Men's Apparel Buyers' Assoc. J., p. 8 (1967).

Macedo, P. B., Napolitano, A., Inadequacies of viscosity theories for B_2O_3, J. Chem. Phys. **49,** No. 4, 1887–1895 (Aug. 15, 1968).

Macek, J. H., Application of the Fock expansion to doubly excited states of the helium atom, Phys. Rev. **160,** No. 1, 170–174 (Aug. 5, 1967).

Madden, R. P., Ederer, D. L., Codling, K., Resonances in the photoionization continuum of Ar I (20–150 eV), Phys. Rev. **177,** No. 1, 136–151 (Jan. 5, 1969).

Madey, T. E., Yates, J. T., Jr., Desorption by electron impact: oxygen adsorbed on tungsten, Surface Sci. **11,** 327–351 (1968).

Maki, A. G., Comment on the fermi resonance constant in ICN, J. Chem. Phys. **50,** No. 5, 2273 (Mar. 1, 1969).

Manning, J. R., Vacancy-wind effect in diffusion and deviations from thermodynamic equilibrium conditions, Can. J. Phys. **46,** No. 23, 2633–2643 (1968).

Marezio, M., Remeika, J. P., Zocchi, M., Cation distribution in the garnet $Eu_3Fe_{1.94}Ga_{3.06}O_{12}$, J. Chem. Phys. **48,** No. 3, 1094–1096 (Feb. 1968).

Matsumura, C., Lide, D. R., Jr., Structure of the alkali hydroxides. III. Microwave spectra of RbOH and RbOD, J. Chem. Phys. **50,** No. 1, 71–75 (Jan. 1, 1969).

Mazur, J., McIntyre, D., Wims, A. M., Asymptotic behavior of the light-scattering function of coiled molocules, J. Chem. Phys. **49,** No. 7, 2896–2904 (Oct. 1, 1968).

McClintock, M., Jennings, D. A., Mizushima, M., Contribution to the Raman line profile in liquids from molecular reorientation, Phys. Rev. Letters **21,** No. 5, 276–278 (July 29, 1968).

McIntyre, D., Sengers, J. V., Study of fluids by light scattering, Chapter 11 in Physics of Simple Liquids, H. N. V. Temperley, J. S. Rowlinson, G. S. Rushbrooke, ed., pp. 449–505 (North Holland Publ. Co., Amsterdam, The Netherlands, 1968).

McKinley, J. D., Jr., Mass spectrometric investigation of the surface reaction of tungsten with chlorine-oxygen mixtures (Proc. 6th Intern. Symp. Reactivity of Solids, Schenectady, N.Y., Aug. 25–30, 1968), Chapter in Reactivity of Solids, J. W. Mitchell, R. C. DeVries, R. W. Roberts, and P. Cannon, ed., pp. 345–351 (John Wiley and Sons, Inc., New York, N.Y., 1969).

Mendlowitz, H., Calculated line strengths for the transitions between the configurations $(3d^3+3d^24s)$ and $3d^24p$ in Ti II, Astrophys. J. **154,** 1099–1110 (Dec. 1968).

Meshkov, S., Ponzini, R., $Su(6)_W$ and high-energy photoproduction, Phys. Rev. **175,** No. 5, 2030–2034 (Nov. 25, 1968).

Mies, F. H., Configuration interaction theory. Effects of overlapping resonances, Phys. Rev. **175,** No. 1, 164–175 (Nov. 5, 1968).

Miller, C. E., Lipsicas, M., Nuclear spin-lattice relaxation in very dilute solutions of orthohydrogen in parahydrogen. Phys. Rev. **176,** No. 1, 273–279 (Dec. 5, 1968).

Mighell, A. D., Reimann, C. W., Mauer, F. A., The crystal and molecular structure of diaquobis-(2,2′-biimidazole) nickel (II) dinitrate, $Ni(C_6H_6N_4)_2(H_2O)_2(NO_3)_2$, Acta Cryst. **B25,** Part 1, 61–66 (Jan. 1969).

Milligan, D. E., Jacox, M. E., Matrix-isolation study of the reaction of F_2 and of F atoms with NCN. The infrared spectra of the species NF_2CN and FNCN, J. Chem. Phys. **48,** No. 11, 4811–4816 (June 1, 1968).

Milligan, D. E., Jacox, M. E., Matrix-isolation study of the vacuum-ultraviolet photolysis of dichlorosilane. The infrared spectrum of the free radical $SiCl_2$, J. Chem. Phys. **49,** No. 4, 1938–1942 (Aug. 15, 1968).

Milligan, D. E., Jacox, M. E., Matrix-isolation study of the vacuum-ultraviolet photolysis of difluorosilane. The infrared and ultraviolet spectra of the free radical SiF_2. J. Chem. Phys. **49,** No. 10, 4269–4275 (Nov. 15, 1968).

Milligan, D. E., Jacox, M. E., Guillory, W. A., Matrix-isolation study of the vacuum-ultraviolet photolysis of trifluorosilane. The infrared spectrum of the free radical SiF_3, J. Chem. Phys. **49,** No. 12, 5330–5335 (Dec. 15, 1968).

Mills, R. M., Flame inhibition with electron attachment as the first step, Combustion and Flame **12,** No. 2, 513–520 (Dec. 1968).

Moore, C. E., Annual report on spectroscopy, Bull. Am. Astron. Soc. **1,** No. 1, 85–86 (Jan. 1969).

Mozer, B., Localized modes, resonant modes and impurity vibrational bands in vanadium alloys, Chapter in Neutron Inelastic Scattering **1,** 55–63 (Intern. Atomic Energy Agency, Vienna, Austria, 1968).

Mulroy, W. J., Kusuda, T., Phillips, C. W., Survey on digital computer programs for heating and cooling load calculations, SICCAP Bull. **2,** No. 2, 4–8 (May 1968).

Nemoto, T., Wait, D. F., Microwave circuit analysis using the equivalent generator concept, IEEE Trans. Microwave Theory Tech. **MTT-16,** No. 10, 866–873 (Oct. 1968).

Newman, M., A bound for the number of conjugacy classes in a group, J. London Math. Soc. **43,** 108–110 (1968).

Newman, M., Maximal normal subgroups of the modular group, Proc. Am. Math. Soc. **19,** No. 5, 1138–1144 (Oct. 1968).

Nimeroff, I., A survey of papers on degree of metamerism, Color Eng. **6,** No. 6, 44–46 (Nov.–Dec. 1968).

Odabasi, H., Spectrum of doubly ionized lanthanum (La III), J. Opt. Soc. Am. **57,** 1459 (1967).

Okabe, H., Photodissociation of HN_3 in the vacuum-ultraviolet production and reactivity of electronically excited NH, J. Chem. Phys. **49,** No. 6, 2726–2733 (Sept. 15, 1968).

Omar, A., Peterson, R. L., On the validity of the Boltzmann relaxation equation, Physica **39,** No. 1, 156–160 (July 1, 1968).

Pechukas, P., Generalized Langevin equation of Mori and Kubo, Phys. Rev. **164,** No. 1, 164–175 (Dec. 5, 1967).

O'Reilly, D. E., Tsang, T., Order-disorder transition in ferroelectric ammonium sulfate, J. Chem. Phys. Letter to Editor **50,** No. 5, 2274–2275 (Mar. 1, 1969).

Pecker, J.-C., Thomas, R. N., Saturation in Fraunhofer lines, Observatory Letter **88,** No. 964, 115–117 (June 1968).

Peiser, J. S., The relative magnitude of jump rates for point-defect paths between equivalent sites around a trap, J. Korean Phys. Soc. **1,** No. 1, 5–8 (Mar. 1968).

Penner, S., Handling high-energy high-power electron beams, Record IEEE 9th Annual Symp. Electron, Ion and Laser Beam Technology, Berkeley, Calif., May 9–11, 1967, No. f–79, 50–61 (1967).

Peterson, R. L., Short-range magnetic order in a modified Weiss molecular-field theory, Phys. Rev. **171,** No. 2, 586–590 (July 10, 1968).

Plummer, E. W., Gadzuk, J. W., Young, R. D., Resonance tunneling of field emitted electrons through adsorbates on metal surfaces, Solid State Commun. **7,** 487–491 (1969).

Pool, K. H., Bates, R. G., Thermodynamics of hydrochloric acid in 95 volume per cent (92.41 mass per cent) ethanol from e. m. f. measurements at 5 to 50 °C, J. Chem. Thermodynamics **1,** 21–29 (1969).

Rhodes, I., The mighty man-computer team, Blanch Anniversary Volume, pp. 277–284 (Aerospace Research Laboratories, Office of Aerospace Research, U.S. Air Force, Arlington, Va., Feb. 1967).

Roach, F. E., The brightness of the zodical light at the ecliptic pole, (Proc. Symp. Meteor Orbits and Dust, Cambridge, Mass., Aug. 9–19, 1965), Smithsonian Contributions to Astrophysics, F. L. Whipple, ed., 11, 225–226 (Smithsonian Institution Astrophysics Observatory, Cambridge, Mass., 1967).

Robbins, C. R., Synthetic $CaTiSiO_5$ and its germanium analogue ($CaTiGeO_5$), Mater. Res. Bull. **3,** 693–698 (1968).

Rush, J. J., Melveger, A. J., Farrar, T. C., Tsang, T., Laser-Raman spectra and hindered rotation in the phosphonium halides, Chem. Phys. Letters **2,** No. 8, 621–624 (1968).

Sadowski, W. L., On some aspects of the eigenfunction expansion of the solution of the nonlinear Vlasov equation (Proc. Computer Simulation of Plasma and Many-Body Problems, Williamsburg, Va., Apr. 19–21, 1967), Natl. Aeronaut. Space Agency Spec. Publ. **153,** 433–440 (1967).

Santoro, A., Weir, C. E., Block, S., Piermarini, G. J., Adsorption corrections in complex cases. Application to single crystal diffraction studies at high pressure, J. Appl. Cryst. **1,** Part 2, 101–107 (June 1968).

Sarachman, T. N., Microwave spectrum of cis-2-butene, J. Chem. Phys. **49,** No. 7, 3146–3149 (Oct. 1, 1968).

Schafft, H. A., Avoiding second breakdown, Proc. XIII Intern. Scientific Congress on Electronics, Rome, Italy, June 1966, pp. 119–130 (Rassegna Internazionale Elettronica Nucleare Teleradiocinematografica, Rome, Italy, 1966).

Schindler, P. W., Heterogeneous equilibria involving oxides, hydroxides, carbonates and hydroxide carbonates (Proc. Symp. Division of Water, Air, and Waste Chemistry, 151st Meeting of the American Chemical Society, Pittsburgh, Pa., Mar. 1966), Book, Equilibrium Concepts in Natural Water Systems, Advances in Chemistry Series **67,** 196–221 (American Chemical Society, New York, N.Y., 1967).

Schmidt, L. B., Case, W. E., Harrington, R. D., Surface dependence of ferrimagnetic resonance fields in polycrystalline NiAl ferrite, Proc. IEEE **56,** No. 7, 1236–1237 (July 1968).

Schweitzer, W. G., Jr., Saturated absorption by neon inside a 6327 Å laser with a mixture of neon isotopes in its gain tube, Appl. Phys. Letters **13,** No. 11, 367–368 (Dec. 1, 1968).

Schwerdtfeger, W. J., Discussion of the paper "Method of estimating corrosion of highway culverts by means of polarization curves," by R. I. Lindberg, Highway Research Record No. 204, Metal Corrosion, Publ. **1535,** p. 8 (National Research Council-National Academy of Sciences, Washington, D.C., 1967).

Shah, J. A., Huber, M. G., Danos, M., Separability of the nuclear residual two-body interaction, Physics Letters **28B,** No. 6, 381–383 (Jan. 6, 1969).

Shapiro, J. T., Madden, R. P., On the optical constants of polystyrene in the vacuum ultraviolet, J. Opt. Soc. Am. **58,** No. 6, 771–775 (June 1968).

Shirley, J. H., Dynamics of a simple maser model, Am. J. Phys. **36,** Part 1, No. 11, 949–963 (Nov. 1968).

Shuler, K. E., Reaction cross sections, rate coefficients and non-equilibrium kinetics (Lecture, NATO Summer School on Theoretical Chemistry, Constance, Germany, Summer 1965), Book, Chemische Elementarprozesse, Ed. H. Hartmann, pp. 1–22 (Springer-Verlag, Berlin, Germany, 1968).

Shumaker, J. B., Jr., Franck-Condon factors for high rotational levels of nitrogen, J. Quant. Spectry. Radiative Transfer **9,** 153–156 (1969).

Shumaker, J. B., Jr., Popenoe, C. H., Experimental test of H_β Stark-broadening theory at high electron densities, Phys. Rev. Letters **21,** No. 15, 1046–1048 (Oct. 7, 1968).

Sieck, L. W., Continuum emission from zenon in the vapor phase induced by absorption of 1470-Å radiation, J. Phys. Chem. **72,** No. 9, 3129–3133 (Sept. 1968).

Sieck, L. W., Xenon-photosensitized decomposition of methane at 1470 A, J. Chem. Phys. **50,** No. 4, 1748–1753 (Feb. 15, 1969).

Silverman, S., Reflections on bioengineering (Proc. Symp. Engineering Significance of the Biological Sciences, Pittsburgh, Pa., Jan. 25–27, 1967), Book, Bioengineering—An Engineering View, pp. 103–106 (San Francisco Press Inc., San Francisco, Calif., June 1968).

Simmons, J. A., Coriell, S. R., Solution of the Stefan problem for whisker evaporation, J. Appl. Phys. **39,** No. 7, 3459–3463 (June 1968).

Smith, E. W., Hooper, C. F., Jr., Comments on ion microfield distributions as used in plasma line broadening theories, J. Quant. Spectry. Radiative Transfer **8,** No. 9, 1617–1619 (Sept. 1968).

Smith, S. J., Photodetachment, Chapter in Methods in Experimental Physics, Vol. 7, Atomic and Electron Physics, B. Bederson and W. L. Fite, ed., pp. 179–208 (Academic Press Inc., New York, N.Y., 1968).

Steel, N. M., Production of synthetic food materials: A statistical survey, Proc. Second Intern. Conf. Women Engineers and Scientists, 30 pages (Women's Engr. Soc., London, England, 1968).

Stevens, M. E., Selected pattern recognition projects in Europe, Pattern Recognition **1,** 103–118 (Nov. 1968).

Steiner, B., Photodetachment of electrons from SH^-, J. Chem. Phys. **49,** No. 11, 5097–5104 (Dec. 1, 1968).

Steiner, B., The cross section for the photodetachment of electrons from I^-, Phys. Rev. **173,** No. 1, 136–142 (Sept. 5, 1968).

Stevens, M. E., Progress and prospects in mechanized indexing (Proc. Symp. on Mechanized Abstracting and Indexing, Moscow, U.S.S.R., Sept. 28–Oct. 1, 1966), UNESCO/NS/209 (United Nations Educational Scientific and Cultural Organization, Paris, France, Apr. 1967).

Sugar, J., Nuclear magnetic dipole moment of ^{165}Ho, J. Opt. Soc. Am. **58,** No. 11, 1519–1523 (Nov. 1968).

Suzuki, G., Quantitative methods for decision making, Book, Management: Concepts and Practices, Ed. F. R. Brown, Chap. VIII, pp. 155–193 (Industrial College of the Armed Forces, Washington, D.C., 1967).

Swanson, N., Codling, K., Excitation of K-shell electrons in Be by soft x-rays and 20-keV electrons, J. Opt. Soc. Am. **58,** No. 9, 1192–1194 (Sept. 1968).

Tantila, W. H., Mahler, R. J., James, L. W., Magnetic parametric nuclear spin saturation, Appl. Phys. Letters **13,** No. 1, 27–29 (July 1, 1968).

Thomas, R. N., Symposium on Wolf-Rayet stars: A summary, Astrophysical Letters **2,** 147–148 (1968).

Toots, J., Fowler, H. A., Marton, L., Reflectance and $1/\epsilon$ resonance of beryllium in the far ultraviolet, Phys. Rev. **172,** No. 3, 670–676 (Aug. 15, 1968).

Truesdell, C., The non-linear field theories of mechanics, Encyclopedia of Physics **III,** Part 3, 602 pages (Springer-Verlag, Berlin, Germany, 1965).

Tschuikow-Roux, E., Photolysis of propene at 1470A, J. Phys. Chem. Note **71,** 2355 (1967).

Utech, H. P., Early, J. G., On the presence of thermal convection in the kinetics experiments of Rigney and Blakely, Acta Met. **15,** No. 7, 1238–1239 (1967).

Van Blerkom, D., Hummer, D. G., A non-LTE theory of overlapping lines near the series limit, Astrophys. J. **154,** 741–750 (Nov. 1968).

Waclawski, B. J., Hughey, L. R., Madden, R. P., Effect of oxygen adsorption on the photoelectron yield from tungsten in the vacuum ultraviolet, Appl. Phys. Letters **10,** No. 11, 305–307 (June 1968).

Wahsweiler, H. G., Greiner, W., Danos, M., Continuum nuclear structure of O^{16} in the eigenchannel reaction theory, Phys. Rev. **170,** No. 4, 893–906 (June 20, 1968).

Wait, D. F., Thermal noise from a passive linear multiport, IEEE Trans. Microwave Theory Tech. **MTT-16,** No. 9, 687–691 (Sept. 1968).

Wang, F. E., DeSavage, B. F., Buehler, W. J., The irreversible critical range in the TiNi transition, J. Appl. Phys. **39,** No. 5, 2166–2175 (Apr. 1968).

Weir, C. E., Piermarini, G. J., Block, S., Crystallography of some high-pressure forms of C_6H_6, CS_2, Br_2, CCl_4, and KNO_3, J. Chem. Phys. **50,** No. 5, 2089–2093 (Mar. 1, 1969).

Weisman, H. M., Information and the discipline of communication sciences, (Proc. American Documentation Institute Annual Meeting, New York, N.Y., Oct. 22–27, 1967), Book, Levels of Interaction Between Man and Information **4,** 8-12 (Thompson Book, Co., Washington, D.C., 1968).

Weisman, I. D., Swartzendruber, L. J., Bennett, L. H., Resonance studies in ferromagnetic Fe_2B and Fe_2Zr, Phys. Rev. **177,** No. 2, 465–471 (Jan. 10, 1969).

Weiss, A. W., Series perturbations and atomic oscillator strengths: The ^2D series of Al I, Phys. Rev. **178,** No. 1, 82–89 (Feb. 5, 1969).

Weissberg, A., Data handling systems, Proc. Second Conf. Technical Information Center Administration, St. David's, Pa., June 14–17, 1965, TICA **2,** Ed. A. W. Elias, Chapt. 7, pp. 75–89 (Spartan Books, Washington, D.C., 1965).

Wildhack, W. A., Improving measurement accuracy for high systems reliability, Electronics **41,** No. 5, 280 (Mar. 4, 1968).

Wims, A. M., McIntyre, D., Hynne, F., Coexistence curve for 3-methylpentane-nitroethane near the critical point, J. Chem. Phys. **50,** No. 2, 616–620 (Jan. 15, 1969).

White, H. S., Jr., Data management and standardization, Mod. Data **2,** No. 5, 52–56 (May 1969).

Wiese, W. L., Dependence of atomic *f*-values on nuclear charge (Proc. Conf. Beam-Foil Spectroscopy, University of Arizona, Tucson, Arizona, Nov. 20–22, 1967), chapt. in Book, Beam Foil Spectroscopy, **II,** 386–406 (Gordon and Breach Publ., New York, N.Y., 1968).

Wiese, W. L., Systematic trends of atomic oscillator strengths in isoelectronic sequences, Appl. Opt. **7,** No. 12, 2361–2366 (Dec. 1968).

Wiese, W. L., Weiss, A. W., Regularities in atomic oscillator strengths, Phys. Rev. **175,** No. 1, 50–65 (Nov. 5, 1968).

Wolcott, N. M., Falge, R. L., Jr., Ferromagnetism of $CrBe_{12}$, Phys. Rev. **171,** No. 2, 591–595 (July 10, 1968).

Wolcott, N. M., Falge, R. L., Jr., Bennett, L. H., NMR studies in paramagnetic and ferromagnetic $CrBe_{12}$, Phys. Rev. Letters **21,** No. 8, 564–549 (Aug. 19, 1968).

Wolfgang, R., Zare, R. N., Branscomb, L. M., Chemical accelerators, Science **162,** No. 3855, 818–822 (Nov. 15, 1968).

Yolken, H. T., Kruger, J., Thermal regeneration of oxide covered iron {100} and {110} surfaces, J. Electrochem. Soc. **114,** No. 8, 796–799 (Aug. 1967).

Yolken, H. T., Kruger, J., Calvert, J. P., Hydrogen in passive films on Fe, Corrosion Sci. **8,** 103–108 (1968).

Younglove, B. A., Polarizability, dielectric constant, pressure, and density of solid parahydrogen on the melting line, J. Chem. Phys. **48,** No. 9, 4181–4186 (May 1, 1968).

Zalubas, R., Present state of analysis of the first spectrum of thorium (Th I), J. Opt. Soc. Am. **58,** No. 9, 1195–1199 (Sept. 1968).

Zwanzig, R., Lauritzen, J. I., Jr., Exact calculation of the partition function for a model of two-dimensional polymer crystallization by chain folding, J. Chem. Phys. **48,** No. 8, 3351–3360 (Apr. 15, 1968).

**Publications for which a price is indicated are available by purchase from the Superintendent of Documents, U.S. Government Printing Office, Washington, D.C. 20402 (foreign postage, one-fourth additional). The NBS non-periodical series are also available from the Clearinghouse for Federal Scientific and Technical Information, Springfield, Va. 22151. Reprints from outside journals and the NBS Journal of Research may often be obtained directly from the authors.*

INDEX TO VOLUME 73C

January to December 1969

A

Page

Absorbed dose 17
Ac 47
Accelerometer 75

B

Ballard, L. D., Epstein, W. S., Smith, E. R., Edelman, S., Optical FM system for measuring mechanical shock 75
Bowman, H. A., Gallagher, W. H., Improved high-precision calibration procedure for reference standard hydrometers ... 57

C

Calibration 57, 75
Calorimeter 17
Cassidy, E. C., Cones, H. N., A Kerr electro-optical technique for observation and analysis of high-intensity electric fields .. 5
Cones, H. N., Cassidy, E. C., A Kerr electro-optical technique for observation and analysis of high-intensity electric fields .. 5

D

D-c 47
Density 57
Design features of a precision ac-dc converter 47
Dielectric liquids 5
Domen, S. R., A heat loss compensated calorimeter and related theorems 17
Doppler 75

E

Edelman, S., Ballard, L. D., Epstein, W. S., Smith, E. R., Optical FM system for measuring mechanical shock 75
Electro-optical measurements 5
Electrostatic field measurements 5
Epstein, W. S., Ballard, L. D., Smith, E. R., Edelman, S., Optical FM system for measuring mechanical shock 75

F

Flach, D. R., Marzetta, L. A., Design features of a precision ac-dc converter 47

G

Gallagher, W. H., Bowman, H. A., Improved high-precision calibration procedure for reference standard hydrometers ... 57

H

Heat flow theorems 17
Heat loss compensated calorimeter and related theorems 17
Heat loss compensation 17
High voltage measurements 5
Hydrometer 57
Hydrometer calibration 57

I

Page

Improved high-precision calibration procedure for reference standard hydrometers 57
Interferometer 1, 75
Interferometer for measuring gradients in both refractive index and thickness of large or small optics 1

J

Joiner, B. L., Student-*t* deviate corresponding to a given normal deviate 15

K

Kerr cell 5
Kerr electro-optical technique for observation and analysis of high-intensity electric fields 5

L

Laboratory measurements of air cavity temperature in a passenger car tire 21
Laser 75
Laser applications 5
Linzer, M., The nuclear quadrupole resonance magnetometer: a new method for the precision measurement of the magnitude and direction of magnetic fields 67

M

Mandel, J., Simpson, B. G., Laboratory measurements of air cavity temperature in a passenger car tire 21
Marzetta, L. A., Flach, D. R., Design features of a precision ac-dc converter 47
Magnetometer 67
Measuring shock 75

N

Nuclear quadrupole resonance 67
Nuclear quadrupole resonance magnetometer: a new method for the precision measurement of the magnitude and direction of magnetic fields 67

O

Operational 47
Optical FM system for measuring mechanical shock 75
Optical homogeneity 1

P

Potential measurements 5
Precision 47
Pulse measurements 5

R

Page

Rectifier 47
Reference hydrometer 57
Refractive index 1

S

Saunders, J. B., An interferometer for measuring gradients in both refractive index and thickness of large or small optics 1
Simson, B. G., Mandel, J., Laboratory measurements of air cavity temperature in a passenger car tire 21
Single-sideband 75
Smith, E. R., Ballard, L. D., Epstein, W. S., Edelman, S., Optical FM system for measuring mechanical shock 75
Specific gravity 57
Standard deviation 15
Standard hydrometer 57
Statistics 15
Student-*t* 15
Student-*t* deviate corresponding to a given normal deviate 15

T

Table of Student-*t* 15
Temperature sensitivity 21
Tire 21
Transfer 47

U

Uncertainties 15

U.S. GOVERNMENT PRINTING OFFICE : 1969 OL—364—586

DUP-C JUNE 46129
UNIVERSITY MICROFILMS INC
SERIALS SECTION
300 NORTH ZEEB ROAD
ANN ARBOR MICHIGAN 48106

UNITED STATES
GOVERNMENT PRINTING OFFICE
DIVISION OF PUBLIC DOCUMENTS
WASHINGTON, D.C. 20402

OFFICIAL BUSINESS

POSTAGE AND FEES PAID
U.S. GOVERNMENT PRINTING OFFICE

JOURNAL OF RESEARCH of the National Bureau of Standards Vol. 73, Nos. 3 and 4 July–December 1969
C. Engineering and Instrumentation

Contents

Page

Design features of a precision ac-dc converter.
Louis A. Marzetta and Donald R. Flach. 47

An improved high-precision calibration procedure for reference standard hydrometers. Horace A. Bowman and William H. Gallagher. 57

The nuclear quadrupole resonance magnetometer: A new method for the precision measurement of the magnitude and direction of magnetic fields. Melvin Linzer. 67

Optical FM system for measuring mechanical shock.
L. D. Ballard, W. S. Epstein, E. R. Smith, and S. Edelman. 75

Publications of the National Bureau of Standards. 79

Index to Volume 73C, January to December 1969. 117

Library of Congress Catalog Card Number: 62–3900

For sale by the Superintendent of Documents, U.S. Government Printing Office, Washington, D.C. 20402. (Order by SD Catalog No. C 13.22/sec. C: 73/3 & 4). Price $1.25 (single copy). Subscription price: $5.00 a year; $1.25 additional for foreign mailing.
UNITED STATES GOVERNMENT PRINTING OFFICE, WASHINGTON : 1969